Universidad Miguel Hernández de Elche

IMMEDIATE AND DEFERRED EPIGENOMIC SIGNATURES OF *IN VIVO* NEURONAL ACTIVATION IN MOUSE HIPPOCAMPUS

Doctoral Thesis presented by

Jordi Fernandez-Albert

- 2019 -

Thesis Director:

Prof. Angel Barco Guerrero

PhD Program in Neuroscience

Instituto de Neurociencias – UMH-CSIC

Sant Joan d'Alacant, 9 de Septiembre 2019

To whom it may concern,

The doctoral thesis entitled "*Immediate and deferred epigenomic signatures of in vivo neuronal activation in mouse hippocampus*" has been developed by myself, Jordi Fernandez-Albert. This thesis includes the following publication, of which I am the first author. I declare that the publication has not been used and will not be used in any other thesis in agreement with my thesis director Prof. Angel Barco Guerrero:

Jordi Fernandez-Albert, Michal Lipinski, María T. Lopez-Cascales, M. Jordan Rowley, Ana M. Martin-Gonzalez, Beatriz del Blanco, Victor G. Corces, and Angel Barco. Immediate and deferred epigenomic signatures of in vivo neuronal activation in mouse hippocampus. Nature Neuroscience, 2019. doi: 10.1038/s41593-019-0476-2 (Public version of the article: bioRxiv, doi: https://doi.org/10.1101/534115)

Yours sincerely,

Doctorando

Dr. Angel Barco Guerrero

Sant Joan d'Alacant, 9 de Septiembre 2019

D. Angel Barco Guerrero, Profesor de Investigación del Consejo Superior de Investigaciones Científicas y Director de esta Tesis Doctoral,

AUTORIZO la presentación de la Tesis Doctoral titulada "*Immediate and deferred epigenomic signatures of in vivo neuronal activation in mouse hippocampus*" y realizada por D. Jordi Fernandez-Albert, bajo mi inmediata dirección y supervisión en el Instituto de Neurociencias (UMH-CSIC) y que presenta para la obtención del grado de Doctor por la Universidad Miguel Hernández.

Y para que conste, a los efectos oportunos, firmo el presente certificado.

Dr. Angel Barco Guerrero

Sant Joan d'Alacant, 9 de Septiembre 2019

D. Miguel Valdeolmillos López, Catedrático y Coordinador del programa de doctorado en Neurociencias del Instituto de Neurociencias de Alicante, centro mixto de la Universidad Miguel Hernández (UMH) y de la Agencia Estatal Consejo Superior de Investigaciones Científicas (CSIC),

CERTIFICO:

Que la Tesis Doctoral titulada "*Immediate and deferred epigenomic signatures of in vivo neuronal activation in mouse hippocampus*" has sido realizada por D. Jordi Fernandez-Albert, bajo la dirección de Dr. Angel Barco Guerrero como director, y doy mi conformidad para que sea presentada a la Comisión de Doctorado de la Universidad Miguel Hernández.

Y para que conste, a los efectos oportunos, firmo el presente certificado.

Dr. Miguel Valdeolmillos López

E-mail :
miguel.valdeolmillos@umh.es
www.in.umh.es

Tel: +34 965 919540
Fax: +34 965 919549

Av Ramón y Cajal s/n
CAMPUS DE SANT JOAN
03550 SANT JOAN D'ALACANT– ESPAÑA

Front cover: High-resolution microscopy image of hippocampal neuronal excitatory cell-nucleus. Green color is the fluorescence of the inner nuclear membrane, emitted by GFP-Sun1 protein.

ACKOWLEDGEMENTS

AGRADECIMIENTOS

AGRAÏMENTS

Quisiera agradecer la realización de mi tesis:

A mi director profesor Angel Barco, por su mentoría y dedicación al conocimiento científico. También por su apoyo en mi desarrollo profesional y la confianza depositada para realizar este trabajo. Gracias.

Al laboratorio de Angel Barco, por el compañerismo y su ayuda cuando la he necesitado, especialmente a aquellos que han participado en el proyecto. Gracias.

A Victor Corces por su mentoría y apoyo al proyecto. Su acogida y la de su laboratorio fueron ejemplares en un momento complicado del trabajo. Especialmente Jordan, Rachel, Xiaowen, Isaac, Yoon Hee, Viviane, Hannah, y Michael. Thanks.

A Maite Lopez por su compañerismo y amistad, trabajando en los momentos más buenos y difíciles del proyecto. Gracias.

A todo el equipo técnico y directivo del Instituto de Neurociencias, que me han acompañado y ayudado estos años. Gracias.

A mis previos mentores científicos los profesores Manuel Irimia y Carles Sindreu que me han guiado y enseñado para poder llegar al objetivo. Gracias.

A mis amigos científicos por su apoyo, sus consejos y los buenos ratos discutiendo ciencia y desconectando. Chelo, Arturo, Victor y Jon. Gracias.

A la més important, la que em riu, em cura, m'estima i m'ensenya. Gràcies per estar allà, sense tu hagués sigut impossible.

A la meva família per poder tornar a casa i no deixar-me caure. Especialment a les meves germanes, les úniques capaces de treure'm sempre un somriure. Merci.

Als meus amics, especialment Rugi, Artur, Enric, Laura, Marti. Gràcies per estar sempre allà, tornar a casa és on vosaltres sou. Merci.

A tots aquells musics, artistes i dissenyadors de jocs que m'han acompanyat a les meves infinites hores de treball i poques de descans.

A totes aquelles persones que no conec, però que segurament han ajudat en el meu dia a dia.

A tots aquells animals que han fet possible aquest coneixement i que el futur de la vida sigui millor.

A tu Yuma, tu segueixes estan allà. Gràcies per ensenyar-me que la vida és amor.

INDEX

ABSTRACT

(English)

Abstract

This thesis describes the genomic regulatory events occurring in the nucleus of hippocampal excitatory neurons of adult behaving mice upon activation. It provides both novel cutting-edge methods in neurogenomics and a repository of novel next generation sequencing datasets with broad utility that open new avenues for the investigation of the genomic mechanisms underlying neuronal plasticity.

The integrative and longitudinal multi-omics analysis of transcriptional and chromatin dynamics after status epilepticus and experience-driven neuronal activation unveils molecular mechanisms that are likely to contribute to metaplasticity in the adult brain. Most of these molecular processes are described here for the first time in the context of neuronal activation *in vivo*. In particular: the identification of transcripts displaying activity-dependent ribosome-engagement; the detection of several species of activity-induced ncRNAs in the nucleus; the description of the dramatic impact of transcriptional bursting in chromatin accessibility at the gene body and enhancers of activity-induced genes; the *de novo* binding of activity-regulated transcription factors; the augmented promoter-enhancer interactions at activity-regulated genes; and the formation of gene loops that bring together the TSS and TTS of actively transcribed genes and may sustain the fast re-loading of RNAPII complexes. Notably, the identification of chromatin occupancy and interaction changes that remain long after the transcriptional burst, particularly those driven by AP1, showed a correlation with deleterious consequences of status epilepticus. Which could underlie the changes in neuronal responsiveness and circuit connectivity observed in these neuroplasticity paradigms, perhaps thereby contributing to a genomic memory.

To reach these findings, I introduce methods that we expect will become standard in the field of Neurogenomics. These include the optimization of procedures for fluorescence-activated nuclear sorting (FANS) and their combination with genetic GFP-tagging of the nuclear envelope, which allowed cell-type specific analyses using a wide range of NGS technologies *in vivo*. In particular, we generated high coverage profiles for ribosomal-bound mRNA-seq (translatome), nuclear RNA-seq (transcriptome), ATAC-seq (chromatin accessibility, TF-footprinting and nucleosome positioning), ChIP-seq (protein-chromatin interactions), and the first Hi-C map (chromatin-chromatin interactions) in hippocampal excitatory neurons, both in the basal state and after activation with a glutamate agonist. Furthermore, the combination of this approach with nuclear immune-staining against Fos allowed the isolation of nuclei from excitatory neuronal-ensembles activated in response to the exploration of a novel context and the investigation of the chromatin changes occurring in these cells in response to experience.

RESUMEN

(Spanish)

Esta tesis describe los eventos reguladores del genoma que ocurren en el núcleo de las neuronas excitadoras del hipocampo en ratones adultos durante la activación. El estudio provee tanto una colección de métodos innovadores en neurogenómica como un novedoso repositorio de datos de NGS con amplia utilidad en el campo, que abrirán nuevos caminos para la investigación de los mecanismos transcripcionales y epigenéticos que participan en la plasticidad neuronal.

El análisis multi-omico integrativo y longitudinal de los dinamismos de la transcripción y la cromatina después del estado epiléptico y la activación neuronal dirigida por la experiencia revela mecanismos moleculares que contribuyen potencialmente a la metaplasticidad en el cerebro adulto. La mayoría de estos procesos moleculares son descritos por primera vez en el contexto de la activación neuronal *in vivo*. En particular: la identificación de transcritos mostrando actividad dependiente de unión al ribosoma; la detección de varias especies de RNAs no codificantes inducidas por actividad en el núcleo; la descripción de el impacto dramático de la actividad transcripcional en la accesibilidad de la cromatina en el cuerpo del gen y en los enhancers de los genes inducidos por actividad; la unión *de novo* de factores de transcripción regulados por actividad; el aumento de las interacciones promotor-enhancer en los genes regulados por actividad; y la formación de lazos génicos que acercan el TSS y el TTS de genes activamente transcritos y que podría sostener la rápida reincorporación de los complejos de RNAPII. Interesantemente, los cambios en la ocupabilidad de la cromatina y las interacciones promotor-enhancer que permanecen tiempo después de la actividad transcripcional, particularmente aquellas dirigidas por AP1, muestran una correlación con las

consecuencias deletéreas del estado epiléptico. Estos cambios de larga duración podrían participar en las alteraciones de la respuesta neuronal y la conectividad del circuito observados en los paradigmas de neuroplasticidad, tal vez contribuyendo a una memoria genómica.

Para llegar a estos descubrimientos, he introducido métodos que esperamos que se conviertan en estándar en el campo de la Neurogenómica. Estos incluyen la optimización de procedimientos de clasificación nuclear activada por fluorescencia (FANS) y su combinación con el etiquetado genético de tipos celulares mediante la expresión de una variante de GFP dirigida a la envuelta nuclear, lo que ha permitido el análisis especifico de tipos celulares usando un amplio rango de tecnologías NGS *in vivo*. En particular, se han generado perfiles con amplia cobertura para mRNA-seq con unión-ribosomal (translación), RNA-seq nuclear (transcripción), ATAC-seq (accesibilidad de la cromatina, huellas de TF y posicionamiento nucleosómico), ChIP-seq (interacciones proteína-cromatina), y el primer mapa de HiC (interacciones cromatina-cromatina) en el hipocampo de neuronas excitadoras, tanto en el estado basal como después de la activación con un agonista de glutamato. Más aún, la combinación de esta aproximación con la immuno-tinción nuclear contra Fos, ha permitido el aislamiento de núcleos de conjuntos de neuronas excitadoras activadas en respuesta a la exploración de un contexto nuevo y la investigación de los cambios en la cromatina de esas células en respuesta a experiencia.

TABLE OF ABBREVIATIONS

3C	chromatin conformation capture
3'-UTR	three prime untranslated region
5hmC	5-hydroxymethylcytosine
5mC	5-methylcytosine
AD-mRNAs	activity-depleted mRNAs
AI-mRNAs	activity-induced mRNAs
AMPA	α-amino-3-hydroxy-5-methyl-4-isoxazolepropionic acid
AP-1	activating protein complex 1
ATAC	assay for transposase-accessibility chromatin
ATP	adenosine triphosphate
BETA	binding and expression target analysis
BRD4	bromodomain- containing protein 4
BAF	*BRG1* - associated factor
CA1	cornus amonis 1
CaMK	calcium/calmodulin-dependent protein kinase
cAMP	cyclic adenosine monophosphate
CBP	CREB-binding protein
CGI	CpG island
ChIP	chromatin immunoprecipitation
ChIA-PET	chromatin interaction analysis by paired-end tag
CHD	chromodomain helicase DNA-binding
circRNA	circular RNAs
CRE	cAMP response element
CREB	cAMP responsive element binding protein

creERT2	cyclization recombination estrogen receptor ligand biding domain for tamoxifen 2
CTCF	CCCTC-binding factor
DA	differential accessibility
DAG	differentially accessible gene
DAR	differentially accessible region
DEG	differentially expressed gene
DET	differentially expressed transcript
DG	dentate gyrus
DI	differential Index
DNA	deoxyribonucleic acid
DNAme	DNA methylation
DNMT	DNA methyltransferase
DSB	DNA double strain break
ecRNA	extracoding RNA
eRNA	enhancer RNA
FANS	fluorescence activated nuclear sorting
FC	fold change
FDR	false discovery rate
GB	gene body
GEO	gene expression omnibus
GFP	green fluorescent protein
GO	gene ontology
GREAT	genomic regions enrichment of annotations
HAT	histone acetyltransferase

HC	home cage
HDAC	histone deacetylase complex
HiC	3C coupled with sequencing
HP1	heterochromatin-associated protein 1
hPTM	histone posttranslational modifications
IA	Induced accessibility
IEG	immediate early gene
INTACT	isolation of nuclei tagged in specific cell types
ISWI	imitation switch
KA	kainic acid
KCl	potassium chloride
LAD	lamina-associated domain
LTP	long-term potentiation
MAPK	mitogen-associated protein kinase
MeCP2	methyl CpG binding protein 2
MEF2	myocyte enhancer factor 2
mRNA	messenger RNA
ncRNA	non-coding RNA
NCS	newborn calf serum
NE	novel exploration
NEB	nuclear extraction buffer
NELF	negative elongation factor
NeuroD1	neurogenic differentiation 1
NGS	next generation sequencing
NIB	nuclear isolation buffer

NMDA	N-methyl-D-aspartate
NRC	nucleosome remodelling complex
nuRNA	nuclear RNA
PBS	phosphate-buffered saline
PCA	principal component analysis
qPCR	quantitative polymerase chain reaction
RA	reduced accessibilty
REB	riboRNA extraction buffer
RIB	riboRNA isolation buffer
riboRNA	ribosomal bound RNA
RNA	ribonucleic acid
RNAPII	RNA polymerase 2
RPM	read per million mapped reads
Sal	saline
SE	status epilepticus
SNP	single nucleotide polymorphism
SRF	serum response factor
TAD	topological-associated domains
TAM	tamoxiphen
TF	transcription factors
TFBS	TF binding sites
TPL	triptolide
TRAP	translating ribosomal affinity purification
TRE	TPA DNA response element
TSE	translational silencing element

TSS	transcription start site
TTS	transcription termination site

INTRODUCTION

1. Brain plasticity

1.1. The excitatory brain

The mammalian brain is a highly compacted tissue composed by great variety of cell types, creating a homeostatic system that support an interconnected circuitry of cells know as neurons. Although the participation of glial cells (non-neuronal cells) to the brain function is remarkable, the electrical properties of neurons have a direct consequence in animal behavior. Furthermore, the brain has the unique ability to constantly adapt animal behavior to the environment changes. This highly plastic component relies on the ability of neurons to compute and store environment inputs along the network (Herring & Nicoll, 2016), creating novel information. There are evidences, that brain-related functions are acquired through competitive pressure. Thus, the contemporary mammals show a clear correlation between their individual cognitive capabilities and their ability to adapt in a changing environment.

Despite the wide range of neuronal types in the mammalian brain, neurons can be classified by its excitatory or inhibitory contribution into the circuitry. Although both neuronal types are necessary to encode information, It has been shown that excitatory neurons contain the major structural changes required to re-balance network connectivity (Turrigiano, 2012; Wefelmeyer et al., 2016). Those changes will occur at discrete groups of neuronal networks, known as memory engrams, whose activation is required and sufficient for the storage and retrieval of information (Liu et al., 2012). These engrams are distributed along different interconnected brain regions, and each region contributes to compute a kind of information. One of the most studied memory systems in mammals is the one supporting contextual fear memories. These

memories show a clear activation of neurons in two well-known brain regions: the hippocampus, which is related with spatial information; and the amygdala, which is related with positive/negative balance of the events (emotions) driving the freezing response to fear. In addition to their anatomical substrate, memories are generally classified in function of their temporal duration in the network: short-term, long-term and remote memories. Each of the memory categories are related with distinct molecular and network events. For instance, long-term and remote memories, can be retrieved long after the creation of the memory, but the coding patterns varies over time, older memories (remote) tend to be less present at subcortical regions and recruited by neo-cortical ensembles (Hofer et al., 2009). At the molecular level, short-term memories can be encoded without the induction of transcription or translation, which are required for long-term and remote memories, a process known as consolidation or memory formation.

1.2. Network plasticity

Changes in the contained information in neurons are thought to occur through changes in network connectivity. At the cellular level, synaptic contacts are the smallest unit of network plasticity, and the majority of these, are forming small protrusions at dendritic arborizations known as spines. This organization will create a compartmentalization along the dendrite for the independent regulation of events through neuron contacts (Spruston, 2008; Tonnesen & Nagerl, 2016). When changes in the network are needed, these are translated into changes in the morphology of the spine and the electrical properties of the synapse, in order to increase or reduce the contact weight within the network. Those

coordinated events in the remodeling of the network architecture, are developed by a cellular process known as synaptic plasticity, considered the structural basis of learning and memory (Yang et al., 2009; Caroni et al., 2012).

Synaptic plasticity involves a wide number of cellular and molecular events within individual neurons. Briefly, after significant synaptic neurotransmitter release and membrane depolarization, the principal second messenger Calcium, will translocate to the cytoplasm and trigger the activation of different metabolic pathways, such as MAPK, CaMKs, and calcineurin-mediated signaling pathways (Sheng et al., 1991; Xing et al., 1996; Bito et al., 1996; Hardingham et al., 1997). The increase of calcium influx will come from the extracellular matrix through ligand-gated ion channels, like NMDA and AMPA glutamate receptors, voltage-gated calcium channels, and through the release from intracellular calcium stores (West et al., 2001). The intracellular activation of these pathways in response to neuronal signaling, will end up activating the transcription of activity-regulated genes and local changes at synapses, such as the surface expression or internalization of glutamate receptors, local mRNA translation, and post-translational modifications of proteins (Figure 1, Flavell & Greenberg, 2008; Thomas & Huganir, 2004; Martin & Zukin, 2006; Wayman et al., 2008; Holt & Schuman, 2013). All together, we will refer to these processes as neuronal activation.

Neurons require the activation of a transient transcriptional program, because the ability to adapt the neuronal network to the environment requires *de novo* synthesis of RNA and proteins necessary for synapse remodeling. The aim of this mechanism is to induce a temporal destabilization of the synaptic contacts that enables molecular changes that will re-balance the network. In

turn, once the synaptic contacts are re-stabilized, will consolidate a change of the neuron weight in the network. In summary, synapse to nucleus signaling create a strong link between environmental changes and external stimuli, neuronal excitability and transcriptional regulation.

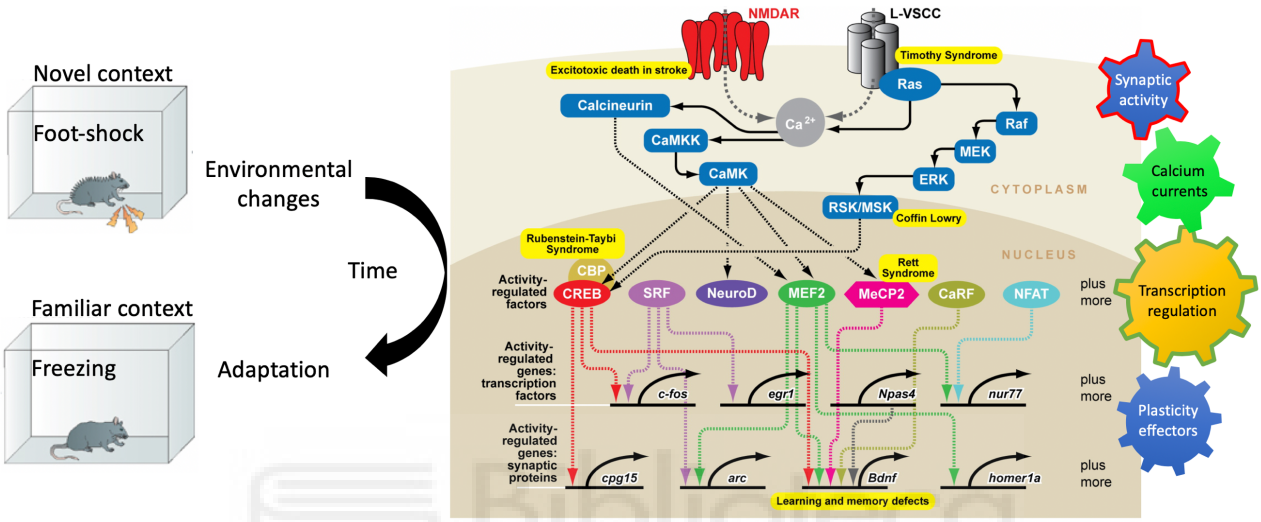

Figure 1. Schema of the signal transduction networks mediating neuronal activity-dependent gene expression, adapted from Flavell & Greenberg, 2008.

2. Activity-driven transcription

2.1. Transcriptional program

The correct regulation of transcription is essential for neuronal activation, because it will drive the transition from short- to long-term forms of neuronal plasticity (Benito & Barco, 2015). The initial wave of transcription induced by synaptic activation is very rapid and transient, induces a group of genes that are not dependent on de novo protein synthesis, known as immediate early genes (IEG). An important number of these IEG encode for proteins that form TF complexes, which once translated, translocate to the nucleus and regulate a

second wave of gene expression known as late response genes (LRG). The majority of these LRGs encodes for effector proteins that participate in neuronal network re-modelling (spine maturation, synapse elimination, dendritic growth, and excitatory/inhibitory balance), rather than in transcription regulation (Sheng & Greenberg, 1990; West & Greenberg, 2011; Mardinly et al., 2016a).

Some of the IEG-encoded TFs known to regulate the expression of LRGs belong to the AP-1, Egr and Nr4a TF-families, as well as the neuronal specific TF Npas4 (Milbrandt, 1988; Christy & Nathans, 1989; Lin et al., 2008). One of the most described neuronal activity gene is Fos, which was the first gene identified as part of the IEG program that respond to the external stimuli in mammals (Greenberg & Ziff, 1984). This gene encodes for an AP1 TF-subunit that will interact with Jun TF-family to create a leucine-zipper heterodimer with a positively charged DNA-binding domain that will selectively interact with the consensus sequence, 5′-TGA(C/G)TCA-3′ (Sheng & Greenberg, 1990). Initially, was though that AP1 would bind within the promoters of the target genes in order to activate its expression (Eferl & Wagner, 2003). Thanks to technological advancements in the field of DNA sequencing, was found that AP1 biding sites were enriched in distal enhancer elements (Malik et al., 2014). Nowadays, it is well stablished that enhancers are distal regulatory sites in the genome that play a major role in the cell type-specific regulation of genes, compared to promoters (Heintzman, et al., 2009; Long et al., 2016). These observations indicate that each cell-type offers a combination of enhancers and TF-biding sequences that specify its function during development and adult. For instance, after external stimuli AP1 complexes bind to different locus repertory between

cell-types (Malik et al., 2014; Vierbuchen et al., 2017), suggesting a differential transcriptional output.

Furthermore, several studies have suggested that varying patterns of neural activity can give rise to unique activity-dependent gene programs (Worley et al., 1993; Dolmetsch et al., 1998; Deisseroth & Tsien, 2001; Belgrad, 2018; Tyssowski et al., 2018). When compared excitatory and inhibitory neurons, the early IEG expression program is very similar and start to be differentiated at the subsequent induced LRGs. Notably, these differences were found with ribosome tagging *in vivo*, which reflects the ongoing translation (Sanz et al., 2009; Mardinly et al., 2016b). Single-cell RNA-seq studies in different brain areas, found the existence of undiscovered cell-types and subtypes (Zeisel et al., 2015). The application of this novel technology in experience-induced transcription paradigms has revealed the levels of activation of neuronal and non-neuronal cells, and the relation between cell-type and cell-state in the brain region of study (Lacar et al., 2016; Hu et al., 2017; Wu et al., 2017; Hrvatin et al., 2018). Cell compartment-specific analysis of transcript presence can be also very informative to explore other mechanism of regulation of gene expression highly relevant in neuronal tissues. For instance, neuronal activation does not only regulate transcription, it also regulates transcript editing, by mechanisms such as intron skipping, and local translation at synapses (Poo et al., 2016; Mauger et al., 2016).

Not only protein coding genes are transcribed during neuronal activation. New sequencing techniques have unveiled novel mechanisms that contribute to the complex transcriptional response to neuronal activation such as the production of different species of non-coding RNAs (ncRNAs). For instance,

enhancer RNAs (eRNAs) that are transcribed at active enhancers and can regulate the expression of the associated mRNA (Kim et al., 2010); circular RNAs (cRNAs) that derivates form coding genes generally generated during alternative splicing (You et al., 2015); and extra-coding RNAs (ecRNAs), which are non-polyadenylated sense-strand RNA encoded by a portion of DNA that surpass the boundaries of the gene (Savell et al., 2016). Despite the number of studies investigating activity-regulated transcripts, there are still outstanding questions about the relationship between the transcriptional program, their regulation and their relevance in *in vivo* during pathology and experience-driven plasticity.

2.2. Epigenetic regulation

By activity-driven transcription we refer to those molecular processes that support the regulated expression of genes necessary to consolidate changes in a cell after being exposed to external stimuli. Ultimately these processes act at the epigenome, a combination of chemical modifications and proteins that interact with the genome and has the ability to integrate signals leading to the regulation of gene expression through changes in chromatin structure.

The epigenetic function is based on the ability of numerous proteins to read and write the genome without alteration of the DNA code, expanding its coding capabilities. The molecular mechanisms underlying epigenetics are not easy to classify or to add boundaries between them because the level of interaction is very dynamic. Generally speaking, proteins and ncRNAs interact directly with the chromatin to regulate the conformation and the transcriptional machinery activity, as well as post-transcriptional mechanism of pre-mRNA

editing. Here, I will classify the chromatin epigenetic changes in five major mechanisms: nucleotide modification, histone posttranslational modification (hPTM), histone variant exchange, nucleosome remodelling and chromatin conformation (Kouzarides, 2007; Figure 2, Aranda et al., 2015). These mechanisms contain complex regulatory layers including proteins and ncRNAs that are relevant in many cellular processes, such as cell differentiation and division, transgenerational passage of the gene-regulation, and integrations of external signals for an adaptive response in post-mitotic cells (Reik, 2007; Goldberg et al., 2007).

During synaptic plasticity, these epigenetic mechanisms play an important role in different stages. If we focus on early neuronal activation, the rapid expression of IEG program is thought to be accomplished with the occupancy of DNA-binding sites by constitutively expressed TFs that respond to second messenger (Ca2+, cAMP). Among these sites, the cAMP response element (CRE), the serum response element (SRE), and the myocyte-specific enhancer factor 2 (MEF2) response element (MRE) that recruit CREB, SRF and MEF2, respectively. The binding sites for these TFs are commonly found in the enhancer or promoter regions of many IEGs induced by neuronal activation, and their activation depends on the ability of these activity-regulated TFs to integrate signals through post-translational changes, such as phosphorylation (Deisseroth et al., 1998; Flavell & Greenberg, 2008; Benito & Barco, 2015). The chromatin state previous to the activation of synaptic plasticity programs is crucial for activation because the access to these sites is strongly influenced by the methylation status of DNA and the presence of hPTMs. In turn, these TFs can modify the epigenome to adapt the next wave of TF encoded by IEGs, such

as *Fos*, *Egr1* and *Npas4*, that will be produced at high levels and regulate the expression of the second wave of neuronal plasticity genes. Numerous questions related with these mechanisms remain unsolved, as it was shown by the recent discovery of the existence of LRGs that are not dependent on *de novo* protein synthesis (Tullai et al., 2017).

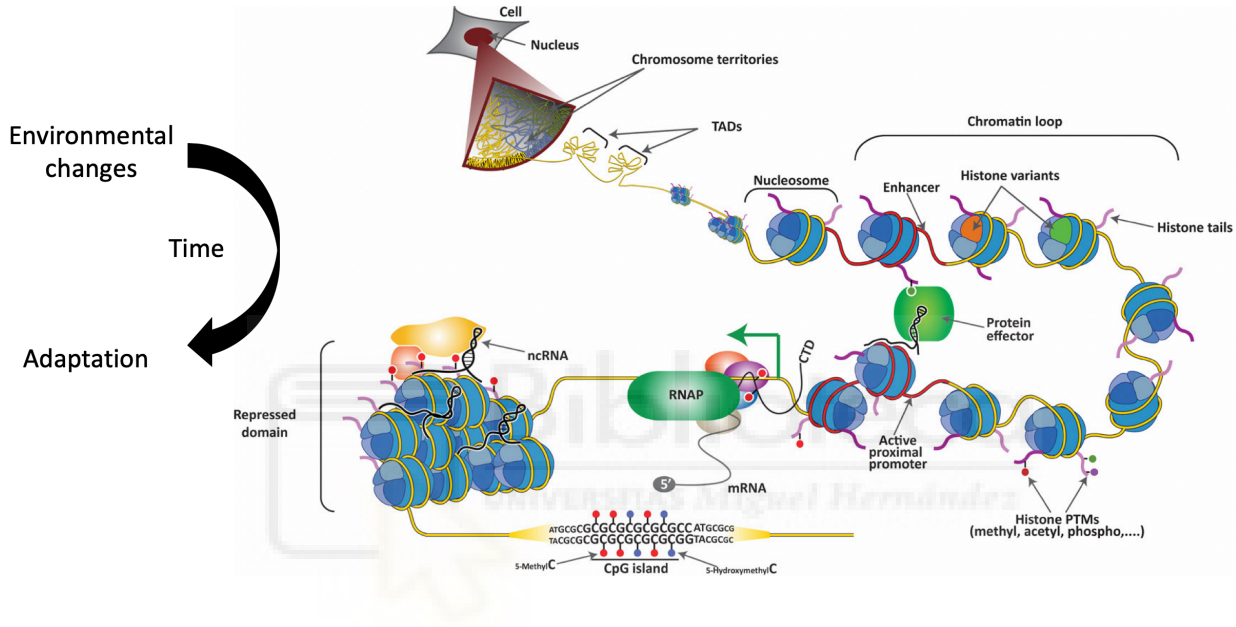

Figure 2. Schema of the Hierarchical layers of chromatin organization in mammalian cells, adapted from Aranda et al., 2015.

2.2.1. DNA modifications

The most studied epigenetic system in mammals is DNA methylation (the presence of 5-methylcytosine, 5mC), initially analyzed on CpG islands (CGIs), which are enriched at promoter regions. Due to the stability of the methyl group on the DNA, 5mC was thought to be less dynamic than other epigenetic marks because it displays clear cell type-specific distribution and its variation is associated with pathology (Jones, 2012). Methylation of the promoter was

initially described as a silencer mark that would recruit CpG binding proteins, such as MeCP2 and other transcription repressor factors. The majority of the CGIs (>80%) are methylated in somatic cells, with the exception of those CGIs found within active regulatory sequences in the cell-type. Often, the promoters are less methylated than the enhancers (Stadler et al., 2011).

Nowadays, it is known that the relationship between DNA methylation and transcription is more complex than outlined above. DNA methylation has positive and negative transcriptional effects at the promoter and the gene body, and can recruit the direct union of transcription factors modulating its binding affinity to the motif (Zhu et al., 2016). There are many evidences of the repressive function of the 5mC at intergenic regions, but the evidence is less clear at intragenic regions where it might show the contrary effect (Jones, 2012). This increased transcription at highly methylated genes seemed to be tissue-specific and interplays with histone modifications during development (see section 2.2.2). Additionally, 5mC presence at the gene bodies, has been related with the regulation of alternative promoters, alternative splicing and spurious transcription (Jones, 2012; Neri et al., 2017; Teissandier & Bourchis, 2017). Notably, the oxidative derivate of 5mC, 5-hydroxymethylcytosine (5hmC), is a less stable epigenetic mark, pinpointing a regulatory function. This methylated derivate is very present in brain tissue, and its presence inhibit the binding of MeCP2, thus, disrupting the repressive function of 5mC (Gabel et al., 2015; Mellén et al., 2017).

In neurons, intragenic 5mC show a negative correlation with transcription activation (Lister et al., 2013). Neuronal activation paradigms, such as contextual fear conditioning, induces the expression of DNA methyltransferases

and DNA de-methylating enzymes (Ma et al., 2009; Sultan et al., 2012; Leach et al., 2012; Gavin et al., 2013; Rudenko et al., 2013), demethylation of memory formation-related genes and methylation of memory-suppressing genes (Miller & Sweatt, 2007; Miller et al., 2010). The maintained activity of the enzymes seems to regulate the temporal expression of the genes (Miller et al., 2010). Also, during memory consolidation, hippocampal neurons induces DNA methylation at regulatory regions located at intergenic and intronic sites (Halder et al., 2016). The relevance of DNMTs in the regulation of synaptic effectors genes, because its inhibition represses LTP induction (Levenson et al., 2006). Interestingly, the expression of IEG like *Fos* and *Egr1* induces de-methylation at the promoter and methylation at the 3' end. The mechanisms that are behind the selection of DNA methylation sites and the relation with the chromatin epigenomic state are still unclear.

2.2.2. Histone modifications

Histones are the protein subunits that interact to form an octameric complex known as nucleosomes, around which 146 bp of DNA is wrapped. There are four families of nucleosome histones: H2A, H2B, H3 and H4. To this we should add histone H1, which acts as a linker between nucleosomes. Numerous modifications occur at the histone tails, Lysine (K), Arginine (R), and Serine (S) residues can be acetylated, methylated, phosphorylated, ubiquitylated, sumoylated, ribosylated and citrullinated (Table1, Chrivia et al., 1993). These changes are expected to alter the affinity of DNA-binding proteins, nucleosome remodelling, chromatin compaction and chromatin interactions. Histone modifications are highly dynamic in active transcriptional regulatory regions,

known as euchromatin, and more stable in inactive and highly compacted genome, known as heterochromatin. These studies give rise to the so called neuronal histone code, hypothesis, which aims to predict the functional output from the epigenomic state.

Table 1. Classes of histone modifications.

CHROM. MODIFICATIONS	RESIDUES	FUNCTIONS
Acetylation	**K**-ac	Transcription, repair, replication, Condensation
Methylation (K)	**K**-me1 **K**-me2 **K**-me3	Transcription, repair
Methylation (R)	**R**-me1 **R**-me2a **R**-me2	Transcription
Phosphorylation	**S**-ph **T**-ph	Transcription, repair, condensation
Ubiquitylation	**K**-ub	Transcription, repair
Sumoylation	**K**-su	Transcription
ADP-ribosylation	**E**-ar	Transcription
Deimination	**R > Cit**	Transcription
Proline Isomerization	**P-cis > P-trans**	Transcription

The interest of several research groups to study histone modifications in neurons, particularly histone acetylation, was influenced by the pioneering work with CREB1 at the Eric Kandel's laboratory. This TF is required for the formation of long-term memories (Yin & Tully, 1996; Silva et al,. 1998). Its activation by serine-133 phosphorylation leads to the recruitment of CBP, a histone acetyltransferase (HAT), to downstream plasticity-related genes.

Nowadays, it is known that HATs are important for the consolidation of memories and brain development in mice (Korzus et al., 2004; Alarcon et al., 2004; Wood et al., 2005; Wood et al., 2006; Chen et al., 2010; Valor et al., 2011; Barrett et al., 2011; Malvaez et al., 2011; Maddox et al., 2013; Lipinski et al., 2019). In turn, histone deacetylases (HDAC) have the opposite effect and function as memory constraints [ref]. HATs and HDACs interact dynamically with each other. Their regulation is often complex and involves several upstream mechanisms, such as phosphorylation, translocation to the nucleus (Lahm et al., 2007) and S-nitrosylation to promote dissociation from chromatin (Gräff et al., 2014). The proteins that bind to acetylated histone tails recruit protein complexes necessary for transcription activation after neuronal activation, such as BRD4 (Korb et al., 2015).

Another important hPTM is lysine methylation. Depending on the degree of histone methylation (me1, me2, me3) and the residue position, the modification is associated with active or repressed transcription (Zhang & Reinberg, 2001; Jenuwein & Allis, 2001). Lysine methylation has been also involved in memory formation and neuronal activation paradigms. For instance, H3K9me2, has been related to transcriptional homeostasis, affecting cell-type specific gene expression and function (Maze et al., 2010; Covington et al., 2011; Anderson et al., 2018). Whereas H3K4me3 is a transcriptionally permissive mark, inhibits the activity of the *de novo* DNA methyltransferase DNMT3A, preventing methylation at CGIs (Guo et al., 2015). However, the interaction between DNMT3B and H3K436me3 increases 5mC at gene bodies of active genes in mESCs, equally, during development intragenic H3K27me3

and 5mC antagonizes polycomb repression (Wu et al., 2010; Baubec et al., 2015).

A direct relationship was found after retrieval of hippocampal dependent memory at the intronic region of the IEG *Npas4*, which shown histone methylation of H3K4me3 and DNA-hydroxy-methylation (5hmC), both appearing to be required for *Npas4* transcription during retrieval (Webb et al., 2017). Neuronal activation increases H3K4me3 correlating with local increases in DNA methylation and reductions in MeCP2 binding (Mellén et al., 2017). The interplay between different histone modifications is highly complex, and can give rise to unexpected output, for instance, when HDACs are inhibited, the increase of H3K9me2 induced by neuronal activation is blocked (Gupta et al., 2010). Furthermore, histone modifications also mark differences between different types of DNA regulatory sequences. For example, the promoters are enriched in H3K4me3 while enhancers show H3K4me1. Notably, also the surrounding levels of DNA methylation are different (Zhou et al., 2011).

2.2.3. Histone variants

The mammalian genome contains multiple copies of each nucleosome histone gene. In addition, there also exist non-allelic and distinct histone isoforms called histone variants. The most studied variants are in the H2A and H3 families, H2AZ and H3.3 respectively, which are replaced by a nucleosome-remodelling complex in an ATP-dependent maner. Each of these variants are involved in different chromatin regulatory mechanisms. H2AZ, is involved in establishing transcriptional competence and nucleosome stability, usually located at the TSS (Weber et al., 2014). H3.3, is involved in nucleosome assembly and is usually

incorporated at transcriptionally active genes (Henikoff & Smith, 2015). This histone variant appears to be the predominant in the H3 family in the adult brain, and its incorporation starts during embryonic development. In neurons, histones seem to be in a continuous turnover (Maze et al., 2015). Both histone variants, H2AZ and H3.3, where shown to be incorporated into the nucleosome during neuronal activation for the regulation of neuronal plasticity and formation of fear memory (Zovkic et al., 2014; Dunn et al., 2017; Stefanelli et al., 2018). The role of the incorporation of histone variants for inducing a new chromatin landscape is not clear, requiring additional studies of their transcriptional effects in memory permanence and reactivation.

2.2.4. Nucleosome remodelling

Chromatin modifiers are known to regulate gene expression by the remodelling of nucleosomes, a crucial mechanism for the activity-induced binding of TFs, but their role during neuronal activation is not well studied. There are four families of nucleosome remodelling complexes (NRCs): BAF, INO80, ISWI and CHD. Their actions can be summarized in the regulation of chromatin compaction, through active sliding, ejecting or restructuring of nucleosomes (Hargreaves & Crabtree, 2011). BAF, is the most studied NRC in neurons, because it is known to interact with the neuronal-activity driven-TF AP1. The ATP-dependent activation of BAF was shown to be required during dendritic and neurite outgrowth induced by neuronal activation (Wu et al., 2007; Vogel-Ciernia et al., 2013; Yoo et al., 2017, Vogel-Ciernia et al., 2017). The published studies in Neurosciences have only investigated the BAF complex, and there is a need to further research in the role of other NRCs during neuronal activation

paradigms. Furthermore, chromatin remodelers are typically large protein complexes in which different combinations of subunits contribute to specify cell type-specific functions. Indeed, neurons have been shown to have their unique combination (Wu et al., 2007).

2.2.5. Chromatin conformation

Histones are protein complexes that pack the DNA in a secondary structure known as chromatin fibers. The different states of chromatin are defined by loose (euchromatin) or dense (heterochromatin) nucleosome packaging, post-translational histone modifications and the presence or absence of transcription regulators. Heterochromatin found at the promoters of actively transcribed genes is characterized by an increased chromatin accessibility, histone acetylation, and nucleosome displacement due to the presence of TF and RNA Polymerase-II Initiation complex. Heterochromatin is enriched in heterochromatin-associated protein 1 (HP1) and repressive histone methylation marks, H3K9me3 and H4K20me3. As we have seen before, these chromatin structures are crucial for sensing the environmental changes and express a transcriptional program to adapt to it. The great number of *cis*-regulatory elements found in the genome, are found principally enriched at intergenic regions, far from promoters. These distal elements, enhancers, will influence the regulation of gene transcription through looping of chromatin generating enhancer-promoter contacts. Thus, how chromatin is spatially organized in the nucleus will drive cell type-specific behavior.

Thanks to the recent combination of chromatin conformation capture (3C) methods with next-generation DNA sequencing many hierarchical

properties of chromosome conformation structures have been described, such as chromatin compartments (Lieberman-Aiden et al., 2009), topologically associating domains (TADs) (Dixon et al., 2012; Nora et al., 2012), sub-TADs (Phillips-Cremins et al., 2013), insulated domains (Dowen et al., 2014) and chromatin loops (Rao et al., 2014). The regions with decondensed chromatin and transcriptionally active genes is often referred to as compartment A, whereas condensed chromatin with transcriptionally silent genes are referred to as compartment B (Rao et al., 2014). Compartments at different chromosomes can interact with compartments at other chromosomes, this higher order of stratification is also in their nuclear position, being silent regions enriched at the nuclear periphery, pericentromeric foci and surrounding nucleolar membranes (Lieberman-Aiden et al., 2009; Padeken & Heun, 2014). Both types of compartments can contain topological-associated domains (TADs), and the loci within come in contact with much more frequency than the loci at other domains (Dekker et al., 2013; Rao et al., 2014). These domains can include lamina-associated domains (LADs), which are condensed chromatin physically contacting with laminin proteins at the nuclear periphery.

Scaffolding proteins are crucial in the regulation of chromosomal conformation, which consists on the regulation of cohesin complex dynamics, CCCTC-binding factor (CTCF) and the accessory proteins. These are usually found at TAD boundaries and chromosomal loops, such as promoter-enhancer interactions. Cohesins form a ring-like structures that entrap distant chromatin fibers into loops, usually highly enriched in active genes in a cell-type specific manner (Nasmyth & Haering, 2009). The cohesin complex is assembled from the CTCF, which it is bound at its DNA binding-sequences at each contact site

of the loop (Rao et al., 2014; Vietri Rudan et al., 2015), creating a loop-bound head-to-head CTCF configuration (Guo et al., 2015). These loops may be required to strongly stimulate transcription because, typically, the preinitiation complex components at the TSS (general TFs and RNA Pol-II) needs to interact with TFs and the mediator complex proteins, such as CBP, that are found at distant enhancers (Vernimmen & Bickmore, 2015). This mediator can load cohesin to the chromatin, promoting the loop formation (Kagey et al., 2010). Again, the interplay between regulatory marks in the epigenome will be crucial for chromatin interactions. For instance, hypermethylation of CTCF binding sites disrupts topological domains and generates ectopic enhancer-promoter interactions (Maurano et al., 2015).

Not many studies of chromatin conformation have interrogated these events during synaptic plasticity. Different models have been proposed to explain how neuronal activity can regulated promoter-enhancer interactions. Recent studies have proposed that neuronal activation of IEG is under the control of enhancer elements that rapidly create the loops in response to stimulation (Bharadwaj et al. 2014; Bharadwaj et al., 2015; Joo et al., 2016). In turn, this process will induce the synthesis of eRNA, which are transcribed in *cis* at active enhancers, and required for the expression of the IEG (Joo et al., 2016). Also, it has been shown that synthesis of eRNA can blocks the negative elongation factor (NELF) at the *Arc* gene (Schaukowitch et al. 2014). Notably, there are many laboratories studying the described participation of lncRNAs in the formation and maintenance of chromatin structures (Keung et al., 2015). A novel event shown to occur during neuronal IEG activation is the formation of DNA strand breaks by topoisomerase, in order to bring together the promoter

and short-range enhancers regions to activate transcription (Madabhushi et al., 2015). This represents a new level of regulation in order to overcome the physical forces that limit small sized loops of chromatin.

2.3. Epigenetics and brain diseases

We have seen that a large volume of scientific literature indicates that activity-dependent transcription is a key part of the neuronal response to synaptic stimulation. As a result, its deregulation is an important feature of many neurological diseases associated with cognitive dysfunction. At the level of DNA modifications, mutations on the methyl-CpG biding domain of the transcriptional repressor MECP2 is linked to Rett syndrome, an autism spectrum disorder (Guy et al., 2011). Co-activators are also implicated in disease, for instance, mutations in CBP are associated with Rubinstein-Taybi syndrome, an intellectual disability accompanied of a facial phenotype (Lopez-Atalaya et al., 2014b). These CBP mutations are correlated with long-term memory deficits and lower histone acetylation levels (Mullins et al., 2016). Mutations on neuronal activated signaling pathways lead to developmental neurological disorders, such as Coffin-Lowry (mutations on ribosomal S6 kinase 2, (Hong et al., 2005)) and Timothy syndrome (mutations on L-VSCC, (Ebert et al., 2013)). Chromatin remodelers also affect neurological disorders, several mutations in NRCs coding genes, including BAF subunits, are associated with Coffin-Siris syndrome and autism spectrum disorders (López & Wood, 2015), demonstrating again the relevance of these protein complexes in cognition (Ronan et al., 2013).

Furthermore, the majority of studies indicate that disease-associated non-coding variants are usually found at cis-regulatory elements and not at protein coding sequences. A recent study revealed that SNPs within AP1 motifs are a common cause of changes in chromatin accessibility in neurons, and suggest to be critical for activity-regulated TFs enhancer selection and LRGs induction (Maurano et al., 2012; Maurano et al., 2015). Moreover, in the context of chromatin conformation, mutations in cohesin subunits genes generate Cornelia de Lange syndrome and demyelination syndromes (Finnsson et al., 2015), and CTCF mutations has been linked to microcephaly (Watson et al., 2014).

All these findings underscore the relevance of characterizing the molecular mechanisms of activity-dependent transcription, in order to understand neurological disorders and network plasticity (Sudhof, 2017). This is the case of epilepsy, a severe neurological condition that has a prevalence of 1% of the population and predisposes the patient to recurrent unprovoked seizures or transient disruption of brain function due to abnormal and uncontrolled neuronal activity, and can lead to brain damage, disability and even death (Urdinguio et al., 2009). The majority of the studies in the mouse model of epilepsy induces a single epileptic seizures or status epilepticus (SE) exposing the mice to the glutamate receptor agonist kainic acid (KA). Several studies showed that the KA-model induces neuronal activation in hippocampal excitatory neurons affecting many synaptic effector genes (Kobow & Blumcke, 2014) after evoking an strong transcriptional response of IEGs (Hevroni et al., 1998; Ben-Ari & Cossart, 2000; Elliott et al., 2003) and rapid changes in chromatin marks and nuclear structure (Sawicka & Seiser, 2012; Huang et al.,

2002; Crosio et al., 2003; Tsankova et al., 2004; Taniura et al., 2006). Despite the efforts in this field, due to technical complexities, it is still lacking a detailed and integrative description of all the events.

3. *Functional Neurogenomics*

An integrated view of the transcriptional and epigenomic changes triggered by neuronal activation *in vivo* is still lacking, partially because of the special challenges derived from brain complexity and cellular heterogeneity. For instance, we do not know whether the molecular processes underlaying neuronal activation, most of which have only been described *in vitro*, also occur in the brain of behaving animals. We also still ignore the mechanisms that sustain the activity-driven transcriptional burst and the nature of the afore predicted genomic memory.

3.1 Next Generation Sequencing

Due to the importance of transcriptional regulation in living organisms, functional genomics is a growing approach in many life sciences fields. A better understanding of the mechanisms of transcriptional regulation within a tissue or cell type is fundamental for inferring molecular functions, and this is also the case for the role of activity-driven transcription in neuronal circuit plasticity. An important trigger of discoveries has been next generation sequencing (NGS) that can generate a large amount of molecular information for the events occurring in a given cell at a time. Great efforts have been made for the creation of new molecular approaches to NGS libraries preparation, resulting in a wide range of tools. An integrative analysis of these tools is the common approach in

functional genomics, as they have different nucleotide resolution and different levels of the system are interrogated (Telese et al., 2013).

A way to classify NGS tools is according to the regulatory level of the chromatin structure interrogated: primary, secondary or tertiary (Figure 3, Risca & Greenleaf, 2015), and within each structure there are different methodologies and resolutions:

- Primary structure: encompasses from 1 nucleotide to a few hundreds nucleotides. There are several techniques that approach this chromatin regulatory layer. Some tools are used to study the single-nucleotide level to usually interrogate sequence variation or nucleotide methylation. Other tools cover from tens to hundreds of nucleotides, because interrogate protein chromatin-binding or histone modifications, such as ChIP-seq. Those tools for analyzing chromatin accessibility, show an intermediate nucleotide range. This is the case for ATAC-seq, this technique uses a transposase to cut the DNA in fragments, and analytically the data can be used to explore several regulatory layers at different nucleotide range, such as footprint of TF-binding (10^1 bp) and nucleosomes position (10^2 bp). There exist also variants of these techniques and the output of data quality, such as ChIP-exo, which aims for a high-resolution of protein DNA-binding sequence for *de novo* motif discovery.
- Secondary structure: refers to local structures formed by nucleosome-nucleosome interactions that range from 10^2 - 10^3 bp resolution. Since there are not NGS technics for interrogating it, it is unknown the relevance of this organizational scale.

- Tertiary structure: encompasses from promoter-enhancer contacts (10^3-10^5 bp) to mega-base (Mb, 10^6 bp) compartments domains. The techniques that approach these regulatory layers base their resolution on the minimal distance between focis to detect a contact. Those that cover thousands of nucleotides usually analyze long-range DNA contacts such as in situ-HiC, which increases its resolution for proximal-contacts by increasing the sequencing depth. Novel variants of 3C techniques are ChIA-PET and Hi-ChIP, which merge HiC and Chip-seq tools to interrogate specific protein-DNA contacts with short-range and long-range interactions by the pulldown of a binding protein that form part of the interaction complex, increasing the resolution of proximal contacts by clearing noisy interaction data in the analysis.

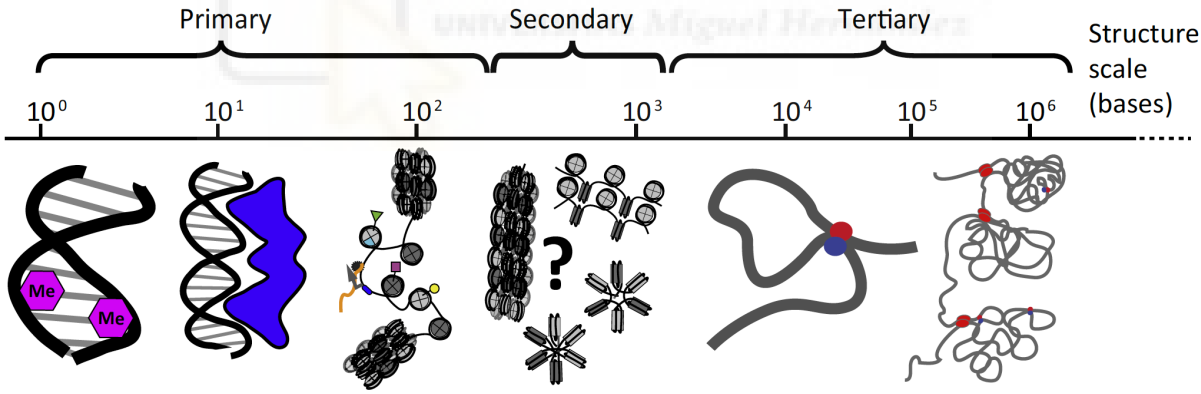

Figure 3. Schema of the Hierarchical structure of chromatin regulatory levels in mammalian cells, adapted from Risca & Greenleaf, 2015.

The conjunctions of all these techniques give to molecular biologists and neuroscientists the ability to obtain a big picture of the genome regulatory processes in cells and tissues. But regulatory genomic processes cannot be

completely understood without the resulting transcriptional output. Transcriptional programs can be approached at many levels, all of them based on RNA-seq, which variates in function of the sequencing strategy: single-end, commonly used for detecting transcript expression; and paired-end, used for detecting transcript variant levels and intron retention. Ongoing transcription can be measured with a conjunctive analysis of RNA-Pol2 and the synthetized transcript with GRO-seq. Ongoing translation can be measured with a conjunctive analysis of transcripts bound to ribosomes with TRAP-seq. And whole transcriptional programs can be covered from the whole cell or by the isolation of cell compartments, such as the nuclear RNA-seq, which will enrich ncRNA and unprocessed RNAs as the events in the nuclei are directly related to transcriptional activity.

3.2 Neuronal activation study approaches

In mammals, these tools have been applied to study activity-driven transcription studies in cellular cultures or brain region of interest. Different methods have been used for inducing neuronal activation, from those that mimic LTP in cellular cultures, to those that induces neuronal activation by exposing the animal to the formation of new memories (Benito and Barco, 2015). The major problems of neuronal cultures are that although neurons can grow and develop synaptic contacts, cells are not in the highly homeostatic brain environment and culture neurons cannot be obtained from adult brains. The major problems of experience-driven neuronal activation are the cellular heterogeneity and the low number of activated neurons. For instance, it has been described that only 5% of the pyramidal excitatory cells from the hippocampus are activated in a

memory spatial task (Liu et al., 2012). Then, although the last gives two levels of complexity, cell-type and activated neurons, are the actual levels to overcome to really describe neuronal activation in its physiological brain function.

Other issues are the methods used to induce neuronal activation. The ones based on drug treatment has been shown to introduce a certain level of variability between studies. Due to the blood brain barrier, the majority of the strategies used in drug-induced neuronal activation *in-vitro* or *ex-vivo* are difficult to replicate *in vivo*, because can only be done by stereotaxic experiments, introducing many uncontrolled variables. On the other hand, the physiologically-induced neuronal activation makes a challenge to catch only activated neurons during the experiment, because only a low number of cells will be activated and the rest of cells will dilute or generate a confounding effect. These facts promote the use of single-cell sequencing in order to describe the distance between cells in function of the transcripts presents in a cell at a certain time. The problem of single-cell sequencing approaches are the limitations in the range of existing methods for functional genomics and the resolution of the data, probably for being a very recent technology.

Overall, to overcome the problem of the number of activated neurons in the hippocampus it has been used drugs such as kainic acid. This drug mimic the epileptic effects with a broad and synchronous activation of excitatory neurons but also from other cell-type such as astrocytes. Still many technical difficulties need to be overcome for the effective application of functional genomics in the adult brain.

3.3 Functional genomics in the adult brain

Traditionally neurons can be differentiated by their anatomic position, morphology, synaptic connection, electrophysiological properties, neurotransmitter identities, and developmental histories. There are a number of studies that suggest the existence of a great, and unknown, diversity of cell types within a tissue, making difficult the studies at the level of genome regulation without the selection of the cell-type. These limitations propelled the increase in the number of studies showing novel approaches for the isolation of the cell-type of interest. In the field of neuroscience, there is an extra issue for those that study the adult brain because of its density and compactivity.

There are two methods that have been frequently used in the past but that have recently lose popularity in functional genomics; these are manual sorting (Sugino et al., 2006) and laser capture microdissection (Emmert-Buck et al., 1996). Both take an important amount of time for isolating a very small number of cells. These methods are useful in the studies of rare population of cells, but the low amount of material obtained can make some epigenetic techniques impossible to apply. Two other methods, currently more popular, are the affinity-based isolation of the cells using antibodies that recognize epitopes expressed in the surface of the cells or in specific structures, and the fluorescence-activated cell sorting (FACS) that will isolate the cells in function of its complexity/size and fluorescence signal.

The compactivity of the adult brain is the major issue for the study of brain genomics and specific methods at the level of tissue disruption and genetic-tagging have been applied to solve this issue. The tissue disruption methods can be classified in those that preserve the membrane integrity and

those that preserve cell compartments. Those that preserve the membrane integrity (Saxena et al., 2012) have two disadvantages. First, because of the compactivity of the tissue is necessary to be treated with enzymes shown to modify transcriptional activity. Second, because the large projections of neurons (axons and dendrites) are lost during tissue disruption. These approaches also have some advantages: Virtually any protein or RNA express in the cell can be used for staining the cells on suspension, and these are the only methods that allow a major picture of what is in the cell cytoplasm. In those methods that aim to preserve cell compartments integrity, can be difficult to understand the events in a process only analyzing a part of the cell, and needs a previous knowledge of the proteins and RNAs contained in the compartment before staining. The pros of the method are that in general only mechanical dissociation is necessary for the isolation of the compartment, and there is a bias in the data towards enriching the functions of a compartment, that may not be appreciated at the whole cell level.

The commented difficulties of information extraction of functional genomics in the adult brain, nowadays promotes the usage of genetic tagging of molecules for the isolation of compartments. This kind of genetic tagging is usually combined with cell type-specific genes or activity-regulated promoters for the isolation of activated neurons in the adult brain. There are several examples of these strategies that are useful in function of the question that needs to be solved: those that aim to isolate RNA and those that aim to isolate DNA. The RNA molecule is primarily found in the cytoplasm and in the nucleus. In the cytoplasm, mature RNAs can be silent or undergoing translation. This is the reason why bulk RNA extraction cannot differentiate between translated and

silent transcripts. The TRAP system was designed to overcome this problem by tagging ribosomes with GFP to isolate the RNA bound to the ribosomes by immunoprecipitation and to assess active translation in the cell (Heiman et al., 2014). Other techniques, such as synaptosome preparation, can be used to isolate RNAs from other cell compartments, like the synaptic buttons, to identify the RNA molecules stored close to the synaptic terminals and available for activity-driven local translation. A novel technique that aim to facilitate the isolation of chromatin from specific cell types uses the expression of chimeric fluorescent nuclear envelope proteins under the control of cell type-specific promoters for pulling-down the tagged nuclei with a method known as INTACT (Mo et al., 2015). All these approaches will help to understand many regulatory events involved in neuronal plasticity and to study transcription and translation regulation in these highly compartmentalized cells.

In the context of this thesis, I introduced new methods to efficiently profile the transcriptome and epigenome of defined neuronal populations in the adult brain. Using these methods, I was be able to generate high-resolution, multi-dimensional and cell-type-specific draft of transcriptional and chromatin alterations associated with neuronal activation in vivo, both under physiological and pathological conditions. Genome-wide screens and analyses provide mechanistic insight into both the rapid changes in gene expression that are initiated after neuronal activity and the more enduring changes that may underlie processes such as epilepsy and memory formation.

OBJECTIVES

This thesis aims to describe the genomic events that underlie neural activity dynamics in the adult mice brain *in vivo*. I will introduce different techniques to uncover several levels of transcriptional regulation in excitatory neurons and use bioinformatical and data science tools to integrate the different levels of information. The specific objectives are:

1. To generate novel mouse models for the isolation of compartment-specific (polysomes and nucleus) and cell type-specific transcripts from excitatory neurons in the adult brain.
2. To develop novel methods for flow-cytometry isolation of neuronal nuclei based on the expression of heterologous fluorescent proteins or antibody tagging of nuclear antigens. Develop the sample preparation compatible with a broad range of next generation sequencing technologies, including RNA-seq, ATAC-seq, ChIP-seq and HiC.
3. To investigate the changes in transcript levels induced during status epilepticus in hippocampal excitatory neurons.
4. To apply ATAC-seq at the isolated cell-nuclei for the study of activity-driven transcription during status epilepticus and memory formation in restricted neuronal ensembles.
5. To develop an integrative multi-omic analysis pipeline for the description of genomic events during neuronal activation.
6. To re-analyse NGS data of previous studies investigating activity-driven transcriptome and epigenome changes in order to expand the description of the genomic events unveiled in my analyses.

MATERIALS AND METHODS

Animals and treatments

The generation of CaMKIIα-creERT2 (Erdmann et al., 2007; from the European Mouse Mutant Archive *EMMA* strain 02125), the cre-dependent riboTRAP (Stanley et al., 2013; Jackson labs, stock #030305) and Sun-1 tagged mice (Mo et al., 2015; Jackson labs, stock #021039) have been previously described. Mice were maintained and bred under standard conditions, consistent with Spanish and European regulations and approved by the Institutional Animal Care and Use Committee. All strains where maintained in a pure C57BL/6J background. Experiments were conducted in 3-6 months old male animals. Mice received intragastric administration of tamoxifen as described in (Fiorenza et al., 2016) when they were ~2 month-old, and we wait 3-4 weeks before experimentation. For the induction of SE by KA (Milestone PharmTech USA Inc.), a concentration of 25 mg/kg was injected intraperitoneally. For the blocking of transcription by TPL (Triptolide from *Tripterygium wilfordii*, Abcam ab120720) a concentration of 0.8 mg/kg was injected intraperitoneally per mice 2 h before the injection of KA or Saline.

Behavioral tasks

For novelty exposure (NE), individually housed mice received 3-4 days of 5 min handling before exposing them to a novel environment. The arena consisted in a white acrylic box of 48 x 48 x 30 cm containing objects with different forms and colors. A total of six mice were individually placed during 60 min before microdissection of the hippocampus and FANS. The novel object location memory test followed the protocol of Vogel-Ciernia et al., 2013. Briefly, one week after saline or KA administration, a total of 8-9 mice per condition were individually habituated to an empty arena (2 exposures of 5 min in consecutive

days). For training, the same mice were placed for 10 min in the arena with two identical objects 24h after the last habituation session. For location memory testing 24 h after training, one of the two objects was moved to a new location. The time spent exploring each object was quantified and a Differential Index (DI = time exploring the displaced object – time exploring the non-displaced object / total time exploring both objects) was calculated.

Immunohistochemistry and microscopy

Mice were anesthetized with intraperitoneal injection of ketamine/xylazine, perfused with 4% paraformaldehyde in PBS and extracted brains were postfixed O/N at 4ºC. Coronal or sagittal vibratome 40 µm sections were obtained, washed in PBS and PBS−0.1% Triton X-100 (PBT). Sections were incubated 30 min with blocking buffer 5% newborn calf serum (NCS, Sigma N4762) – PBT, and incubated O/N at 4ºC with the primary antibodies diluted in 5% NCS-PBT. The primary antibodies used in this study are α-NeuN (1:2000, Chemicon MAB377), α-GAD67 (1:800, Millipore MAB5406), α-Fos (1:500, Synaptic Systems 226004) and α-GFP (1:1000, Aves Labs GFP-1020). After primary antibody incubation and washing with PBS, sections were incubated with a-Guinea Pig IgG (H+L) Alexa 594 (1:400, Invitrogen #A-11075) for fluorescent labeling. Nuclei were counterstained with a 1 nM DAPI solution (Invitrogen) before mounting with Fluoromount (Sigma). Images were taken using Olympus confocal inverted microscope and processed using ImageJ.

Ribosomal-RNA immunoprecipitation sequencing

TRAP immunoprecipitation followed the original protocol described in Heiman et al., 2014 with small changes in the extraction step. Hippocampi were micro-dissected after cervical dislocation, washed in PBS and submerged into

ribosomal extraction buffer (REB-LOW: 150 mM KCl, 10 mM $MgCl_2$, 20 mM Hepes-KOH (pH 7.8), 1% IGEPAL CA-630, 0.5 mM β-mercaptoethanol, 1x proteinase inhibitors (cOmplete EDTA-free, Roche), 60 U/ml RNasin Plus RNasa (Promega N2611), 100 ug/ml cycloheximide). Tissue was homogenized (25 times with pestle A and B) using a Dounce homogenizer (K8853000002, Kontes-DWK). A total of six hippocampi were pooled together and nuclear supernatant was obtained by centrifugation at 2000xg 4ºC for 10 min. Next steps followed the original protocol.

Fluorescent Activated Nuclei Sorting (FANS)

Novel protocol was designed for the maximum efficiency and specificity, a total of 1M nuclei/mice. Hippocampi were microdisected after cervical dislocation, rapidly washed in PBS and extracted with the dounce homogenizer (Sigma) with 1ml of Nuclear extraction buffer (NEB: 250 mM sucrose, 25 mM KCl, 5 mM $MgCl_2$, 20 mM Hepes-KOH (pH 7.8), 0.5% IGEPAL CA-630, 65 mM β-gycerol, 1mM β-mercaptoethanol, 1x proteinase inhibitors (Roche, cOmplete EDTA-free), 0.2 mM spermine, 0.5 mM spermidine, 60 U/ml RNasin Plus RNasa (Promega N2611), 5% NCS). Tissue was disrupted 15 times with pestle A and B, as described above. In case of nuclei fixation, formaldehyde was added in a final concentration of 1% after extraction, incubated at room temperature in rotation for 10', and blocked in rotation with 1,25 mM gycline. Hippocampi from 3 (SE experiments) to 6 (NE experiment) mice were pooled during filtration in a 35 um mesh capped tube. In case of nuclear staining the nuclei pool was split in two tubes of 750 ul total NEB and were stained during 30 min with the primary antibody α-Fos-Alexa647 (1:40, sc-52 AF647) or α-NeuN (1:100, Chemicon MAB377) at 4ºC in rotation. In case of α-NeuN, the secondary antibody Alexa

Fluor-conjugated IgG (1:1000, Life Technologies) was incubated during 15' more at 4ºC in rotation. Nuclei were stained 10 min with DAPI at a final concentration of 0.01 mM. After incubation, the nuclei preparation was diluted in Optiprep (O) density gradient medium (60% iodixianol, Sigma D1556) up to a concentration of 22%. A density gradient was prepared in 13 ml ultracentrifugue tube containing at the bottom a layer of O-44% and an upper layer of O-22% with the nuclear extraction. The tube was centrifuged at 7,500 rpm for 23 min at 4ºC and nuclear fraction was collected and transferred into a tube with the same volume of nuclear isolation buffer (NIB: 340 mM sucrose, 25 mM KCl, 5 mM $MgCl_2$, 20mM Hepes-KOH (pH 7.8), 65 mM β-glycerol, 1x proteinase inhibitors (cOmplete EDTA-free, Roche), 0.2 mM spermine, 0.5 mM spermidine, 60 U/ml RNasin Plus RNasa (Promega N2611), 5% NCS). Nuclei populations were selected with FACS Aria III (BD Biosciences), selecting DAPI staining, singlet nuclei, Sun1-GFP positive, and sorted into a tube with NIB. Flow cytometry data was analyzed and plot in *Flowjo* v10.

RT-qPCR and RNA library construction

Bulk RNA extraction from dissected hippocampi was done with TRI reagent (Sigma-Aldrich). For TRAPped RNA, after O/N incubation, beads were washed 3-4 times in ribosomal extraction buffer (RIB-HIGH: 350 mM KCl, 10 mM $MgCl_2$, 20 mM Hepes-KOH (pH 7.8), 1% IGEPAL CA-630, 0.5 mM β-mercaptoethanol) and re-suspended in 350 ul of RLT for purification with RNeasy Micro kit (Qiagen 74004). For nuclear RNA, after FANS, 2 millions nuclei were pelleted at 4ºC 1,000 g for 7 min and re-suspended in RLT for purification with RNeasy Micro kit (Qiagen 74004). qPCR was performed in Applied Biosystems 7300 real-time PCR unit. RNA samples were reverse transcribed using RevertAid

First-Strand cDNA syntesis kit (Fermentas) and quantified using Eva Green qPCR reagent mix. Samples were assayed in duplicates and the results were normalized to *Gapdh* transcript levels. The sequences of the primers used in RT-qPCR assays are:

Fos Fw	5´-GCTTCCCAGAGGAGATGTCTGT
Fos Rv	5´-GCAGACCTCCAGTCAAATCCA
Npas4 Fw	5´-CTGGCCCAAGCTTCTTCTCA
Npas4 Rv	5´-TCCATGCTTGGCTTGAAGTCT
Arc Fw	5´-GCAGGAGAACTGCCTGAACAG
Arc Rv	5´-AAGACTGATATTGCTGAGCCTCAA
Plp1 Fw	5'-CTTTGGCGACTACAAGACCAC
Plp1 Rv	5'-ACAGTCAGGGCATAGGTGATG
Gfap Fw	5´-GGACAACTTTGCACAGGACCTC
Gfap Rv	5´-TCCAAATCCACACGAGCCA
Bdnf Fw	5´-GAAGGTTCGGCCCAACGA
Bdnf Rv	5´-CCAGCAGAAAGAGTAGAGGAGGC
Gapdh Fw	5’-CATGGACTGTGGTCATGAGCC
Gapdh Rv	5’-CTTCACCACCATGGAGAAGGC

RNA-seq, library preparation and sequencing were performed at facilities in the Center for Genomic Regulation (CRG, Barcelona, Spain). Truseq libraries were prepared from ribo-depleted total RNA in the case of nuRNA-seq and from polyA-selected mRNA in the case of riboRNA-seq. Samples were sequenced (single-end, 50 bp length) using a Illumina HiSeq2500 apparatus with a depth of at least 80M reads in nuRNA and 30M reads in riboRNA (**Supp. Table 8a**).

ATAC assay and library construction

After FANS 50K nuclei were pelleted at 4ºC 1,000 g for 7 min, re-suspended in 50 ul of transposition reaction (Illumina FC-121-1030) and gently pipette to resuspend the nuclei. The assay of transposase-accessibility chromatin coupled to massive sequencing (ATAC-seq) experiments were conducted as the original protocol (Buenrostro et al., 2013). Briefly, nuclei were incubated with tn5 during 30 min at 37ºC, and immediately purified with MinElute PCR purification kit (Qiagen 28004). In order to reduce PCR induced biases during library preparation, after the first 5 PCR cycles, 10% of the sample was monitored with SYBR-green qPCR for 20 cycles to calculate the 25% of saturation per sample (any sample needed more than 12 PCR cycles in total). Libraries were purified with MinElute PCR purification kit (Qiagen 28004). ATAC-assay was performed in an Applied Biosystems 7300 real-time PCR unit using Eva Green qPCR reagent mix. Samples were assayed in duplicates and results were normalized to *Gapdh* promoter insertion levels. The sequences of the primer pairs used in ATAC-qPCR assays are:

Heterochromatin Fw	5´-CTACCGAGTGTTGATTGCCGT
Heterochromatin Rv	5´-TGATGCAAGTGTCAAGCTCAATG
Fos-promoter Fw	5´-GCAGTCGCGGTTGGAGTAGT
Fos-promoter Rv	5´-CGCCCAGTGACGTAGGAAGT
Gfap-promoter Fw	5´-TACCAGAAAGGGGGTTCCTT
Gfap-promoter Rv	5´-AACTCCTCTCACCCCACTGA
Gapdh-promoter Fw	5’-TTCACCTGGCACTGCACAA
Gapdh-promoter Rv	5’-CCACCATCCGGGTTCCTATAA

For ATAC-seq, sequencing (paired-end, 50bp length) was performed at the CRG facilities (Barcelona, Spain) using a Illumina HiSeq2500 apparatus and a depth of at least 100M reads per sample (**Supp. Table S8a**).

ChIP- assay and ChIP library construction

For Bulk ChIP the whole hippocampi from two mice were microdissected and pooled together. For sorted ChIP after FANS, 2 millions nuclei were pelleted at 4ºC 2,000 g for 7 min and re-suspended in SDS-lysis buffer or RIPA-PBS buffer. ChIP was conducted as previously described (Lopez-Atalaya et al., 2013) using the anti-H3K4me3 (Millipore 07-473), anti-H3K27ac (Abcam ab4729), anti-CBP (sc583x) and anti-RNAPII (sc901x). ChIP-assay was performed in an Applied Biosystems 7300 real-time PCR unit using Eva Green qPCR reagent mix. Samples were assayed in duplicates and results were normalized to input. The sequences of the primer pairs used in ChIP-qPCR assays are:

Camk2a-promoter Fw	5´-GAGTCCTAGAGAGCATGGGG
Camk2a-promoter Rv	5´-TGCATACACAGTGCTTCCAAA
Heterochromatin Fw	5´-CTACCGAGTGTTGATTGCCGT
Heterochromatin Rv	5´-TGATGCAAGTGTCAAGCTCAATG

For ChIP-seq, library preparation and sequencing (single-end, 50bp length) were performed at the CRG facilities (Barcelona, Spain) in a Illumina Hi2500Seq apparatus with a depth of 40M reads per sample (**Supp. Table 8a**).

In situ Hi-C library construction

After FANS 2M nuclei were pelleted at 4ºC 2,000 g for 10 min. The nuclei were resuspended in ice-cold HiC lysis buffer and the original in situ Hi-C protocol by

Rao et al., 2014 was followed. Libraries were prepared with TruSeq and sequenced (paired-end 50bp) with Illumina NovaSeq apparatus at the Hudson Alpha sequencing facility (Alabama, AL, USA) with a depth of 1B reads per sample (**Supp. Table 8a**).

Genomic data processing and access

All sequenced datasets adapters were trimmed using *cutadapt* v1.18 (Martin, 2011) and aligned to mm10. Only reads with mapq > 30 and mapping to nuclear chromosomes were used for the posterior analysis. Data was processed with the extensive use of custom scripts and Samtools v1.9 (Li et al., 2009), bedtools v2.26.0 (Quinlan and Hall, 2010) and DeepTools v3.1.0 (Ramirez et al., 2016). Whole genome alignments were normalized to RPM (read per million sequenced reads) and visualized using IGV v2.3.92 (Thorvaldsdottir et al., 2013). The datasets generated in this study are listed in **Supp. Table 8a** and can be accessed at the GEO repository using the accession number GSE125068. The previously generated datasets deposited in public servers used in specific analyses are listed in **Supp. Table 8b**.

RNA-seq data: Reads were aligned with HISAT2 v2.1.0 (Kim et al., 2015). For a clear comparison between riboRNA and nuRNA datasets, reads were annotated to exons from Ensemble (GRCm38.89) and quantified using Rsubreads v1.26 (Liao et al., 2014). Differential expression analysis was performed in DESeq2 v1.10.0 (Love et al., 2014) counting for batch and treatment effect. Genes with FDR<0.1 and log2FC > +/-1 were considered significantly changed. Transcriptome analyses used the datasets GSE74971 (Halder et al., 2016) and GSE77067 (Lacar et al., 2016) applying the same cut-offs used in our study. Comparison of principal neurons (this study) to cortical

neurons and embryonic stem cells from GSE96107 (Bonev et al., 2017) was done using FPKM values from each dataset. GO terms where analyzed using PANTHER v14 with Fisher's Exact with FDR multiple test correction, cut-off was done by the number of genes associated to category (< 2,000 genes), the number of DEG associated to the category (> 3 genes) and fold enrichment > 3 (p-value < 0.05). Over-Representation Enrichment Analysis (ORA) was performed with WebGestalt, and the use of the DisGeNET human database (Bauer-Mehren et al., 2010; Queralt-Rosinach et al., 2016).

ATAC-seq data: Reads were aligned with bowtie2 v2.2.6 (Langmead, B. & Salzberg et al., 2012). Duplicated reads were removed with Picardtools v2.17 and only paired reads were used for the posterior analysis (the KA-6h biological replicate 1 had to be down-sampled). The same pipeline was applied to ATAC-seq datasets from (GSE63137; Mo et al., 2015) and (GSE82015; Su et al., 2017). Peak calling was done with MACS2 (Zhang et al., 2008) in the merged samples that were going to be compared for Differential Accessible Regions (DARs), quantified using Rsubreads on called peaks with FDR < 1e-5. For Differential Accessible Genes (DAGs) reads were annotated to the whole gene region from Ensembl (GRCm38.89), quantified using Rsubreads v1.26. DARs and DAGs analysis was performed using DESeq2 v1.10.0 counting for batch and treatment effect. Regions or Genes with FDR < 0.1 and log2FC > +/-1 were considered significantly changed. The analysis of changes in TPL and NE experiments, were performed in the DESeq2 including in the experiment design the comparisons with KA-1h and Saline respectively that support the reduced n for the rlog calculation and value transformations. Unfortunately, due to the broad increase of accessibility at the gene bodies, we could not subtract

polymerase driven transcriptional events from putative enhancers located at introns; the enhancer regions considered in this study were those positioned a more than 1 Kb from the TSS (upstream) or TTS (downstream) of annotated Ensembl genes (GRCm38.89). GO terms enrichment for DAGs were analyzed using PANTHER with Fisher's Exact with FDR multiple test correction, cut off was done by the number of genes associated to category (< 2000 genes), the number of DEG associated to the category (> 3 genes) and fold enrichment > 3 (p-value < 0.05). Disease ontology from genes associated to DARs was done with GREAT v3.0 (McLean et al., 2010) using standard parameters. Promoter and enhancers regions were clustered with unsupervised method (k-means with linear normalization method) using seqMiner v1.3.4 (Ye et al., 2011). The *phastCons* score was obtained from the multiple alignments of 59 vertebrate genomes (60way Placental) to the mouse genome mm10 (Siepel et al., 2005; Pollard et al., 2010). Motif analysis was done at the promoter and enhancer sites with HOMER v4.8 using validated database from ChIP-seq experiments. Motifs were classified by families (i.e. TRE motif is recognized by a number of proteins that form the AP1 complex) and by the detection of the related protein coding genes in our nuRNA-seq datasets. Predictive analysis of DARs and expression changes was done using BETA v1.0.7 basic activating/repressive function prediction with the Ensembl reference (GRCm38.89) and DEG from our nuRNA-seq datasets. Nucleosome occupancy information was retrieved with the *NucleoATAC* algorithm v0.3.4 (Schep et al., 2015); the shifting analysis was conducted using custom R scripts 500 bp around the TSS. Digital footprint was done in DARs promoters/enhancers using the adapted *Wellington* algorithm for tn5 (Piper et al., 2013). ATAC-seq datasets from KA-1h were used to detect the

footprints during SE (FDR < 0.01) and in the longitudinal analysis (p-value < 1e-10).

ChIP-seq data: Reads were aligned with bowtie2 v2.2.6. Chip-seq meta-analyses used data generated by (Kim et al., 2010; Malik et al., 2014; Halder et al., 2016; Scandaglia et al., 2017); in some cases the positions had to be trans-mapped to mm10. Peak calling was done with MACS2 v2.1.1 with default parameters.

HiC data: Hi-C datasets were processed using the Juicer pipeline (Durand et al., 2016) to align reads to the mm10 genome, filter duplicates, perform matrix normalizations, and obtain the eigenvector. Reads with a mapping quality >= 30 and binned at 25 Kb were used in all downstream analyses. Distance normalization was done using the formula $\frac{(observed-expected)}{(expected+1)}$. Significant enhancer -promoter interactions were called using Fit-Hi-C v1.1.3 (Ay et al., 2014) separately for each dataset with an FDR of 0.05. Fit-Hi-C interactions were compared across samples using the distance normalized signal. Intragenic interactions were visualized across genes with high and low nucRNA-seq signal categorized by the top and bottom quartiles respectively. High intensity interactions known as CTCF loops were identified via HiCCUPS v1.7.6 (rao et al., 2014) in each dataset and differential loops were searched for by selecting for 2-fold changes in interaction signal in a combined total list of loops. To examine the most dramatically changed loops in the published Hi-C data for *in vitro* differentiated cortical neurons (CN) and embryonic stem cells (ES) (GSE96107; Bonev et al., 2017), we searched for 4-fold changes and then plotted the average distance normalized Hi-C signal in each dataset. One-dimensional interaction plots were derived by isolating all Hi-C interaction signal

with each specified anchor. Because *Nptx2* lied at the border of two 25 Kb bins, the average interaction signal across both bins was used.

Statistical analyses

Set of mice with the same age and sex were raised in the same conditions and randomly allocated to the different experimental groups. Blinding was not applied in the study because animals need to be controlled by treatment conditions. No statistical methods were used to pre-determine sample sizes but our sample sizes are similar to those reported in similar publications (Mo et al., 2015). In addition, sample size was estimated according to data variance and correlation between biological replicates and the distance to control condition. No data was excluded from the analyses. All statistical analyses were two-tailed. For pairwise comparison of averages, data were tested for normality using Shapiro's test. If any of the two samples were significantly non-normal, a non-parametric Mann-Whitney U/Wilcoxon rank-sum test was executed instead. When variances between groups were the same, a 2-way ANOVA was applied in the riboRNA-qPCR experiments. For multiple comparisons Kruskal-Wallis test was applied and Dunn test when the number of observations were unequal between groups. Bonferroni-corrected pairwise tests were used where appropriate post-hoc to correct for multiple comparisons. P values were considered to be significant when $\alpha < 0.05$. Assuming the linear relation of the data, correlation was used. Bar plots and cumulative plots centered regions indicate the mean ± s.e.m, unless otherwise indicated. Heat maps show Euclidean clusters. For one-dimensional interaction plots, changes in interactions were significant if above the 99.9% confidence interval derived from all the fold changes in the plot.

For data availability see inventory of Supplementary tables in page 125.

RESULTS

Author contributions: I performed most of the experiments and bioinformatical analyses. M.L. collaborated in the characterization of the models and performed ChIP-seq experiments. M.T.L-C. collaborated in bioinformatical analyses and figures preparation. M.J.R. conducted Hi-C analyses. A.M-G. collaborated in the preparation of Hi-C samples and performed some immunostaining analyses. B.dB. provided important reagents. V.G.C. supervised the Hi-C experiment and analyses. A.B. supervised all other aspects of the project. Together with my thesis director, I conceived the study, designed the experiment and wrote the original draft of the article.

Title: Immediate and deferred epigenomic signatures of in vivo neuronal activation in mouse hippocampus

Author list: [1]Jordi Fernandez-Albert, [1,#]Michal Lipinski, [1,#]María T. Lopez-Cascales, [2,#]M. Jordan Rowley, [1,3]Ana M. Martin-Gonzalez, [1]Beatriz del Blanco, [2]Victor G. Corces, and [1,4]Angel Barco

Author affiliations:

[1] Instituto de Neurociencias (Universidad Miguel Hernández-Consejo Superior de Investigaciones Científicas), Sant Joan d'Alacant, Alicante, Spain.

[2] Department of Biology, Emory University, Atlanta, GA, USA.

[3] Nencki Institute of Experimental Biology PAS, 02-093, Warsaw, Poland.

[#]Equal contribution

[4] Corresponding author: Angel Barco, Instituto de Neurociencias (Universidad Miguel Hernández – Consejo Superior de Investigaciones Científicas), Av Santiago Ramón y Cajal s/n, Sant Joan d'Alacant 03550, Alicante, Spain. Tel: +34 965 919232. Email: abarco@umh.es

DOI: 10.1038/s41593-019-0476-2

Abstract

Activity-driven transcription plays an important role in many brain processes, including those underlying memory and epilepsy. Here, we combine genetic tagging of nuclei and ribosomes with RNA-seq, ChIP-seq, ATAC-seq and Hi-C to investigate transcriptional and chromatin changes occurring in mouse hippocampal excitatory neurons at different timepoints after synchronous activation during seizure and sparse activation by novel context exploration. The transcriptional burst is associated with an increase in chromatin accessibility of activity-regulated genes and enhancers, *de novo* binding of activity-regulated transcription factors, augmented promoter-enhancer interactions, and the formation of gene loops that bring together the TSS and TTS of induced genes and may sustain the fast re-loading of RNAPII complexes. Some chromatin occupancy changes and interactions, particularly those driven by AP1, remain long after neuronal activation and could underlie the changes in neuronal responsiveness and circuit connectivity observed in these neuroplasticity paradigms, perhaps thereby contributing to metaplasticity in the adult brain.

Introduction

Activity-dependent transcription is a key part of the neuronal response to synaptic stimulation and is essential for the transition from short- to long-term forms of neuronal plasticity [1, 2]. As a result, its deregulation is an important feature of many neurological diseases associated with cognitive dysfunction [3]. This is the case for epilepsy, a severe neurological condition that predisposes the patient to recurrent unprovoked seizures or transient disruption of brain function due to abnormal and uncontrolled neuronal activity, and can lead to brain damage, disability and even death. Beyond this pathological setting, activity-dependent transcription is also thought to contribute to the changes in circuit connectivity and neuronal responsiveness that are necessary for memory formation [1, 4]. Thus, it has been hypothesized that the formation of long-term memory, which requires the activation of tightly regulated transcriptional programs during learning, relies not only on synaptic changes but also on modifications in the chromatin of activated neurons [5, 6]. These epigenetic changes may contribute to long-lasting or permanent changes in the expression and responsiveness of genes involved in synaptic function, thereby representing a sort of genomic memory.

New sequencing techniques have unveiled novel processes that contribute to the complex transcriptional response to neuronal activation, such as activity-regulated intron skipping, double-strand breaks, and the production of different species of non-coding RNAs (ncRNAs), including enhancer (eRNAs) and extracoding RNAs (ecRNAs) [7-13]. Despite this progress, an integrated view of the transcriptional and epigenomic changes triggered by neuronal activation *in vivo* is still lacking, partially because of the special challenges derived from

brain complexity and cellular heterogeneity [1]. For instance, we do not know whether the processes mentioned above, most of which have only been described *in vitro,* also occur in the brain of behaving animals. We also still poorly understand the mechanisms that sustain the activity-driven transcriptional burst and the nature of the afore predicted genomic memory.

Here, we introduce methods to efficiently profile the transcriptome and epigenome of defined neuronal populations in the adult brain. Using these methods we were able to generate the first high-resolution, multi-dimensional and cell-type-specific draft of transcriptional and chromatin alterations associated with neuronal activation *in vivo*, both under physiological (novel context exploration) and pathological (status epilepticus). Our genome-wide screens and analyses provide molecular insight into both the rapid changes in gene expression that are initiated after neuronal activity and the more enduring changes that may underlie processes such as epilepsy and memory formation.

Results

Nuclear tagging enables neuronal-specific genomic screens and reveals broad changes to the nuclear transcriptome upon status epilepticus

To investigate the transcriptional and chromatin changes specifically occurring in forebrain principal neurons upon activation, we produced mice in which the nuclear envelope of these neurons is fluorescently tagged [14] (**Fig. 1a-b**). This genetic strategy combined with fluorescence activated nuclear sorting (FANS) allowed us to isolate this neuronal nuclei type from adult brain tissue (**Supp. Fig. 1a-c**). After FANS, sorted nuclei can be used in different applications, from nuclear RNA (nuRNA) quantification (**Supp. Fig. 1d**) to chromatin

immunoprecipitation (ChIP) (**Supp. Fig. 1e**) and enzymatic treatments like the assay for transposase-accessible chromatin (ATAC) (**Supp. Fig. 1f**). FANS represents a substantial improvement over cell sorting because it prevents the stress response triggered by neuronal dissociation that can occlude activity-induced changes. Moreover, since our method does not require the use of antibodies against GFP, it can be combined with immunolabeling for secondary sorting to increase the specificity of the cellular population under investigation.

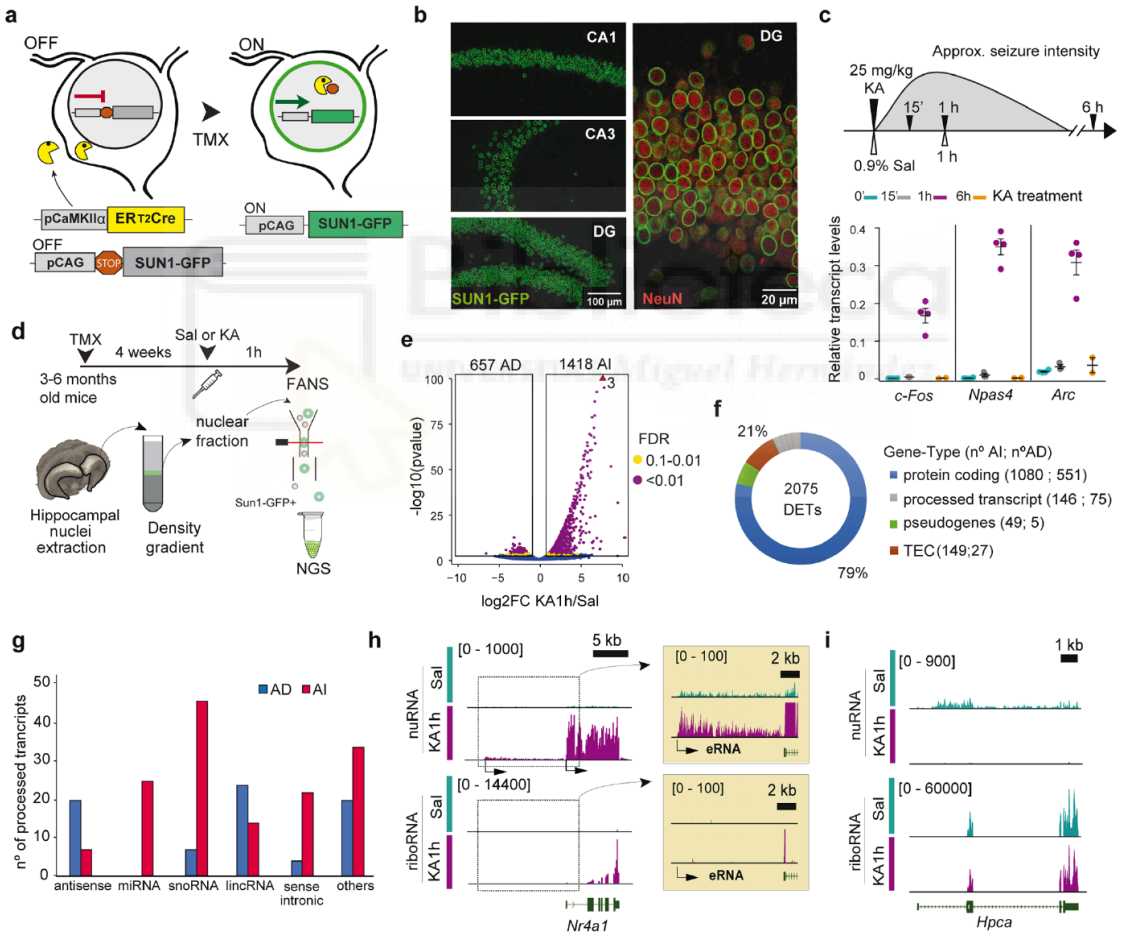

Figure 1. SE triggers broad changes of the nuclear transcriptome. a. Crossing of the TMX-inducible Cre-driver line CaMKII-creERT2 with mice that express SUN1-GFP in a Cre-recombination-dependent manner allows the tagging of the nuclear envelope in forebrain principal neurons for subsequent FANS-based isolation. **b.** Confocal images of principal hippocampal neurons in the CA1, CA3 and DG subfields stained against GFP (green) and the

neuronal marker NeuN (red). Similar results were obtained in 6 independent experiments. **c.** Top: Scheme depicting seizure strength and duration in KA-treated animals. Mice were injected with KA (25 mg/kg) and sacrificed at various time points (0': n = 4; 15': n = 3; 1 h: n = 4; 6 h: n = 2, biologically independent samples). Bars indicate mean ± s.e.m. As a reference, control mice were treated with saline and sacrificed 1 h after treatment. Bottom: RT-qPCR assays show transient IEG induction. **d.** Experimental design for KA-induced neuronal activity, nuclei isolation and application of next generation sequencing (NGS) techniques. **e.** Volcano plot showing the significance and p-value distribution after differential gene expression analysis using DESeq2. AD: activity decreased; AI: activity induced (Sal: n = 2; KA-1h: n = 2, biologically independent samples). **f.** Transcript classification according to ENSEMBL for DETs 1 h after KA. TEC: To be Experimentally Confirmed. **g.** Number of processed transcript species detected for DETs 1 h after KA in the nuRNA-seq screens. miRNA: micro RNA; snoRNA: small nucleolar RNA; lincRNA: long interspersed non-coding RNA. **h.** The nuRNA-seq screen detects activity-induced eRNA and other nucleus-resident ncRNAs. We also present the riboRNAseq tracks for comparison. Values represent counts in RPM (read per million). The arrows indicate transcript directionality. **i.** Genomic track for the gene encoding hippocalcin (*Hpca*), a calcium-binding protein that is highly expressed in the hippocampus and downregulated upon SE. Values represent counts in RPM.

Exposure to the glutamate receptor agonist kainic acid (KA) is often used to model a single epileptic seizure episode – *aka* status epilepticus (SE) – in experimental animals. SE evokes a strong transcriptional response in the hippocampus that includes the transient transcription of immediate-early genes (IEGs) [15, 16] and rapid changes in chromatin marks and nuclear structure [17-20]. Nuclear envelope-tagged mice were treated with 25 mg/Kg of KA, which causes a strong and synchronous activation in all the hippocampal subfields leading to a robust but transient induction of IEGs (**Fig. 1c**). We used FANS to isolate nuRNA from hippocampal principal neurons of KA- and saline-treated mice

(**Fig. 1d** and **Supp. Fig. 1g**). This screen detected over 2,075 differentially expressed transcripts (DETs) (**Fig. 1e** and **Supp. Table 1**), unveiling a broader impact and less skewed distribution than previous studies of activity-induced transcription [2]. We observed the induction of a rich variety of transcripts, including eRNAs and other nucleus-resident species (**Fig. 1f-h**). These profiles did not present the typical enrichment for 3' sequences observed in mRNA-seq and covered both exons and introns (**Fig. 1h** and **Supp. Fig. 1h**). These results indicate that nuRNA-seq is particularly well suited for studying dynamic transcriptional responses because the signal precisely reflects the time point in which the transcripts are produced. As a result, nuRNA-seq provides a finer detection of activity-induced changes, particularly for transcripts that are already expressed in the basal state. It also unveils the transient downregulation of hundreds of transcripts (**Fig. 1e, i**), including many genes involved in basal metabolism (**Supp. Fig. 1i**).

Compartment-specific transcriptomics reveals the uncoupling of the SE-induced neuronal transcriptome and translatome

We next used the same genetic approach to tag ribosomes and identify the pool of mRNAs that are translated in response to seizures (i.e., the activity-induced neuronal translatome) (**Fig. 2a-c** and **Supp. Fig. 2a**). Translating ribosomal affinity purification (TRAP) [21] led to an enrichment for neuron-specific transcripts and depletion of glia-specific transcripts (**Fig. 2d** and **Supp. Fig. 2b**). The sequencing (referred to as riboRNA-seq) and analysis of TRAPped mRNAs retrieved 189 differentially translated genes (DTGs) (**Fig. 2e, Supp. Fig. 2c-e** and **Supp. Table 2**). Most of these DTGs are protein-coding (**Fig. 2f** and **Supp. Fig. 2f)** and relate to Gene Ontology (GO) functions such as *Transcription*

cofactor activity, *Kinase activity*, *Histone acetyltransferase* and *Chromatin binding*, being the nucleus the most enriched cellular component (**Supp. Fig. 2g**, red bars). Notably, the small set of activity-depleted mRNAs is also related to transcriptional regulation (**Supp. Fig. 2g**, blue bars), which further underscores the importance of transcriptional and epigenetic regulation in activity-dependent processes.

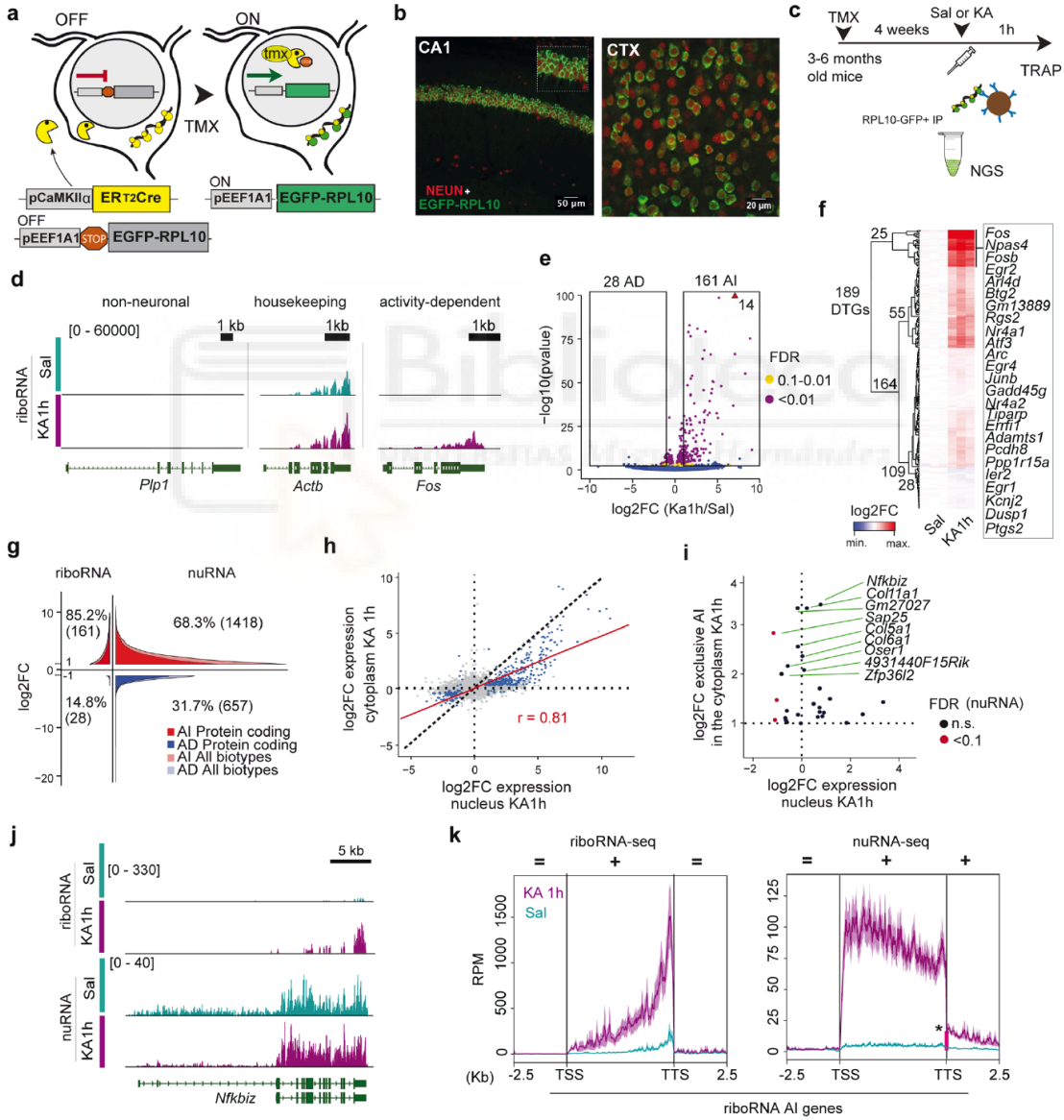

Figure 2. Compartment-specific transcriptomics reveals changes in neuronal transcripts production and translation. a. Crossing the TMX-inducible Cre-driver line CaMKII-creERT2

with mice that express GFP-L10a in a Cre-recombination-dependent manner allows the tagging of ribosomes in forebrain principal neurons for subsequent IP-based isolation. **b.** Confocal images of principal neurons in the CA1 subfield and cortex stained against GFP (green) and the neuron marker NeuN (red). Similar results were obtained in 3 independent experiments. **c.** Experimental design for KA-induced neuronal activation and ribosomal RNA isolation. **d.** Genomic snapshots for representative examples of glia-specific (*Plp1*), housekeeping (*ActB*) and activity-induced (*Fos*) genes. Values indicate the levels of counts in RPM. **e.** Volcano plot showing the significance and p-value distribution after differential transcript abundance analysis using DESeq2. AD: activity decreased; AI: activity induced. Sal: n = 3, KA-1h: n = 3, biologically independent samples. **f.** Heatmap of fold changes in DTGs retrieved in the riboRNA-seq screen. **g.** Density distribution of DTGs and DETs in the riboRNAseq and nuRNAseq screens, respectively. Colors indicate the distribution of protein coding *vs* all biotypes. **h.** Correlation of fold change (FC) values for genes significantly regulated (FDR < 0.1, 372 genes) in both datasets (blue). All other detected genes are labeled in gray. Cytoplasm: Sal: n = 3, KA-1h: n = 3; nucleus: Sal: n = 2, KA-1h: n = 2, biologically independent samples. The Pearson's correlation index is shown. **i.** Scatter plot of log2 FC for genes exclusively upregulated in the cytoplasm (FDR < 0.1; Sal: n = 3, KA-1h: n = 3, biologically independent samples) and its FC value in the nucleus (colors indicate FDR significance in nuRNA-seq analysis: n.s.: FDR > 0.1 in nuRNA-seq; Sal: n = 2; KA-1h: n = 2, biologically independent samples). **j.** Comparison of nuRNA-seq and riboRNA-seq tracks in *Nfkbiz*. The vertical scale shows counts in RPM. **k.** Metagene mapability profiles for riboRNA-seq (Sal: n = 3, KA-1h: n = 3) and nuRNA-seq (Sal: n = 2, KA-1h: n = 2) samples at genes upregulated in both datasets. The red bar to the right indicates the significant difference downstream of the TTS in nuRNA-seq. The solid lines indicate the mean and the shaded lines the s.e.m.

The availability of neuronal-specific riboRNA-seq and nuRNA-seq data provides a unique opportunity for the dissection of RNA-related mechanisms involved in the response to activation. First, the comparison of the number, magnitude and distribution of the changes confirmed the special suitability of

nuRNA-seq for transcriptional dynamics studies (**Fig. 2g** and **1h-i**). Second, despite these differences, we observed a robust correlation between changes in both screens demonstrating the coordinated regulation of RNA transcription and export upon neuronal activation (**Fig. 2h**). Third, we identified a small number of transcripts that escape the general correlation. These mRNAs show an increase in riboRNA-seq profiles but no change, or even a decrease in nuRNA-seq profiles. This pattern suggests that activity-dependent regulation of these transcripts occurs at the translational levels rather than at the transcriptional level (**Fig. 2i** and **Supp. Fig. 2h**, discordant). Notably, some of these genes are known to be post-transcriptionally regulated in other cell types [22]. This is the case with *Nfkbiz* (**Fig. 2j**), which encodes an atypical member of the NF□B family and harbors a translational silencing element (TSE) in the 3' UTR that destabilizes the mRNA [23, 24]. Fourth, we observed striking differences in the transcription termination site (TTS) of IEG transcripts obtained after nuclear and ribosome-bound RNA isolation (**Fig. 2k** and **Supp. Fig. 2i**). The nuclear transcripts were consistently longer, extending several hundred base pairs after the annotated TTS (**Fig. 2k**, red bar). This observation indicates that activity-induced ecRNAs, which have been postulated to prevent gene inactivation in embryonic neuronal cultures [8], are also produced in the adult brain. Overall, these findings underscore the value of parallel compartment-specific transcriptome analyses to unveil novel regulatory mechanisms.

The activity-induced transcriptional burst causes a dramatic increase in chromatin accessibility at IEGs

To precisely correlate transcriptional differences with changes in chromatin occupation and TF binding, we next assessed chromatin accessibility by ATAC-

seq [25]. The combination of FANS and ATAC-seq revealed that the chromatin accessibility profile of hippocampal neurons (**Supp. Fig. 3a-c**) is dramatically altered during SE (**Fig. 3a**). The differential accessibility screen retrieved more than 30,000 differentially accessible regions (DARs) (**Fig. 3b** and **Supp. Table 3a**), providing a deeper survey of activity-dependent changes than previous analyses [26] (**Supp. Fig. 3d-f**). While KA-induced increase of chromatin accessibility was primarily observed within gene regions, particularly within close proximity of the TSSs (< 1 Kb), modest chromatin closing occurred more frequently at intergenic regions (**Supp. Fig. 3g**). Overall, the most prominent changes in chromatin accessibility correspond to the opening of gene regions (**Fig. 3c**)

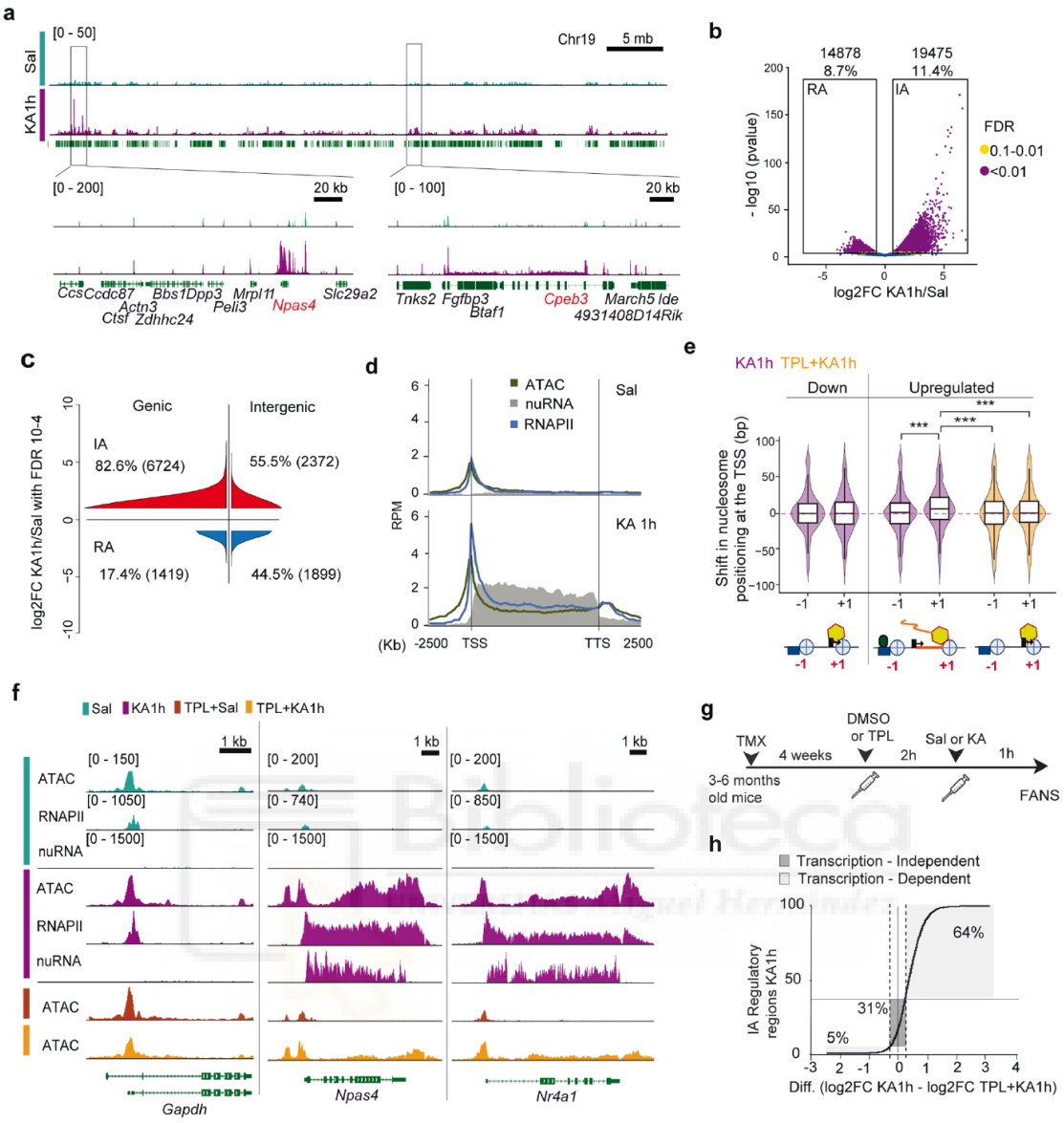

Figure 3. Neuronal activation causes a dramatic increase in accessibility at activity-regulated genes associated with the transcriptional burst. a. Genomic profile at the chr19 locus containing the activity-induced genes *Npas4 and Cpeb3* (in red). **b.** Volcano plot showing the significance value distribution after DAR analysis using DESeq2; upper values indicate number of regions and percentage of all the accessible regions detected. RA: Reduced accessibility; IA: Increased accessibility. Sal: n = 2, KA-1h: n = 2, biologically independent samples. **c.** Density distribution of highly significant intragenic and intergenic DARs (FDR < 10^{-4}) after DESeq2 analysis. RA: Reduced Accessibility; IA: Increased Accessibility. Sal: n = 2, KA-1h: n = 2. Values obtained by DESeq2 analysis. **d.** Metagene plot for ATAC-seq (Sal: n = 2, KA-1h: n = 2), RNAPII-ChIP-seq (Sal: n = 1, KA-1h: n = 1) and nuRNA-seq signals at upregulated

genes 1 h after saline or KA administration retrieved by DESeq2 analysis. (log2FC > 3; FDR < 0.1; Sal: n = 2, KA-1h: n = 2). **e.** Violin plot showing the shift in the distribution of nucleosome positioning at the TSS of downregulated and upregulated genes 1 h after KA (purple density plot) or after TPL+KA treatment (orange density plot). The boxplot indicates the median, interquartile range and min./max. The dashed red line indicates no shift at 0. KA-1h: n = 2, TPL+KA-1h: n = 1. ***: p-adjusted < 0.00001 in *pos hoc* Dunn test for Kluskal-Wallis with multiple comparisons. **f.** Top: Genomic snapshots of ATAC-seq, nuRNA-seq and RNAPII-ChIP-seq profiles in control and activity-regulated genes 1 h after saline or KA administration. Bottom: Impact of TPL in ATAC-seq profiles. Values indicate the levels of counts in RPM (read per million). **g.** Experimental design for the TPL blockage of KA-induced changes. **h.** Distribution of the difference of log2FC for "KA-1h" and "TPL+KA-1h" at the DARs detected in KA-1h. The DARs considered to be transcription independent (log2 FC difference smaller than ± 0.25) occupy the gray box.

We next used binding and expression target analysis (BETA) to integrate ATAC-seq and RNA-seq data [27] and found that the increase in chromatin accessibility throughout the gene body is an excellent predictor of transcriptional activation ($p < 3.86x10^{-36}$, **Supp. Fig. 4a**). ATAC-seq data correlated with changes in the riboRNA-seq and nuRNA-seq screens (**Supp. Fig. 4b**), but correlation was stronger and depended on more genes in the case of nuRNA-seq (**Supp. Fig. 4c** and **Supp. Table 3b**). These comparisons revealed a very prominent increase in accessibility at the gene body of activity-induced genes that extended beyond the TTS and narrowly matched transcript production (**Fig. 3d)**. We next investigated the relationship between changes in accessibility, transcription and RNA polymerase II complex (RNAPII) binding. Experiments in neuronal cultures have suggested that IEGs may have pre-assembled RNAPII at the TSS in the basal state [28]. RNAPII poising is however not evident *in vivo*. Although we detected a modest presence of RNAPII at the promoter of rapid

response genes in saline-treated mice, SE triggered a robust *de novo* binding (**Fig. 3d**). Nucleosome positioning at the TSS of activity-regulated genes showed a shift of the +1 nucleosome in activity-induced genes, also reflecting the *de novo* entrance of RNAPII (**Fig. 3e**) [29]. In addition to promoter binding, neuronal activation increased RNAPII occupancy of the gene body and the TTS in activity-regulated genes matching the production of extended nuclear transcripts (**Fig. 3d, f**) and enhanced intragenic accessibility (**Supp. Fig. 4d**). These results suggest that the enhanced accessibility at IEGs reflects the continuous passage of the RNAPII. To assess this hypothesis, we examined the effect of triptolide (TPL), a drug that inhibits transcription initiation [30, 31], in chromatin accessibility changes (**Fig. 3g**). Both IEG induction (**Supp. Fig. 4e**) and increased accessibility in the gene body of upregulated genes (**Fig. 3f** and **Supp. Table 3c**) were reduced in animals treated with TPL before KA administration. The impact of TPL on DARs was more prominent in the genes that show the largest changes (**Supp. Fig. 4f**) and stronger in gene bodies than TSSs (**Supp. Fig. 4g**), thereby confirming that most of these changes are directly derived from the traffic of RNAPII during the transcriptional burst. Administration of TPL also prevented the nucleosome shift at the TSS caused by the entry of new RNAPII complexes (**Fig. 3e**, orange violins). Interestingly, our analyses show that about 30% of the regions with altered accessibility in response to KA were not affected by TPL (**Fig. 3g-h**), indicating that other mechanisms, such as the *de novo* binding of activity-regulated transcription factors (TF) and the recruitment of co-activators, also contribute to activity-dependent changes in the chromatin.

TF and transcriptional co-activator binding at activity-regulated enhancers

Similar to TSSs and intragenic sequences (**Fig. 3d**), SE-induced changes at extragenic regions (> 1 Kb from gene body) also correlate with transcriptional changes in the proximal genes (**Supp. Fig. 5a**). To explore these changes in greater detail, we classified the accessible extragenic regions in the chromatin of mature excitatory neurons into promoters and putative enhancers distinguishing between regions with a stronger or weaker epigenetic signature (**Fig. 4a**). Promoters were characterized by the prominent presence of RNAPII and H3K4me3, along with a depletion of H3K4me1. In contrast, putative enhancers presented enrichments for the histone post-translational modifications (HPTM) H3K4me1 and H3K27ac and binding of the transcriptional co-activator and lysine acetyltransferase CREB-binding protein (CBP). About 10% of these promoter regions and 25% of the putative enhancer regions showed changes in accessibility during SE (**Supp. Fig. 5b**). Notably, these changes were consistent with ChIP-seq profiles for the binding of RNAPII and CBP upon SE, indicating that the changes are driven by the activity-dependent recruitment of transcriptional complexes. While promoters and strong enhancers showed robust activity-dependent binding of both RNAPII and CBP, weak enhancers only showed CBP binding (**Supp. Fig. 5c**), indicating that they may be poised for activation [32]. Consistent with this view, we detected an activity-dependent increase in H3K27 acetylation at the same sites (**Supp. Fig. 5d**) in primary cultures of embryonic cortical neurons stimulated with KCl [33]. Furthermore, activity-dependent CBP recruitment and increased H3K27 acetylation occurred at both TPL-sensitive and TPL-resistant sites (**Supp. Fig. 5e-f**), which suggests that CBP recruitment and enhancer activation may be

independent of RNAPII action. Intriguingly, 75% of the activity-induced-transcripts are associated with activity-driven changes in accessibility (**Fig. 4b** and **Supp. Fig. 5g**), but only 25% of promoters and 10% of enhancers displaying increased accessibility are linked to activity-induced transcripts (**Supp. Fig. 5h**). This discrepancy indicates that synaptic activity triggers a large number of chromatin changes that are not directly associated with transcription in the nearest gene.

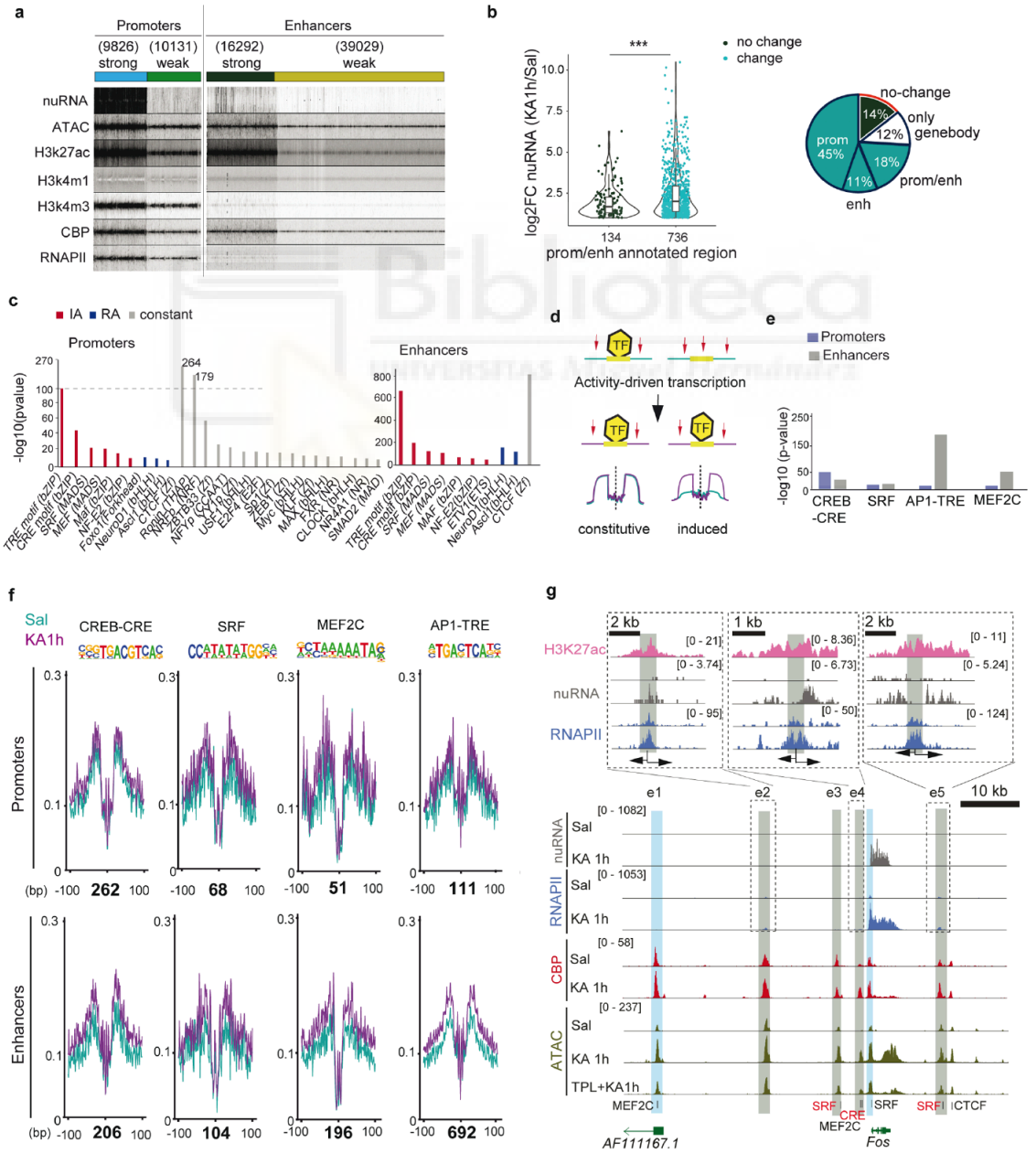

Figure 4. Neuronal activation induces TF-binding at extragenic sites. a. K-mean clustering for accessible extragenic regions (± 5 Kb) generated using the profiles of ATAC-seq, nuRNAseq, and ChIP-seq for RNAPII, CBP, H3K27ac, H3K4m3 and H3K4m1 in hippocampal chromatin of naïve animals (this study and [49, 50]). **b**. Left: Violin plot shows the log2FC distribution and number of upregulated nuclear transcripts with promoter/enhancer annotations that change (cyan dots) or do not change (black dots) during SE. ***: The boxplot indicates the median, interquartile range and min./max. Sal: n = 2, KA-1h: n = 2; p-adjusted value = 2.10^{-16} in Kruskal-Wallis test. Right: The sector graph shows the percentage of regions according to their annotation and change upon SE. **c**. Motif enrichment after HOMER analysis at detected promoter/enhancer accessible regions from reduced accessibility (RA, blue), increased accessibility (IA, red) and constant (gray) regions. Sal: n = 2, KA-1h: n = 2. **d.** Scheme of digital footprinting analysis. Red arrows indicate sites accessible to tn5 cutting. Occupied TF-binding sites are more protected than the immediate surrounding. **e.** Motif enrichment significance after HOMER analysis at detected footprints in IA-promoters and –enhancers. Sal: n = 2, KA-1h: n = 2. **f.** Digital footprinting at enriched motifs and number of motifs detected (values correspond to normalized tn5 insertions). **g.** As an example, the snapshot shows nuRNAs, ATAC-seq, RNAPII and CBP binding at regions flanking *Fos* in saline, KA-1h and TPL+KA-1h samples (values in RPM). Annotations label the detected footprints (in red, less stringent footprints) and classification for the regions (blue: promoters; gray: enhancers). The upper insets zoom on enhancers with detected eRNAs. Arrows indicate transcript directionality.

We next investigated the abundance of TF binding sites at accessible regions that show a significant increase, reduction or no change in accessibility upon SE. The promoters and enhancers showing an increase in accessibility were enriched for motifs recognized by TFs involved in neuronal plasticity processes such as AP1 (TRE) and CREB (CRE) [2]. In turn, the promoters and enhancers displaying reduced accessibility showed enrichment for motifs associated with neuronal identity such as NeuroD1 (**Fig. 4c**). This result pinpoints again to a competition between activity-regulated genes and other

highly expressed neuronal genes for the basal transcriptional machinery. Interestingly, constitutive promoters and enhancers were both enriched in CTCF binding sites, suggesting that the general architecture of the chromatin in neurons is not severely altered upon activation. To directly assess the occupancy of these sites before and during SE, we analyzed their digital footprints in ATAC-seq profiles (**Fig. 4d**). Occupancy by the activity-regulated TFs CREB, SRF, AP1 and MEF2C was detected in promoter and enhancer regions. While the footprint for the CREB family was stronger in promoters than in enhancers, the footprints of AP1 and MEF2C presented the opposite pattern (**Fig. 4e-f**). Upon SE, constitutive activity-regulated TFs, such as SRF and CREB, did not show large changes in their footprint although we could detect some *de novo* binding at enhancer regions (**Fig. 4f-g** and **Supp. Fig. 6a**). In contrast, AP1 showed a robust increase in occupancy at enhancer regions (**Fig. 4f-g,** and **Supp. Fig. 6a**) that, consistent with the *de novo* synthesis of AP1 proteins, was highly sensitive to TPL (**Supp. Fig. 6b-c**). ChIP-seq data for CREB, SRF and Fos in cortical neurons demonstrate the occupancy of these sites by the corresponding TFs after KCl stimulation [7, 33], suggesting that both modes of activation trigger the same genomic mechanisms (**Supp. Fig. 6d**). Consistent with the recently postulated role of the acquisition of signal-regulated DNA elements in gene regulatory regions in the evolution of cognitive abilities [34], these footprints are evolutionary conserved (**Supp. Fig. 6e**).

Physiological and pathological neuronal activation share common mechanisms but trigger distinct epigenomic signatures

To investigate whether the genomic events described above are exclusive to pathological neuronal over-activation or can also be observed after neuronal

activation in physiological conditions, we next explored chromatin changes triggered by the exploration of a novel and rich spatial context. This experience is known to induce IEG transcription in sparse neuronal assemblies in the hippocampus of rodents [35] (**Fig. 5a** and **Supp. Fig. 7a**). Nuclear envelope-tagged mice were subjected to novelty exploration (NE) for 1 h; we next used FANS and Fos immunostaining to isolate the small percentage of neuronal nuclei responding to this experience (25,000 $Sun1^+/Fos^+$ nuclei from the hippocampi of 6 novelty-exposed mice, **Fig. 5b** and **Supp. Fig. 7b**). We also isolated the same number of $Sun1^+/Fos^-$ nuclei for direct comparison of activated and non-activated neurons from the same animal. Both types of nuclei were processed for ATAC-seq to produce the first map of learning-related chromatin accessibility changes. Although the comparison of Fos^+ and Fos^- neurons revealed less numerous and more modest changes (**Fig. 5c**, **Supp. Fig. 7c** and **Supp. Table 4**), there was a large overlap between the NE- and SE-induced DARs. Principal component analysis (PCA) showed that Fos^+ nuclei clustered with the KA-1h samples, while Fos^- nuclei clustered with the samples of saline-treated mice (**Supp. Fig. 7d-e**). Similar to our SE study, chromatin accessibility changes in gene bodies correlated with nuclear transcript induction upon NE [36] (**Supp. Fig. 7f**), and digital footprinting revealed a clear enrichment for AP1 and Mef2c binding at activity-regulated enhancers, albeit less TF motifs were detected in NE than in SE (**Fig. 5d**).

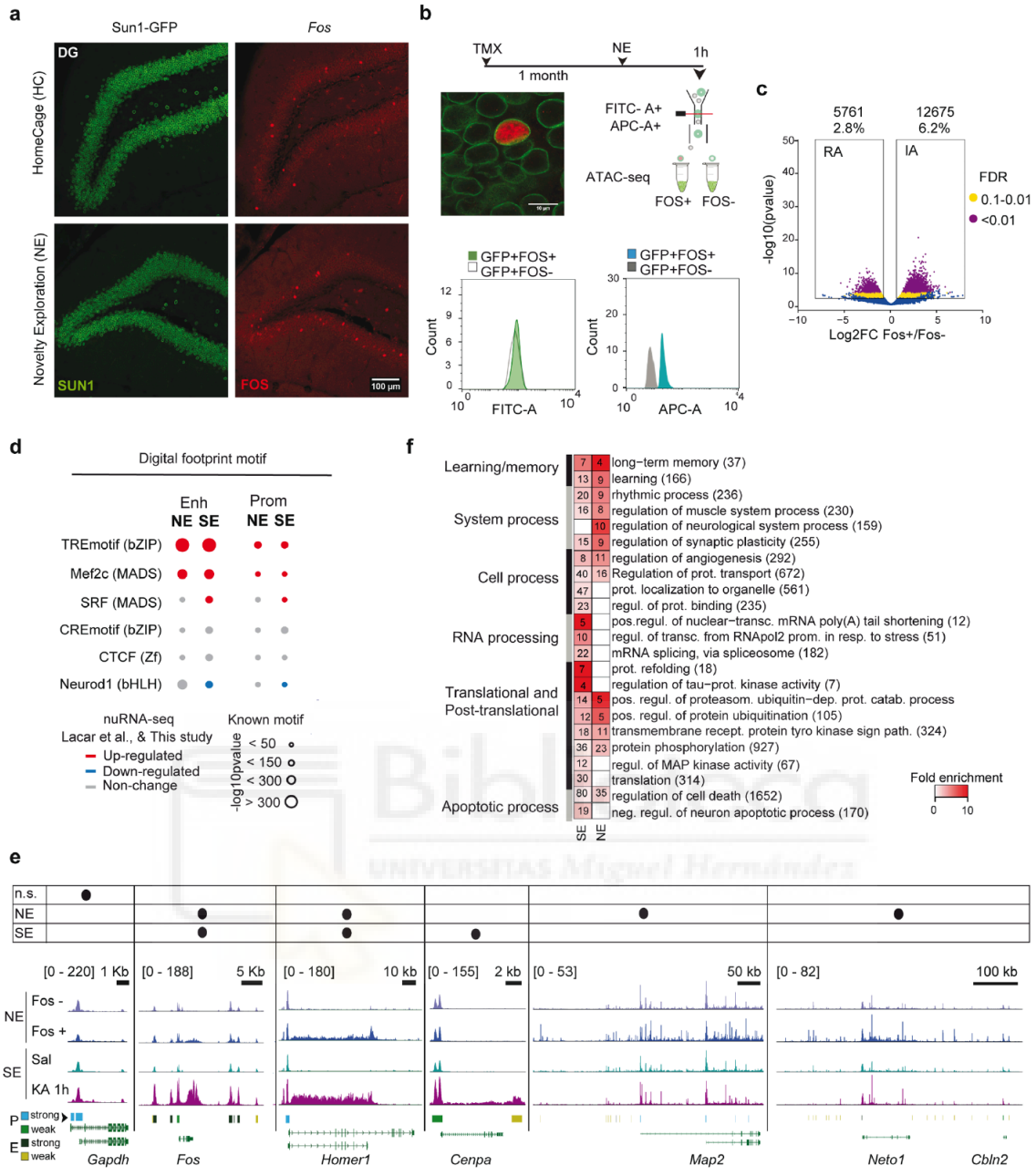

Figure 5. Physiological and pathological neuronal activation share common mechanisms but trigger distinct genomic signatures. a. Confocal images of granular neurons in the dentate gyrus (DG) of mice maintained in their homecages or exposed to 1 h of novelty exploration (NE). Brain slices were stained against GFP (green) and Fos (red). Similar results were obtained in 3 independent experiments. **b.** Experimental design of the approach used to study chromatin changes in neurons activated by 1 h of NE. Bottom: channel filtering of flow cytometry signal for Sun1-GFP^{+} (FITC-A) singlet nuclei and differences in Fos staining (APC-A).

Similar results were obtained in 3 independent experiments. **c.** Volcano plot showing the significance value distribution after differential accessible regions analysis; upper values indicate number of regions and percentage of all the accessible regions detected. RA: Reduced accessibility; IA: Increased accessibility. Fos^-: n = 1, Fos^+: n = 1, directly related (obtained from the same animals) samples. Values obtained after DESeq2 analysis including in the experiment design the comparisons with KA-1h and Sal condition to support the reduced n for value transformations. **d.** Digital footprinting at enhancer and promoter sites in NE and SE, indicating the motif enrichment (circle size) and the associated TF expression change in NE [36] and SE (this study) nuRNA-seq datasets (upregulated TFs are shown in red, downregulated one in blue, and those not changed in gray). **e.** Comparison of ATAC-seq tracks for physiologically (Fos^+ *vs* Fos^- neurons) and chemically activated (Sal *vs* KA-1h) neurons, at the DEG in the SE (this study) and NE [36] nuRNA-seq datasets. The table indicates the increase in accessibility at the gene body and nuRNA upregulation per each condition. Bottom bars indicate the regions classified as strong or weak at promoters and enhancers. Values indicate the levels of counts in RPM. **f.** Heatmap of fold enrichment for biological process GO terms in genes displaying increased accessibility in the NE and SE datasets. Values correspond to the number of genes associated with each term.

Although most of the genes responding to NE at the chromatin accessibility and transcriptional levels were retrieved during SE, a subset of genes was unique to this paradigm (**Fig. 5e**). Consistently, GO enrichment analyses reveled a greater enrichment for neuronal plasticity and memory functions in the NE-specific set, while the SE-specific genes were related to the modification and processing of RNA and protein, including the regulation of Tau and kinases involved in neurophysiopathology [37] (**Fig. 5f**). The comparison of chromatin accessibility profiles also revealed noticeable differences between SE and NE (**Supp. Fig. 7c** and comparison of **Supp. Fig. 7g** and **Supp. Fig. 5h**). For instance, the TF footprints detected at DARs exclusive to the NE situation

do not show *de novo* RNAPII or CBP binding after SE (**Supp. Fig. 7h**). However, the same sites displayed reduced DNA methylation and enhanced H3K4me1 and H3K27ac (two HPTMs associated with enhancer activation) after fear conditioning in a new context [38] (**Supp. Fig. 7i**). These results underscore both the common mechanisms and the stimuli-dependent differences in the genomic signature of pathological versus physiological activation of principal neurons.

Longitudinal analyses unveil chromatin changes that remain long after SE

Next, we investigated the duration and reversibility of the transcriptional and chromatin accessibility changes triggered by neuronal activation. Towards this end, we expanded our study of the epigenetic and transcriptome signature of synchronous hippocampal neuron activation to 6 h and 48 h after SE. In the case of nuRNA-seq, the longitudinal analysis revealed a dynamic scenario in which the broad initial transcriptional response led to a secondary wave of changes at 6 h that still affected thousands of transcripts but with more moderate changes, while 48 h after SE the neuronal transcriptome was largely restored to the basal situation (**Fig. 6a, Supp. Fig. 8a-d** and **Supp. Table 5**). Of note, there were more genes downregulated than upregulated at later time points, which contrasts with the oppositely skewed distribution observed during SE. Some of these downregulated genes are related to potassium and calcium transport, likely reflecting the late homeostatic response (**Supp. Fig. 8e**).

In contrast, the longitudinal analysis of chromatin accessibility changes (**Supp. Table 6**) did not reveal the same restoration to the original state. The samples corresponding to 48 h after KA approached the control samples (Sal), but did not overlap (**Fig. 6a**). Indeed, a relatively large subset of DARs (>

10,000), particularly those located at intergenic regions, persists 48 h after SE (**Fig. 6b-c** and **Supp. Fig. 8f-i**). Moreover, although BETA revealed a clear correlation between augmented transcript production and accessibility for each time point **(Fig. 6d**), the extragenic regulatory regions exhibiting increased accessibility at 48 h showed a better correlation with transcriptional changes at 1 h and 6 h than at 48 h.

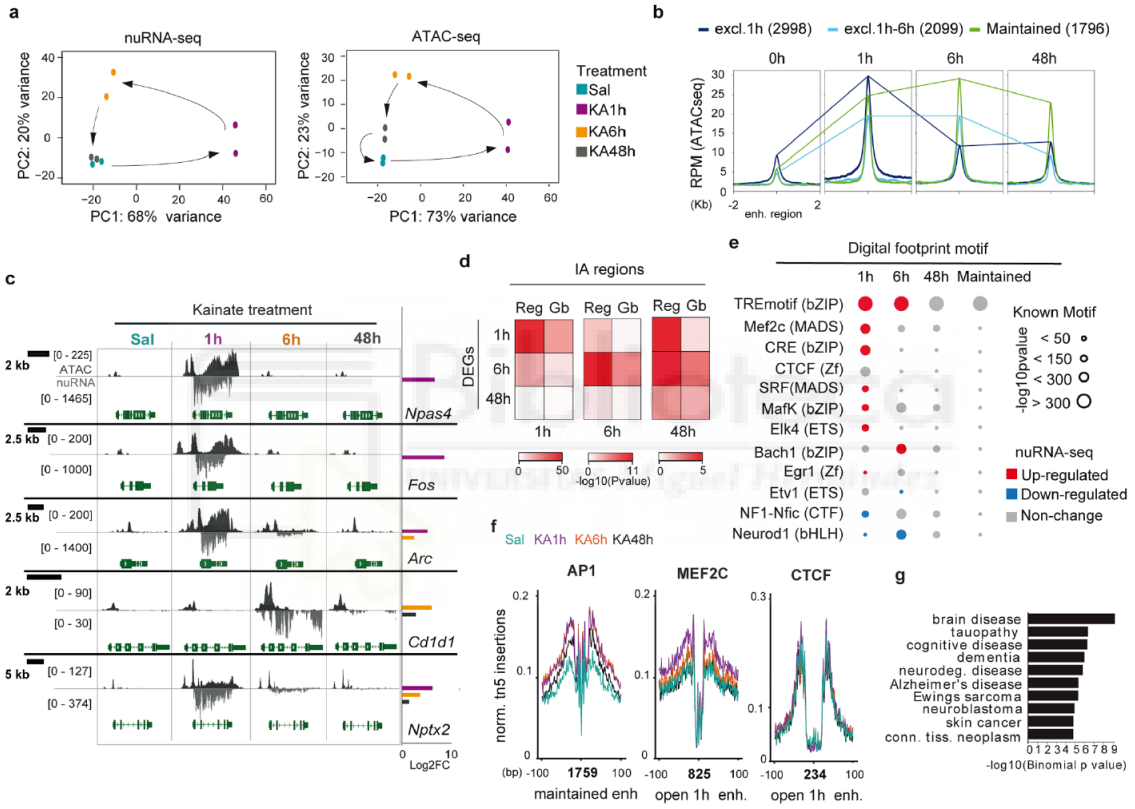

Figure 6. Long-lasting chromatin accessibility changes are associated with AP1 binding and disease. a. Principal component analysis for nuRNA-seq (left) and ATAC-seq (right) datasets. Sal and KA-48h samples overlap distant from KA-1h samples. The separation of KA-6h samples suggests an independent second wave of transcriptional changes (Sal: n = 2, KA-1h: n = 2, KA-6h: n = 2, KA-48h: n = 2; same number of biologically independent samples in ATAC-seq and nuRNA-seq). **b.** ATAC-seq signal at activity-regulated enhancers that show increased accessibility (IA) exclusively at 1 h, at 1 h and 6 h, or maintained for 48 h. **c.** Snapshots for ATAC-seq and nuRNA-seq tracks at the different time points. The examples

illustrate the diversity of profiles under the general denomination of IEG. *Fos* and *Npas4* present a very rapid and transient induction associated with dramatic changes in the accessibility of the chromatin at the gene body, while other IEGs, such as *Arc* and *Nptx2*, maintain their induction for hours or even days after SE. Late response genes, such as *Cd1d1*, increase transcription and chromatin accessibility long after SE. Right bars show significant (FDR < 0.1) log2FC for nuclear transcripts after DESeq2 analysis at each time point (Sal: n = 2, KA-1h: n = 2, KA-6h: n = 2, KA-48h: n = 2; same number of biologically independent replicates in ATAC-seq and nuRNA-seq). Values are shown in RPM. **d.** Heatmap showing the significance after BETA analysis for increased accessibility (IA) regions and transcript levels in each time point at promoter/enhancer (Reg) and gene bodies (Gb) (Sal: n = 2, KA-1h: n = 2, KA-6h: n = 2, KA-48h: n = 2; same number of biologically independent replicates in ATAC-seq and nuRNA-seq). **e.** Digital footprinting at enhancer/promoter sites in SE dynamic, indicating the motif enrichment (circle size) and the associated TF expression change in NE nuRNA-seq datasets. Red: upregulated; blue: downregulated; gray: no-change. **f.** Footprinted AP1, Mef2c and CTCF sites at 0 h, 1 h, 6 h, and 48 h after KA detected on enhancer DARs presenting increased accessibility during SE (open 1h) and maintained from 1 to 48 h. The number of motifs detected is indicated below the graph. **g.** Genes associated with the enhancer-overlapping DARs that show a maintained increase in accessibility are disease-related (Sal: n = 2, KA-1h: n = 2, KA-6h: n = 2, KA-48h: n = 2).

Digital footprint analysis at those regions displaying long-lasting changes revealed a specific enrichment for AP1 binding, while the enrichment for other activity-regulated TFs such as MEF2C, was only detected at earlier time points (**Fig. 6e-f**). Notably, AP1 sites also show stable accessibility changes after electrical stimulation of dentate gyrus neurons [26]. ChIP-seq data for Fos binding upon KCl stimulation of cortical neurons [7, 33] is consistent with the occupancy of these sites (**Supp. Fig. 9a**). Interestingly, the AP1 sites presenting long-lasting changes after SE also respond to novelty exploration (**Supp. Fig 9b**), which further underscores the biological relevance of these sites. This binding signal

might correspond to Fos-Jun dimers or to other TFs of the same family that recognize the same motif [26]. Although the activity-induced transcription of AP1 genes is highly transient (**Fig 6e**), at the protein level, Fos immunoreactivity persists even 6 h after SE (**Supp. Fig. 9c**). Therefore, we cannot discard that a reduced number of AP1 molecules induced during seizure could still remain bound at specific loci at later time points. Notably, the genomic regions displaying long-lasting changes are associated with genes involved in brain diseases related to protein accumulation **(Fig 6g),** thus linking these changes with pathological traits. Consistent with this notion, mice that underwent SE displayed both memory deficits (**Supp. Fig. 9d**) and impaired induction of *Fos* (**Supp. Fig. 9e**) when subjected to a novel object location memory task (which is known to be hippocampal dependent). The *Fos* locus is surrounded by several regions that display long-lasting changes in occupancy, including sustained AP1 binding at putative enhancers located close to the neighbor gene *Jdp2* (**Supp. Fig. 9f**), which encodes for a repressor of AP1. These results suggest that the "silent" changes retrieved in our longitudinal study might affect the future responsiveness of the neuron and thereby contribute to hippocampal dysfunction in the epileptic brain.

Activity-driven transcription is associated with the formation of gene loops and stronger promoter-enhancer interactions

Our multi-omic analysis indicates that activity-driven transcription is associated with a rapid increase in chromatin accessibility and RNAPII occupancy that extends over the gene limit and points to the participation of structural proteins that topologically delimit locus responsiveness. In addition, we also detected a delayed response in the form of long-lasting changes in chromatin occupancy

that suggest the existence of a genomic memory in the form of protein binding or architectural modifications. To test these hypotheses, we investigated the 3D chromatin architecture of activated hippocampal neurons 1 h and 48 h after SE using Hi-C (**Supp. Fig. 10a**). This genome-wide and fully unbiased chromatin conformation capture technique enables the analysis of compartments, CTCF loops and gene loops [39]. We combined our FANS procedure with Hi-C to generate the first draft of DNA interactions in 25 Kb bins for excitatory neurons of adult behaving mice both in the basal situation and during SE (**Fig. 7a**). Compartments were generally similar to those reported for cortical neurons differentiated *in vitro* (**Supp. Fig. 10b**) [40]. Furthermore changes in gene expression during neuronal differentiation correlate with similar changes to compartments in these *in vitro* differentiated neurons and adult neuronal tissue (**Supp. Fig. 10c-d**).

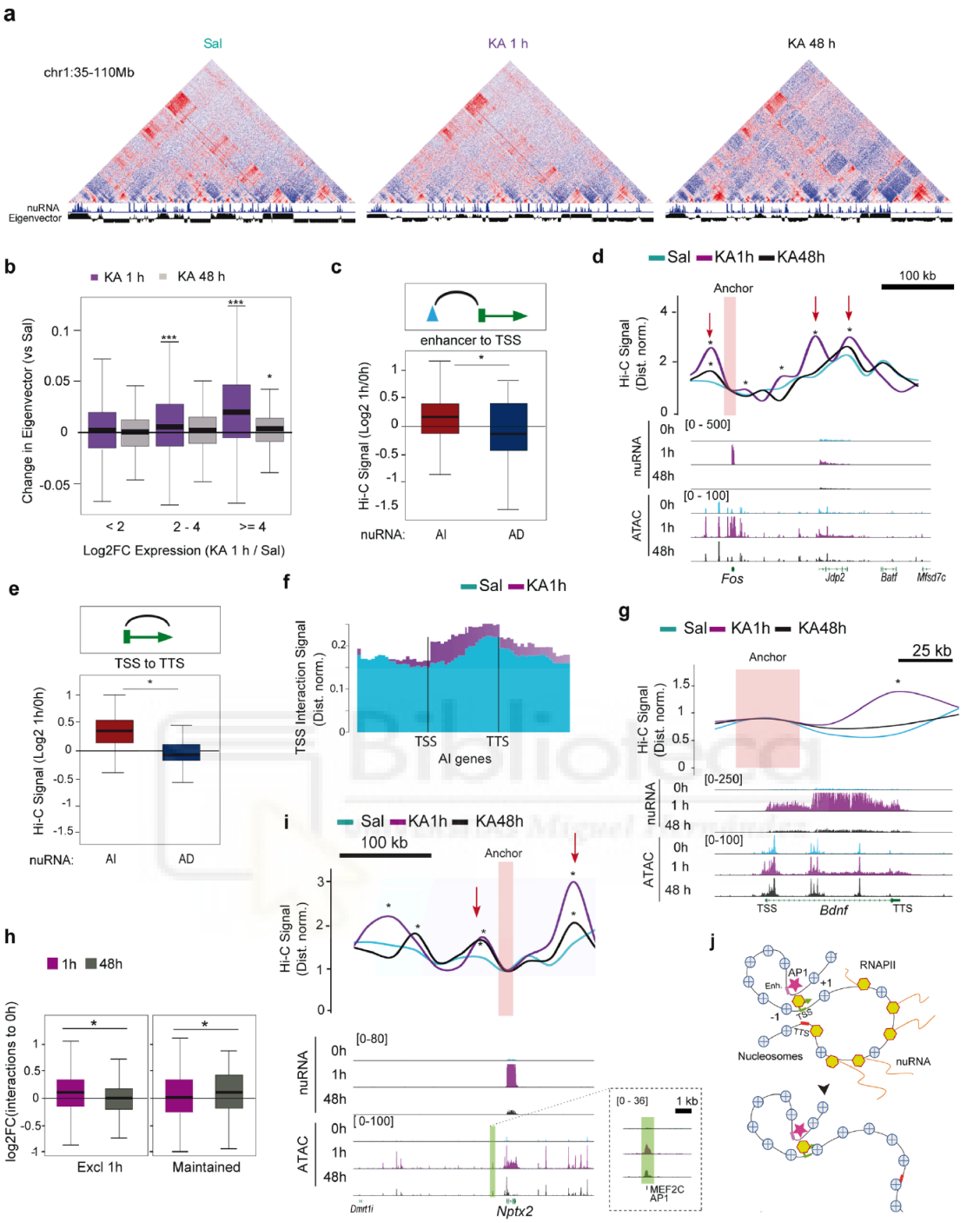

Figure 7. Neuronal activation induces gene loops and strengthens TSS-enhancer interactions. a. Hi-C maps of normalized distances in chromatin samples of saline and KA-treated mice 1 and 48 h after drug administration. Note the segregation of active and inactive chromatin in both situations, represented by positive and negative eigenvectors at the top and the augmented inflection (red arrow) in a SE-induced locus. **b.** Difference in the compartmental eigenvector 1 h (purple boxplot) or 48 h (gray boxplot) after KA treatment compared to Sal at

genes with increased expression 1 h after KA treatment as retrieved by DESeq2. Hi-C, Sal: n = 2, KA-1h: n = 2, KA-48h: n = 2; nuRNA-seq, Sal: n = 2, KA-1h: n = 2 biological replicates. The boxplot indicates the median, interquartile range and min./max. Two-sided statistic test, ***: p < 0.001, *: p < 0.05 Wilcoxon sum rank test for each compared to < 2 FC. **c.** Changes to Fit-Hi-C interaction signal 1 h after KA between differential ATAC-seq peaks and TSSs of activity-induced (red boxplot) or activity-decreased (blue boxplot) genes as detected by DESeq2 analysis. The boxplot indicates the median, interquartile range and min./max. Two-sided statistic test, *: p < 0.05 Wilcoxon rank sum test. Sample sizes are the same than in panel b. **d.** Top: Snapshot of the *Fos* locus presenting *de novo* promoter-enhancer interactions in response to SE. Red arrows indicate significant activity-driven interactions 1 h after KA. Significant differences were tested for enrichment in KA-1h samples using a one-sided confidence interval using all interaction bins in the immediate vicinity (n = 21). Significance was assigned if fold change was above a 99.9% confidence interval giving rise to p < 0.001. Bottom: Genomic profiles at the different time points. Values are in RPM. **e.** Changes to gene loop signal (TSS-TTS) 1 h after KA for activity-induced (red boxplot) an activity-reduced (blue boxplot) genes detected by nuRNA-seq and DESeq2 analysis. The boxplot indicates the median, interquartile range and min./max. Two-sided statistic test, *: p < 0.05 Wilcoxon rank sum test. Sample sizes are the same than in panel b. **f.** Metagene plot for TSS interaction signal at upregulated genes 1 h after saline or KA administration (compare with **Fig. 3d**). **g.** Snapshot of the *Bdnf* locus presenting the increased interaction between the TSS and the TTS. Significant differences were tested and assigned as indicated in panel d (n = 16). **h.** Changes to the Fit-Hi-C 1 h and 48 h interaction signals between the TSSs of activity-induced genes and DARs located at enhancers and showing increased accessibility only at 1 h (Excl 1h) or from 1 h to 48 h (Maintained) according to our DESeq2 analysis. The boxplot indicates the median, interquartile range and min./max. Significance was assigned using a two-sided Wilcoxon rank sum test. Left boxplot: n = 774, p < 0.001. Right boxplot: n = 269, p = 0.03. **i.** Genomic screenshots for *Nptx2* (an example of activity-regulated gene that does not return to basal expression and maintains some proximal chromatin accessibility changes after 48 h). The Hi-C inset for *Nptx2* shows augmented interactions with an upstream enhancer that remains slightly over the basal level even after 48 h. Red arrows indicate significant activity-driven interactions. Values show counts

in RPM. Significant differences were tested and assigned as indicated in panel d (n = 81). **j.** Scheme summarizing the main features of the immediate and deferred epigenetic signature of neuronal activation.

We sought after activity-regulated CTCF loops using HiCCUPS [41], but while we detect differences in CTCF loops between embryonic stem cells [40], *in vitro* differentiated neurons [40] and adult principal neurons, we did not detect significant activity-driven changes, suggesting that CTCF loops are largely invariant during neuronal activation (**Supp. Fig. 10e-f**). This lack of change is consistent with our TF binding site enrichment and digital footprint analyses (**Fig. 4c** and **Supp. Fig. 6c**). We however detected changes in the interactions of activity-induced genes with nearby DARs (**Supp. Fig. 10g**). The differences in compartmental eigenvector strongly correlated with the observed increase in transcription of activity-regulated genes 1 h after KA treatment (**Fig. 7b**, purple boxes). To test this on a genome-wide scale, we used Fit-Hi-C to retrieve a list of significantly enriched pairwise intra-chromosomal interactions (**Supp. Table 7**). Our analyses revealed enhanced interactions between proximal extragenic DARs and the TSS of activity-induced genes (**Fig. 7c**), such as the IEG *Fos* (**Fig. 7d**), and between the TSS and TTS of activity-induced genes (**Fig. 7e-f**). We then evaluated the appearance of gene loops between the TSS and TTS of genes with high levels of nuRNA-seq signal, and found increased formation upon SE (**Supp. Fig. 10h**). These gene loops between the TSS and the TTS of strongly induced genes (**Supp. Fig. 10i** and **Fig. 7g** show *Bdnf* as an example) may be essential for supporting the fast transcriptional rate of these loci. Their detection, together with the robust increase in gene body accessibility and

intragenic RNAPII signal (**Fig. 3d**), point to a continuous re-loading of the RNAPII complex at IEGs during SE.

We next investigated if these activity-induced interactions persist beyond the transcriptional burst. Hi-C maps were consistent with ATAC-seq profiles and presented largely restored compartments **(Fig. 7b**, gray boxes) but incomplete restoration of site-specific interactions 48 h after SE **(Fig. 7h-l** and **Supp. Fig. 10j-k**; see also black lines in **7d** and **7g**). In some genes such as *Nptx2*, encoding a synaptic protein involved in excitatory synapse formation [42], the chromatin change was associated with enhanced transcription and strengthening of the interaction between the promoter and a proximal enhancer (**Fig. 7i**). Together with the identification of long-lasting changes in chromatin occupancy, these intriguing results support the notion of a genomic memory in the form of architectural modifications that originate from past transcriptional activity (**Fig. 7j**).

Discussion

Here, we investigated the transcriptional and chromatin changes occurring in neuronal nuclei of adult behaving mice upon activation. To gain cell-type specificity, we genetically tagged the nuclei and polysomes of excitatory hippocampal neurons for their isolation and use in several sequencing methods. Subsequent multi-omics analyses revealed an unexpectedly broad and dynamic scenario with multiple levels of activity-dependent regulation. For instance, the improved temporal resolution obtained by nuRNA profiling revealed that the robust induction of IEGs is accompanied by the downregulation of numerous metabolism genes, suggesting that the activity-induced transcriptional burst

transiently hijacks the transcriptional machinery. In turn, the delayed downregulation of genes involved in ion transport and synaptic transmission may contribute to homeostatic plasticity mechanisms that compensate for prolonged activation and stabilizes neuronal firing [43]. Our nuRNA-seq screen also reveals the production of ecRNA in activity-induced genes that may finetune the activity of these loci and contribute to transcriptional memory [8]. Furthermore, its comparison with translatome data identifies genes in which synaptic activity specifically regulates ribosome engagement. We cannot discard a delayed impact also at the translational level.

Further integration of nuRNA-seq with ATAC-seq, RNAPII ChIP-seq and Hi-C maps obtained in the same activation paradigm demonstrates for the first time that the robust transcription of IEGs during SE relies on the formation of gene loops that bring together the TSS and the TTS and might favor the continuous re-loading of the RNAPII complex. Such organization has been described for highly transcribed genes in yeast [44, 45] and *Drosophila* cells [39], but not in neurons. Our analyses also identified hundreds of *de novo* or strengthened promoter-enhancer interactions and thousands of TF binding events in the chromatin of hippocampal excitatory neurons upon activation. Although some of these changes are transcription-independent and rely on the post-translational modification of TFs (e.g., phosphorylation), many others, such as the AP1 binding detected after both physiological and pathological stimulation, are transcription-dependent. Interestingly, the comparison of chromatin changes associated with physiological and pathological neuronal activation demonstrates that, in addition to common mechanisms, there are remarkable differences in the scope and magnitude of the changes. These

large-scale and dynamic adjustments of genome topology likely contribute to the rapid and coordinated transcriptional response associated with neuronal activation in both paradigms. The technical developments introduced here in combination with recent progress in tagging neuronal ensembles that participate in the encoding of a particular experience [46] open up the possibility of longitudinal studies of chromatin changes linked to memory engrams.

Notably, our longitudinal analyses in the context of SE retrieved changes in chromatin occupancy that persist even 2 days after stimulation. In particular, changes in the occupancy of AP1-binding sites are detected long after the shutdown of the encoding loci and constitute a prominent part of the deferred epigenomic signature of neuronal activation. This conclusion is in agreement with the recent observation of stable accessibility changes in granular neurons 24 h after electrical stimulation and the postulated role of Fos in initiating neuronal activity-induced chromatin opening [26]. Intriguingly, a recent large-scale study of accessible *cis*-regulatory elements across multiple human tissues revealed that SNPs within AP-1 motifs, including disease-associated non-coding variants, are often associated with changes in chromatin accessibility [1, 47]. Consistent with this link, our functional genomics analyses indicate that these long-lasting changes may relate to brain disorders such as cognitive dysfunction, dementia and neurodegenetative diseases. In a broader context, the enduring changes in accessibility that are associated with *de novo* AP1 binding to distal regulatory regions of activity-induced genes and with enhanced promoter-enhancer interactions may influence future activity of the loci. AP1 has been recently shown to recruit the BAF chromatin-remodeling complex to enhancers to locally augment chromatin accessibility [48]. Therefore, the robust

induction of AP1 subunits in response to activity might produce an excess of proteins to guarantee the occupancy of these sites and the priming effect. Since many of these loci play important roles in regulating synaptic plasticity and excitability, the experience fingerprints that persist in the chromatin may act as a form of metaplasticity by influencing the future response of the neuron to the same or other stimuli.

Acknowledgments: We thank E. Herrera, T. Ferrar, J.P. Lopez-Atalaya and Y. Ruan for critical reading of the manuscript, and R. Olivares, N. Cascales, A. Caler and the personnel of the sequencing facility at the CRG (Barcelona, Spain) and HudsonAlpha (Alabama, USA) for technical assistance. J.F-A. and M.T.L-C. are recipients of fellowships from the Spanish Ministry of Science and Innovation (MICINN). A.B. research is supported by grants SAF2017-87928-R and SEV-2017-0723 from MICINN co-financed by ERDF, PROMETEO/2016/026 from the Generalitat Valenciana, and RGP0039/2017 from the Human Frontiers Science Program Organization (HFSPO). M.J.R. is supported by the National Institutes of Health (NIH) Pathway to Independence Award K99/R00 GM127671. V.G.C. research is supported by the U.S. Public Health Service Award (R01) GM035463 from the NIH. The content is solely the responsibility of the authors and does not necessarily represent the official views of the NIH. The Instituto de Neurociencias is a “Centre of Excellence Severo Ochoa”. **Competing interests statement:** The authors do not express any conflict of interest.

References

1. Yap, E.L. & Greenberg, M.E. Activity-Regulated Transcription: Bridging the Gap between Neural Activity and Behavior. *Neuron* **100**, 330-348 (2018).

2. Benito, E. & Barco, A. The neuronal activity-driven transcriptome. *Mol Neurobiol* **51**, 1071-1088 (2015).

3. West, A.E. & Greenberg, M.E. Neuronal activity-regulated gene transcription in synapse development and cognitive function. *Cold Spring Harbor perspectives in biology* **3** (2011).

4. Eagle, A.L., Gajewski, P.A. & Robison, A.J. Role of hippocampal activity-induced transcription in memory consolidation. *Rev Neurosci* **27**, 559-573 (2016).

5. Sweatt, J.D. The emerging field of neuroepigenetics. *Neuron* **80**, 624-632 (2013).

6. Lopez-Atalaya, J.P. & Barco, A. Can changes in histone acetylation contribute to memory formation? *Trends Genet* **30**, 529-539 (2014).

7. Kim, T.K.*, et al.* Widespread transcription at neuronal activity-regulated enhancers. *Nature* **465**, 182-187 (2010).

8. Savell, K.E.*, et al.* Extra-coding RNAs regulate neuronal DNA methylation dynamics. *Nature communications* **7**, 12091 (2016).

9. You, X.*, et al.* Neural circular RNAs are derived from synaptic genes and regulated by development and plasticity. *Nat Neurosci* **18**, 603-610 (2015).

10. Crepaldi, L.*, et al.* Binding of TFIIIC to sine elements controls the relocation of activity-dependent neuronal genes to transcription factories. *PLoS Genet* **9**, e1003699 (2013).

11. Madabhushi, R., *et al.* Activity-Induced DNA Breaks Govern the Expression of Neuronal Early-Response Genes. *Cell* **161**, 1592-1605 (2015).

12. Cho, J., *et al.* Multiple repressive mechanisms in the hippocampus during memory formation. *Science* **350**, 82-87 (2015).

13. Mauger, O., Lemoine, F. & Scheiffele, P. Targeted Intron Retention and Excision for Rapid Gene Regulation in Response to Neuronal Activity. *Neuron* **92**, 1266-1278 (2016).

14. Mo, A., *et al.* Epigenomic Signatures of Neuronal Diversity in the Mammalian Brain. *Neuron* **86**, 1369-1384 (2015).

15. Ben-Ari, Y. & Cossart, R. Kainate, a double agent that generates seizures: two decades of progress. *Trends Neurosci* **23**, 580-587 (2000).

16. Elliott, R.C., Miles, M.F. & Lowenstein, D.H. Overlapping microarray profiles of dentate gyrus gene expression during development- and epilepsy-associated neurogenesis and axon outgrowth. *J Neurosci* **23**, 2218-2227 (2003).

17. Huang, Y., Doherty, J.J. & Dingledine, R. Altered histone acetylation at glutamate receptor 2 and brain-derived neurotrophic factor genes is an early event triggered by status epilepticus. *J Neurosci* **22**, 8422-8428 (2002).

18. Tsankova, N.M., Kumar, A. & Nestler, E.J. Histone modifications at gene promoter regions in rat hippocampus after acute and chronic electroconvulsive seizures. *J Neurosci* **24**, 5603-5610 (2004).

19. Crosio, C., Heitz, E., Allis, C.D., Borrelli, E. & Sassone-Corsi, P. Chromatin remodeling and neuronal response: multiple signaling pathways induce specific histone H3 modifications and early gene expression in hippocampal neurons. *J Cell Sci* **116**, 4905-4914 (2003).

20. Taniura, H., Sng, J.C. & Yoneda, Y. Histone modifications in status epilepticus induced by kainate. *Histol Histopathol* **21**, 785-791 (2006).

21. Dougherty, J.D. The Expanding Toolkit of Translating Ribosome Affinity Purification. *J Neurosci* **37**, 12079-12087 (2017).

22. Schott, J.*, et al.* Translational regulation of specific mRNAs controls feedback inhibition and survival during macrophage activation. *PLoS Genet* **10**, e1004368 (2014).

23. Yamazaki, S., Muta, T., Matsuo, S. & Takeshige, K. Stimulus-specific induction of a novel nuclear factor-kappaB regulator, IkappaB-zeta, via Toll/Interleukin-1 receptor is mediated by mRNA stabilization. *J Biol Chem* **280**, 1678-1687 (2005).

24. Behrens, G.*, et al.* A translational silencing function of MCPIP1/Regnase-1 specified by the target site context. *Nucleic Acids Res* **46**, 4256-4270 (2018).

25. Buenrostro, J.D., Giresi, P.G., Zaba, L.C., Chang, H.Y. & Greenleaf, W.J. Transposition of native chromatin for fast and sensitive epigenomic profiling of open chromatin, DNA-binding proteins and nucleosome position. *Nature methods* **10**, 1213-1218 (2013).

26. Su, Y.*, et al.* Neuronal activity modifies the chromatin accessibility landscape in the adult brain. *Nat Neurosci* **20**, 476-483 (2017).

27. Wang, S.*, et al.* Target analysis by integration of transcriptome and ChIP-seq data with BETA. *Nat Protoc* **8**, 2502-2515 (2013).

28. Saha, R.N.*, et al.* Rapid activity-induced transcription of Arc and other IEGs relies on poised RNA polymerase II. *Nat Neurosci* **14**, 848-856 (2011).

29. Schep, A.N., *et al.* Structured nucleosome fingerprints enable high-resolution mapping of chromatin architecture within regulatory regions. *Genome Res* **25**, 1757-1770 (2015).

30. Wang, Y., Lu, J.J., He, L. & Yu, Q. Triptolide (TPL) inhibits global transcription by inducing proteasome-dependent degradation of RNA polymerase II (Pol II). *PLoS ONE* **6**, e23993 (2011).

31. Jonkers, I., Kwak, H. & Lis, J.T. Genome-wide dynamics of Pol II elongation and its interplay with promoter proximal pausing, chromatin, and exons. *eLife* **3**, e02407 (2014).

32. Creyghton, M.P., *et al.* Histone H3K27ac separates active from poised enhancers and predicts developmental state. *Proc Natl Acad Sci U S A* **107**, 21931-21936 (2010).

33. Malik, A.N., *et al.* Genome-wide identification and characterization of functional neuronal activity–dependent enhancers. *Nature Neuroscience* **17**, 1330-1339 (2014).

34. Hardingham, G.E., Pruunsild, P., Greenberg, M.E. & Bading, H. Lineage divergence of activity-driven transcription and evolution of cognitive ability. *Nat Rev Neurosci* **19**, 9-15 (2018).

35. Guzowski, J.F., *et al.* Mapping behaviorally relevant neural circuits with immediate-early gene expression. *Curr Opin Neurobiol* **15**, 599-606 (2005).

36. Lacar, B., *et al.* Nuclear RNA-seq of single neurons reveals molecular signatures of activation. *Nature communications* **7**, 11022 (2016).

37. Tai, X.Y., *et al.* Hyperphosphorylated tau in patients with refractory epilepsy correlates with cognitive decline: a study of temporal lobe resections. *Brain* **139**, 2441-2455 (2016).

38. Halder, R., *et al.* DNA methylation changes in plasticity genes accompany the formation and maintenance of memory. *Nat Neurosci* **19**, 102-110 (2016).

39. Rowley, M.J. & Corces, V.G. Organizational principles of 3D genome architecture. *Nat Rev Genet* **19**, 789-800 (2018).

40. Bonev, B., *et al.* Multiscale 3D Genome Rewiring during Mouse Neural Development. *Cell* **171**, 557-572 e524 (2017).

41. Rao, S.S., *et al.* A 3D map of the human genome at kilobase resolution reveals principles of chromatin looping. *Cell* **159**, 1665-1680 (2014).

42. Xiao, M.F., *et al.* NPTX2 and cognitive dysfunction in Alzheimer's Disease. *eLife* **6** (2017).

43. Fernandes, D. & Carvalho, A.L. Mechanisms of homeostatic plasticity in the excitatory synapse. *J Neurochem* **139**, 973-996 (2016).

44. Hampsey, M., Singh, B.N., Ansari, A., Laine, J.P. & Krishnamurthy, S. Control of eukaryotic gene expression: gene loops and transcriptional memory. *Adv Enzyme Regul* **51**, 118-125 (2011).

45. Laine, J.P., Singh, B.N., Krishnamurthy, S. & Hampsey, M. A physiological role for gene loops in yeast. *Genes Dev* **23**, 2604-2609 (2009).

46. DeNardo, L. & Luo, L. Genetic strategies to access activated neurons. *Curr Opin Neurobiol* **45**, 121-129 (2017).

47. Maurano, M.T., *et al.* Large-scale identification of sequence variants influencing human transcription factor occupancy in vivo. *Nat Genet* **47**, 1393-1401 (2015).

48. Vierbuchen, T.*, et al.* AP-1 Transcription Factors and the BAF Complex Mediate Signal-Dependent Enhancer Selection. *Mol Cell* **68**, 1067-1082 e1012 (2017).

49. Del Blanco, B.*, et al.* CBP and SRF co-regulate dendritic growth and synaptic maturation. *Cell Death Differ* Mar 8. doi: 10.1038/s41418-019-0285-x (2019).

50. Scandaglia, M.*, et al.* Loss of Kdm5c Causes Spurious Transcription and Prevents the Fine-Tuning of Activity-Regulated Enhancers in Neurons. *Cell reports* **21**, 47-59 (2017).

Supplemental figures:

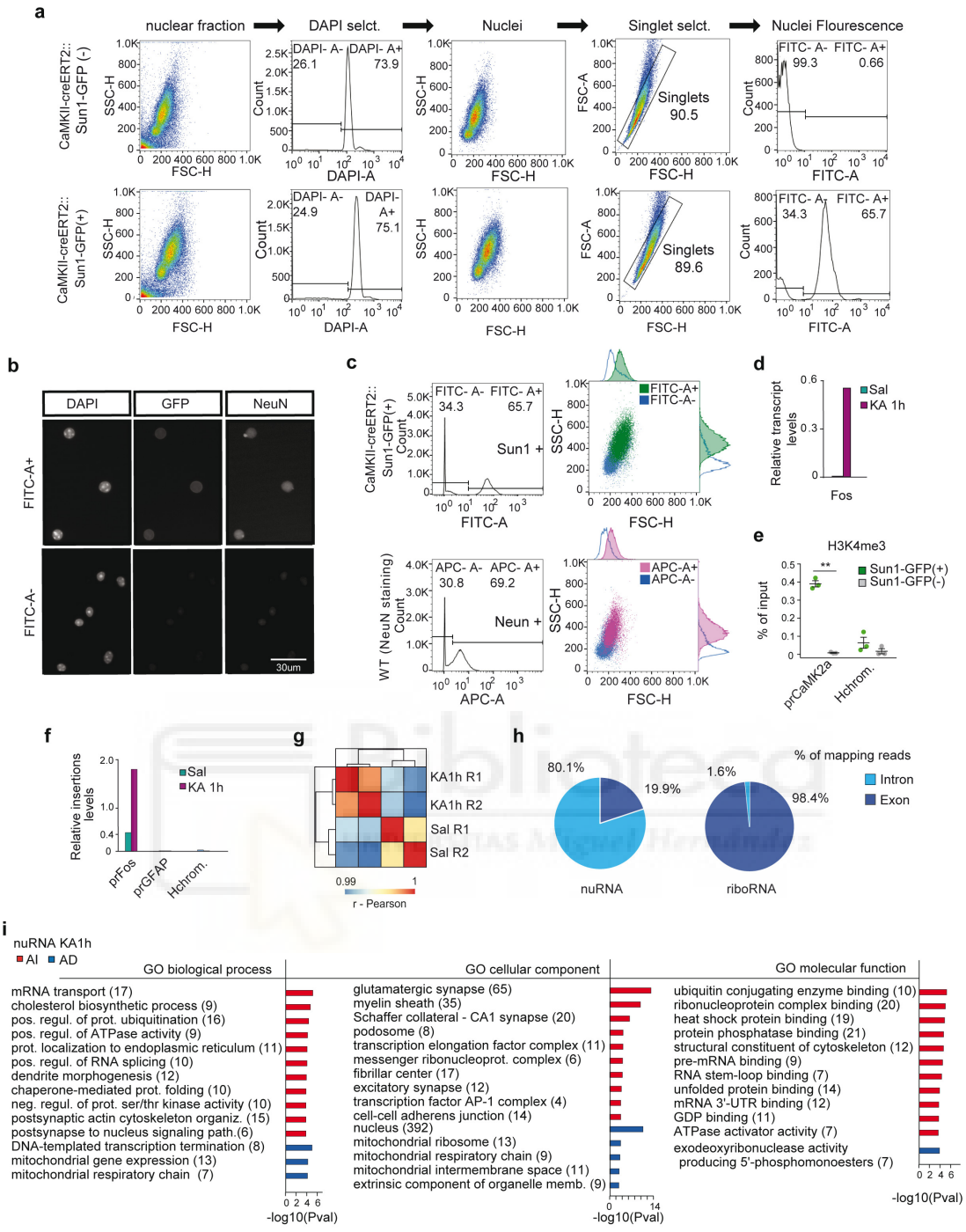
a
nuclear fraction
DAPI selct.
Nuclei
Singlet selct.
Nuclei Flourescence
CaMKII-creERT2:: Sun1-GFP (-)
CaMKII-creERT2:: Sun1-GFP(+)
SSC-H
FSC-H
DAPI-A
FSC-A
FITC-A
Count
DAPI- A- 26.1
DAPI- A+ 73.9
Singlets 90.5
FITC- A- 99.3
FITC- A+ 0.66
DAPI- A- 24.9
DAPI- A+ 75.1
Singlets 89.6
FITC- A- 34.3
FITC- A+ 65.7
b
DAPI
GFP
NeuN
FITC-A+
FITC-A-
30um
c
Sun1 +
FITC-A+
FITC-A-
APC- A- 30.8
APC- A+ 69.2
Neun +
WT (NeuN staining)
APC-A
APC-A+
APC-A-
d
Relative transcript levels
Sal
KA 1h
Fos
e
H3K4me3
Sun1-GFP(+)
Sun1-GFP(-)
% of input
prCaMK2a
Hchrom.
f
Relative insertions levels
prFos
prGFAP
g
KA1h R1
KA1h R2
Sal R1
Sal R2
r - Pearson
h
% of mapping reads
Intron
Exon
80.1%
19.9%
1.6%
98.4%
nuRNA
riboRNA
i
nuRNA KA1h
AI
AD
GO biological process
mRNA transport (17)
cholesterol biosynthetic process (9)
pos. regul. of prot. ubiquitination (16)
pos. regul. of ATPase activity (9)
prot. localization to endoplasmic reticulum (11)
pos. regul. of RNA splicing (10)
dendrite morphogenesis (12)
chaperone-mediated prot. folding (10)
neg. regul. of prot. ser/thr kinase activity (10)
postsynaptic actin cytoskeleton organiz. (15)
postsynapse to nucleus signaling path.(6)
DNA-templated transcription termination (8)
mitochondrial gene expression (13)
mitochondrial respiratory chain (7)
-log10(Pval)
GO cellular component
glutamatergic synapse (65)
myelin sheath (35)
Schaffer collateral - CA1 synapse (20)
podosome (8)
transcription elongation factor complex (11)
messenger ribonucleoprot. complex (6)
fibrillar center (17)
excitatory synapse (12)
transcription factor AP-1 complex (4)
cell-cell adherens junction (14)
nucleus (392)
mitochondrial ribosome (13)
mitochondrial respiratory chain (9)
mitochondrial intermembrane space (11)
extrinsic component of organelle memb. (9)
-log10(Pval)
GO molecular function
ubiquitin conjugating enzyme binding (10)
ribonucleoprotein complex binding (20)
heat shock protein binding (19)
protein phosphatase binding (21)
structural constituent of cytoskeleton (12)
pre-mRNA binding (9)
RNA stem-loop binding (7)
unfolded protein binding (14)
mRNA 3'-UTR binding (12)
GDP binding (11)
ATPase activator activity (7)
exodeoxyribonuclease activity producing 5'-phosphomonoesters (7)
-log10(Pval)

Supplementary Figure 1. KA-induced neuronal activation causes broad changes in the nuclear transcriptome. a. Step by step analysis and channel filtering (percentage of the filtered population indicated within the channel) of flow cytometry signal for the specific isolation of florescent singlet nuclei. Shown the comparison of intrinsic fluorescence in Sun1-GFP$^-$ (above) *vs* Sun1-GFP$^+$ (below) mice. Similar results were obtained in 25 independent experiments. **b.** Images of isolated nuclei immunostained with antibodies against GFP and the neuronal marker NeuN. Similar results were obtained in 3 independent experiments. **c.** Comparison of nuclear size of Sun1- GFP$^+$ (green) and wildtype nuclei stained with NeuN (pink). Similar results were obtained in 3 independent experiments. **d.** RT-qPCR in nuclear RNA showing Fos transcript levels in GFP positive nuclei after KA-induced SE (levels referred to GAPDH expression). **e.** ChIP-qPCR assay analysis for H3K4me3 in GFP positive and negative nuclei showing FANS specificity (values are normalized to input). Hchrom: heterochromatin; pr: promoter. Sun1-GFP(-) n = 3; Sun1-GFP(+) n = 3, biologically independent samples. Bars indicate mean ± s.e.m. Two-sided t-test, **: p-value < 0.005. **f.** ATAC-qPCR assay showing specificity and promoter changes 1 h after KA-induced neuronal activation in GFP positive nuclei (levels referred to the *Gapdh* promoter). Hchrom: heterochromatin; pr: promoter. **g.** Pearson correlation matrix between normalized samples clustered by Euclidian dendrogram. Sal n = 2; KA-1h n = 2, biologically independent samples. **h.** Percentage of nuRNA-seq reads aligned into exons and introns. For comparison, we also present the values for riboRNA-seq samples. **i.** GO enrichment analysis for protein-coding DETs that are activity-induced (AI, red bars) or activity-depleted (AD, blue bars) by SE after PANTHER analysis. The number of genes associated with each GO term is indicated. Sal n = 2; KA-1h n = 2, biologically independent samples.

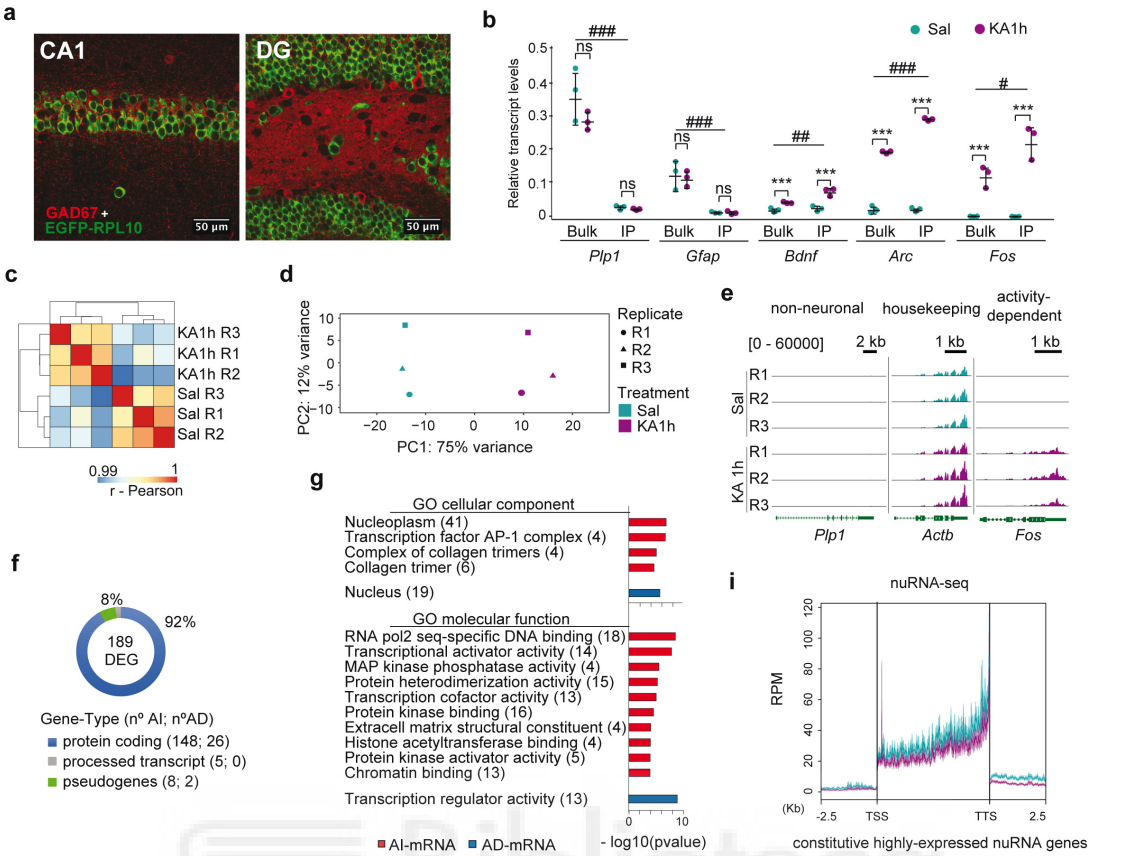
a
CA1
DG
GAD67 +
EGFP-RPL10
50 µm
b
Sal
KA1h
Relative transcript levels
Bulk
IP
Plp1
Gfap
Bdnf
Arc
Fos
c
KA1h R3
KA1h R1
KA1h R2
Sal R3
Sal R1
Sal R2
r - Pearson
d
PC2: 12% variance
PC1: 75% variance
Replicate
Treatment
e
non-neuronal
housekeeping
activity-dependent
Actb
f
8%
92%
189 DEG
Gene-Type (nº AI; nºAD)
protein coding (148; 26)
processed transcript (5; 0)
pseudogenes (8; 2)
g
GO cellular component
Nucleoplasm (41)
Transcription factor AP-1 complex (4)
Complex of collagen trimers (4)
Collagen trimer (6)
Nucleus (19)
GO molecular function
RNA pol2 seq-specific DNA binding (18)
Transcriptional activator activity (14)
MAP kinase phosphatase activity (4)
Protein heterodimerization activity (15)
Transcription cofactor activity (13)
Protein kinase binding (16)
Extracell matrix structural constituent (4)
Histone acetyltransferase binding (4)
Protein kinase activator activity (5)
Chromatin binding (13)
Transcription regulator activity (13)
AI-mRNA
AD-mRNA
- log10(pvalue)
i
nuRNA-seq
RPM
TSS
TTS
constitutive highly-expressed nuRNA genes
h
AI
Discordant
AD
riboRNA
nuRNA
Egr1
Egr2
Egr3
Arc
Bdnf
Col6a1
Zfp108
Zfp128

Supplementary Figure 2. SE-induced RNA translation activates nucleus-related functions. a. Confocal images of principal hippocampal neurons in the DG and CA1 subfield of CaMKII-creERT2::GFP-L10a mice stained against GFP (green) and the interneuron marker GAD67 (red). Cells positive for GAD67 do not express GFP. Similar results were obtained in 3 independent experiments. **b.** RT-qPCR assay comparing transcript levels before IP (Bulk) and after immunoprecipitation (IP). Note that fold changes for IEG induction were larger after TRAPping. Sal n = 3; KA-1h n = 3, biologically independent samples. Bars indicate mean ± s.e.m. 2-way ANOVA p-values: * = treatment effect (KA 1h *vs* Sal); # = procedure effect (IP *vs* Bulk). */#: $p < 0.05$; **/##: $p < 0.01$; ***/###: $p < 0.001$; ns: non significant. **c.** Pearson correlation matrix between normalized riboRNA-seq samples clustered by Euclidian dendrogram. Sal n = 3; KA-1h n = 3, biologically independent samples. **d.** Principal component analysis of riboRNA-seq samples. Sal n = 3; KA-1h n = 3, biologically independent samples. **e.** Genomic snapshots for each replicate riboRNA-seq track at representative examples of non-neuronal (*Plp1*), housekeeping (*ActB*) and activity-induced (*Fos*) genes. Values indicate the number of counts in RPM. **f.** Gene biotype classification for DTGs 1h after KA. **g.** GO enrichment analysis for protein-coding genes displaying enhanced (red bars) or reduced (blue bars) translation upon SE after PANTHER analysis. The number of genes associated with each GO term is indicated. Sal n = 3; KA-1h n = 3, biologically independent samples. **h.** Comparison of nuRNAseq and riboRNAseq tracks for representative transcripts that are either detected as upregulated or downregulated in both screens (but showing largest changes in nuRNA-seq), or that show discordant changes in the two screens. Values indicate the levels of counts in RPM. **i.** Metagene mapability profiles for nuRNA-seq at a group of constitutive highly expressed genes. Compare the region downstream of the TTS for this group and the IEGs presented in **Fig. 2k**; the two groups contain the same number of genes.

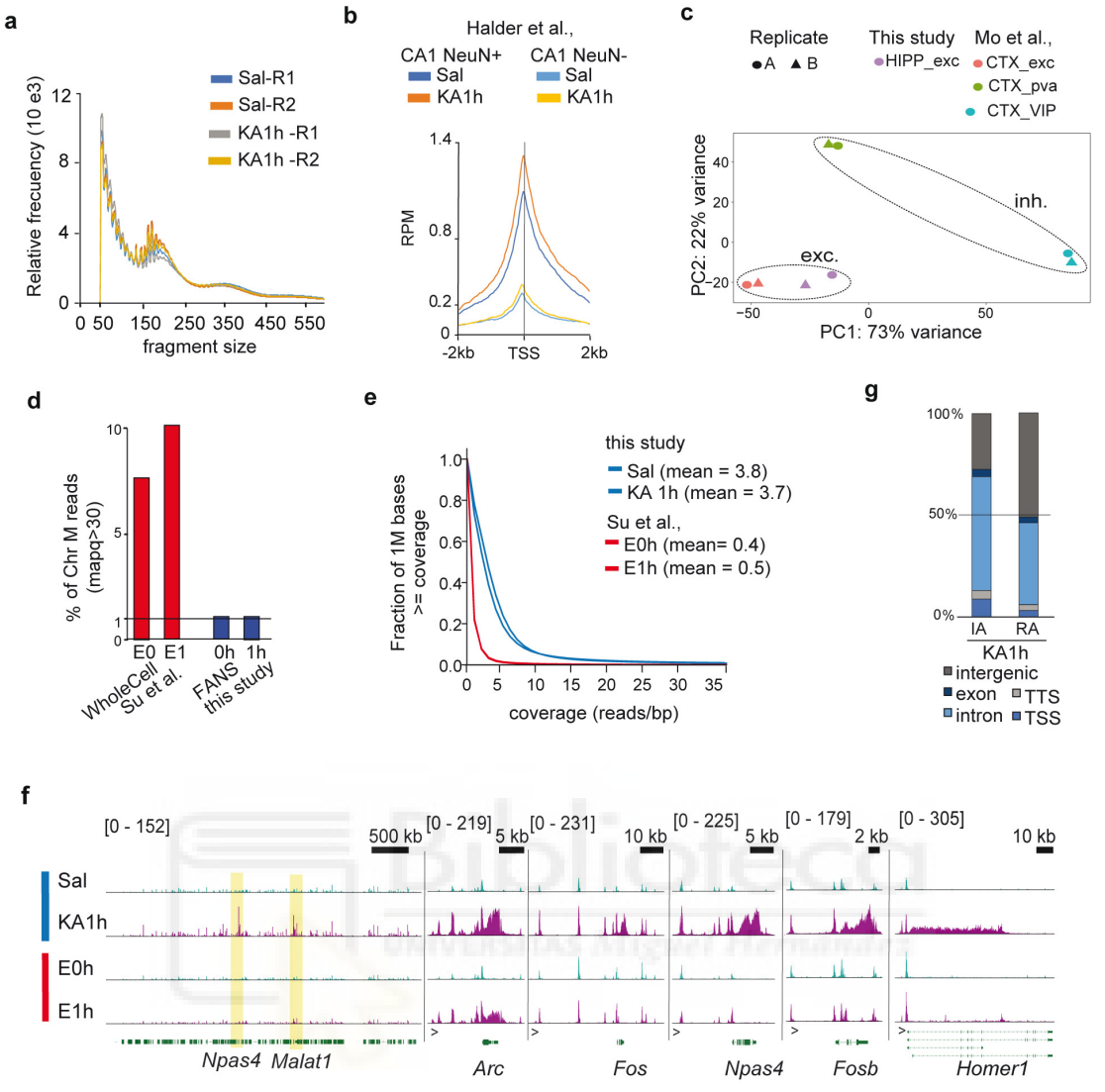
a
Relative frecuency (10 e3)
fragment size
Sal-R1
Sal-R2
KA1h -R1
KA1h -R2
b
Halder et al.,
CA1 NeuN+
CA1 NeuN-
Sal
KA1h
RPM
-2kb
TSS
2kb
c
Replicate
A B
This study
HIPP_exc
Mo et al.,
CTX_exc
CTX_pva
CTX_VIP
PC2: 22% variance
PC1: 73% variance
inh.
exc.
d
% of Chr M reads (mapq>30)
E0 E1 0h 1h
WholeCell Su et al.
FANS this study
e
Fraction of 1M bases >= coverage
coverage (reads/bp)
this study
Sal (mean = 3.8)
KA 1h (mean = 3.7)
Su et al.,
E0h (mean= 0.4)
E1h (mean = 0.5)
g
100%
50%
0%
IA RA
KA1h
intergenic
exon
intron
TTS
TSS
f
[0 - 152]
[0 - 219]
[0 - 231]
[0 - 225]
[0 - 179]
[0 - 305]
500 kb
5 kb
10 kb
5 kb
2 kb
10 kb
Sal
KA1h
E0h
E1h
Npas4
Malat1
Arc
Fos
Npas4
Fosb
Homer1

Supplementary Figure 3. Transcriptional bursting increases accessibility at IEGs. a. Fragment size distribution in ATAC-seq libraries. **b.** ATAC-seq signal at the TSS of highly expressed genes in $NeuN^+$ *vs* $NeuN^-$ CA1 cells (Halder et al. 2016, *Nat Neurosci* 19, 102-10). **c.** PCA of accessibility profiles shows similarity between cortical (Mo et al. 2015, *Neuron* 86, 1369-84) and hippocampal excitatory neurons (this study). CTX_exc: cortical excitatory neurons, n = 2 ; CTX_VIP: vasoactive intestinal peptide-expressing interneurons, n = 2; CTX_PV: parvalbumin-expressing interneurons, n = 2; HIPP_exc: hippocampal excitatory neurons, n = 2, biologically independent samples. **d.** Percentage of reads mapped into nuclear and mitochondrial chromosomes in this study and (Su et al. 2017, *Nat Neurosci* 20, 476-83). **e.** Genome coverage in this study and (Su et al. 2017, *Nat Neurosci* 20, 476-83). E0 and E1: chromatin profiling coverage before (E0) and 1 h after synchronous electrical neuronal activation (E1). **f.** Comparison of genomic profiles at control and activity-regulated genes, including an extended view of the *Npas4* locus. Discrepancies may result from the superior genomic coverage and intrinsic differences between stimulation paradigms (chemical *vs.* electrical) and composition of the samples (hippocampal glutamatergic neurons nuclei *vs.* microdissected DG tissue). **g.** Distribution of genomic features along differentially accessible regions.

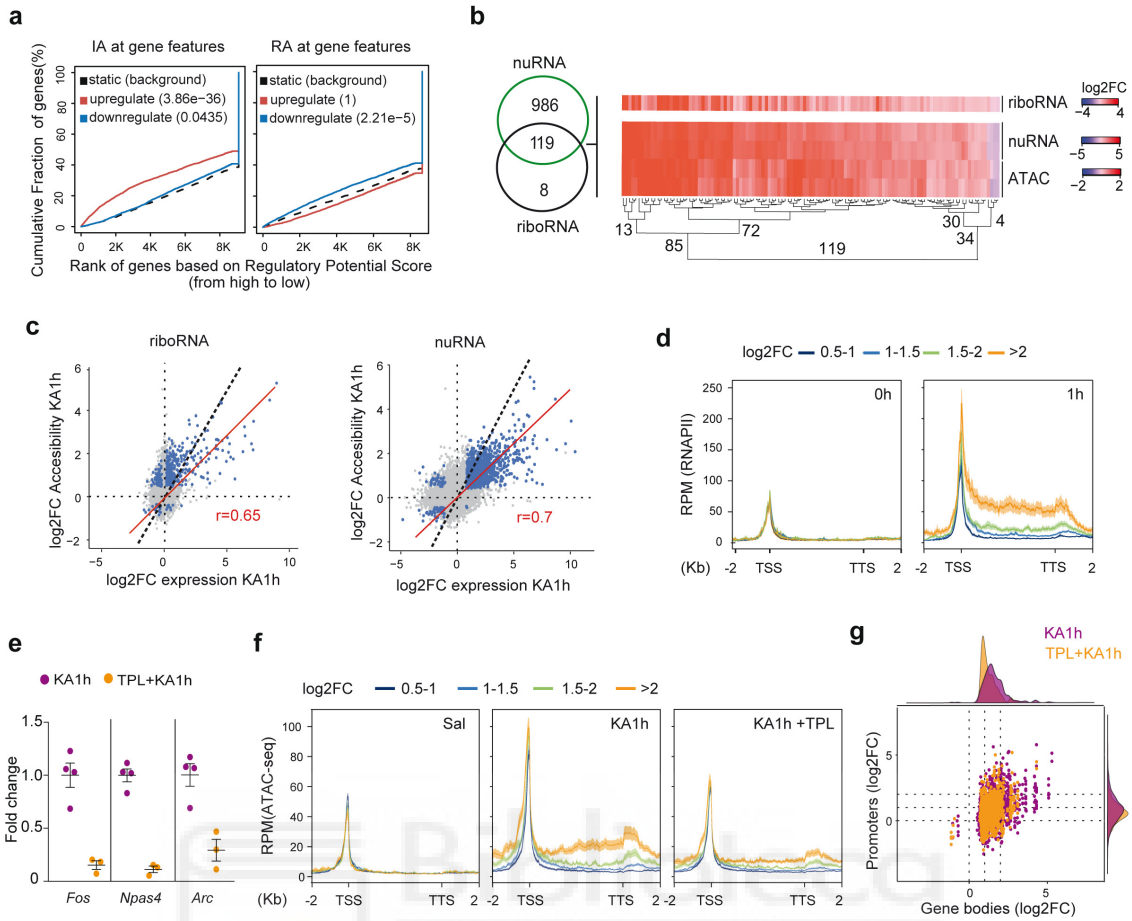
a
IA at gene features
RA at gene features
static (background)
upregulate (3.86e−36)
downregulate (0.0435)
upregulate (1)
downregulate (2.21e−5)
Cumulative Fraction of genes(%)
Rank of genes based on Regulatory Potential Score
(from high to low)
b
nuRNA
986
119
8
riboRNA
log2FC
riboRNA
nuRNA
ATAC
c
riboRNA
nuRNA
log2FC Accesibility KA1h
log2FC expression KA1h
r=0.65
r=0.7
d
log2FC 0.5-1 1-1.5 1.5-2 >2
0h
1h
RPM (RNAPII)
(Kb) -2 TSS TTS 2
e
KA1h TPL+KA1h
Fold change
Fos
Npas4
Arc
f
log2FC 0.5-1 1-1.5 1.5-2 >2
Sal
KA1h
KA1h +TPL
RPM(ATAC-seq)
g
KA1h
TPL+KA1h
Promoters (log2FC)
Gene bodies (log2FC)

Supplementary Figure 4. Correlation of changes in chromatin accessibility and transcription. a. Predictive analysis of activating/repressive function for accessibility changes at regions displaying increased (IA) or reduced accessibility (RA) within the gene body and correlation with changes in nuclear transcript levels. **b.** Left: Overlap between activity-induced genes detected in the nuRNA-seq and riboRNA-seq screens that show increased accessibility. Right: Heatmap representation of changes in accessibility and transcript levels in the 119 overlapping genes. **c.** Scatter plots showing the correlation between chromatin accessibility changes at gene bodies (Y-axis) and transcript levels determined by DESeq2 analysis (X-axis: left graph, riboRNA; right graph, nucRNA). Blue dots label genes significantly regulated by KA (FDR < 0.1). riboRNA: Sal n = 3; KA-1h n = 3; nuRNA: Sal n = 2; KA-1h n = 2, biologically independent samples. The Pearson's correlation indexes are shown **d.** Metagene plot of RNAPII occupancy in AI genes (nuRNA-seq) split according to increased gene body accessibility (FDR > 0.1) after DESeq2 analysis. RNAPII: Sal n = 1, KA-1h n = 1. **e.** RT-qPCR assays show the inhibition of IEG induction by TPL after KA-induced neuronal activation. Sal n = 4; KA-1h n = 4; TPL+KA-1h n = 3, biologically independent samples; $p < 0.001$ in the three genes. Bars indicate mean ± s.e.m. **f.** Metagene plot of ATAC-seq signal in Sal, KA-1h and KA+TPL samples; genes were split as in panel d. **g.** TPL effect on the accessibility at gene bodies and TSSs of activity-regulated genes.

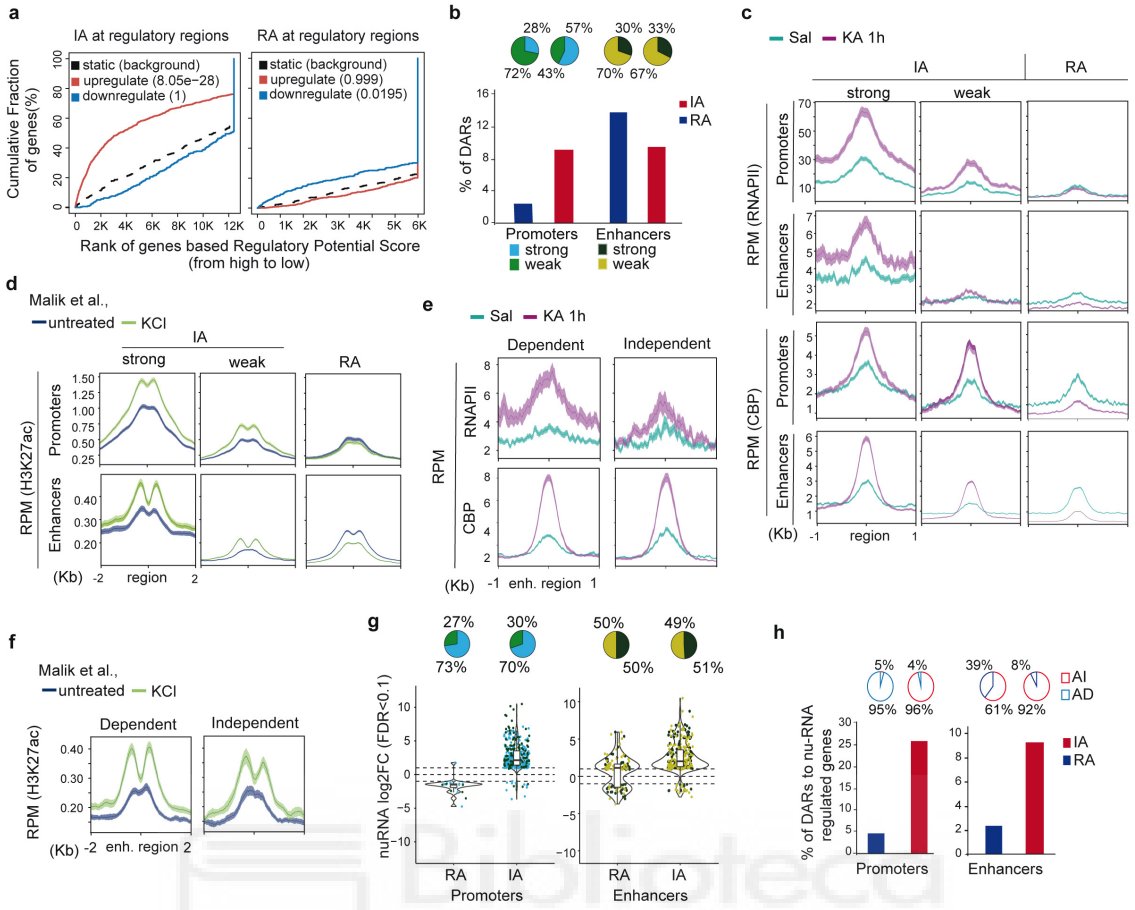

Supplementary Figure 5. Activity-dependent TF-biding. a. BETA analysis of accessibility changes at extragenic regions and associated changes in expression. IA: increased accessibility; RA: reduced accessibility. **b.** Bar plot comparing the percentages of DARs at accessible promoters and enhancers. Upper sector plots indicate percentage of strong/weak signal at IA and RA regions. **c**. Signal for RNAPII and CBP binding 1 h after KA. We compare IA and RA regions; IA regions are split between weak and strong promoters/enhancers. The solid lines indicate the mean and the shaded lines the s.e.m. RNAPII: Sal n = 1, KA-1h n = 1; CBP: Sal n = 1, KA-1h n = 2, biologically independent samples. **d**. Signal of activity regulated profiles for H3K27ac 1 h after KCl (Malik et al. 2014, *Nat Neurosci* 17, 1330-39) using the same classification than in panel c. **e.** Signal for RNAPII and CBP 1h after KA in transcriptional-dependent and independent regions. The solid lines indicate the mean and the shaded lines the s.e.m. RNAPII: Sal n = 1, KA-1h n=1; CBP: Sal n = 1, KA-1h n = 2, biologically independent samples. **f.** Signal of H3K27ac 1 h after KCl (Malik et al. 2014, *Nat Neurosci* 17, 1330-39) using the same classification than in panel e. The solid lines indicate the mean and the shaded lines the s.e.m. Untreated n = 2; KCl n = 2, biologically independent samples. **g.** Violin plots show the log2FC distribution of activity-regulated genes in KA-1h annotated with reduced (RA) or increased accessibility (IA) sites at promoters and enhancers. Note the detection of opposing changes in chromatin accessibility and transcript levels suggests the activity-dependent release of transcriptional repressors. Sector plot shows the percentage of strong and weak enhancers annotated at those genes. The boxplot indicates the median, interquartile range and min./max. Dots are colored in according to their weak or strong enhancer annotation. nuRNA: Sal n = 2, KA-1h n = 2; ATAC-seq: Sal n = 2, KA-1h n = 2, biologically independent samples. **h**. Bar plot comparing the percentage of promoter/enhancer DARs annotated to nuRNA-seq regulated genes (FDR < 0.1) after DESeq2 analysis. Upper sector plots show percentage of activity-induced (AI) and depleted (AD) genes associated with IA and RA regions. nuRNA: Sal n = 2, KA-1h n = 2; ATAC-seq: Sal n = 2, KA-1h n = 2, biologically independent samples.

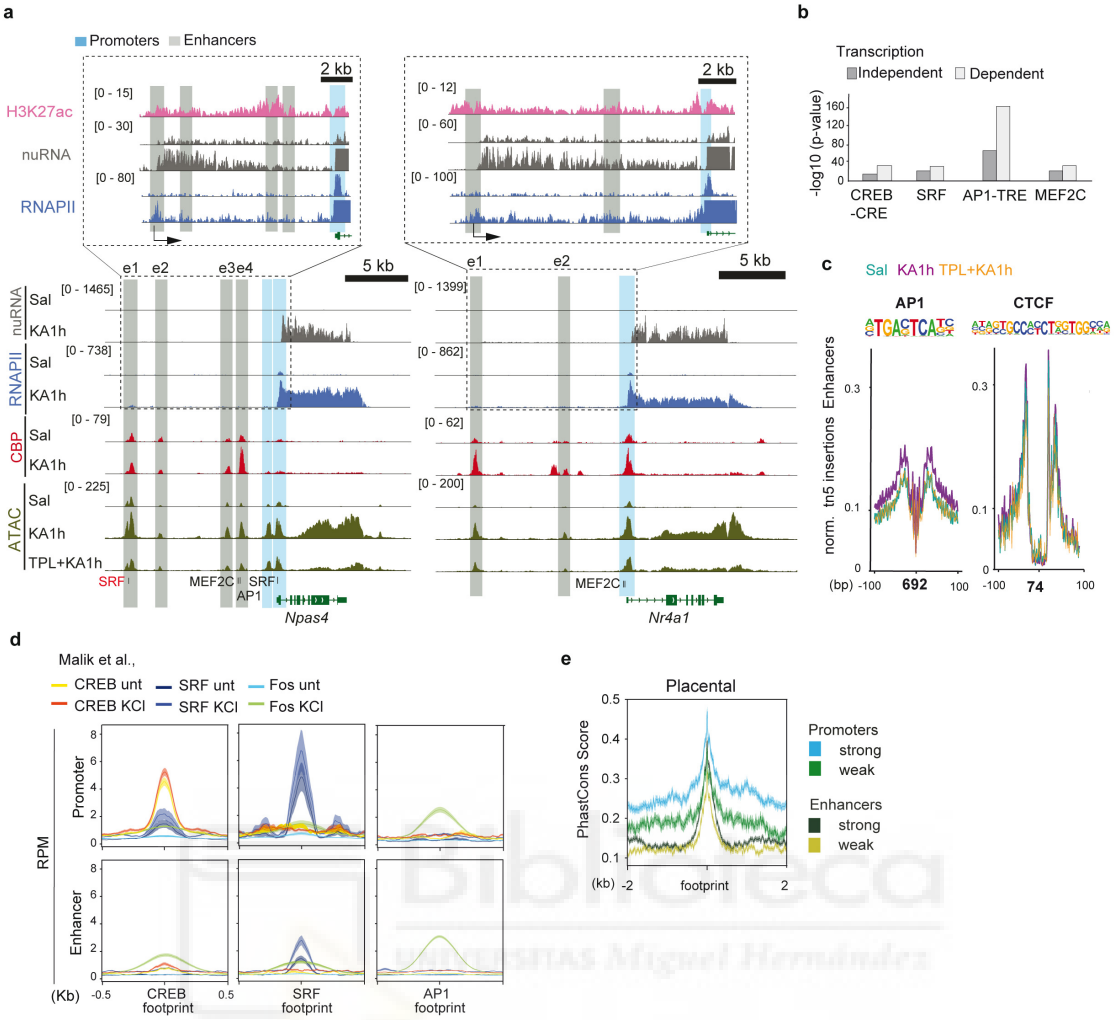

Supplementary Figure 6. Activity-dependent changes of TF footprints. a. Genomic snapshot of nuRNAs, ATAC-seq, RNAPII and CBP binding in saline, KA-1h and TPL+KA-1h samples at the *Npas4* and *Nr4a1* loci (values in RPM). Annotations label the detected footprints (in red, less stringent footprints) and classification for the regions (blue: promoters; gray: enhancers). Zoom-in inset shows upstream eRNA activity and H3K27 acetylation profile. **b.** Motif enrichment at transcription-dependent and -independent enhancers for the indicated activity-regulated TFs. **c.** Plots compare the digital footprint at AP1 and CTCF motifs in saline, KA-1h and TPL+KA-1h datasets (value correspond to normalized tn5 insertions). The bottom numbers correspond to the motifs detected in KA-1h. **d.** Signal for CREB, SRF and Fos binding 1 h after KCl stimulation of neuronal cultures (Malik et al. 2014, *Nat Neurosci* 17, 1330-39) at the detected footprints 1 h after KA in IA promoters/enhancers. The solid lines indicate the mean and the shaded lines the s.e.m. CREB: unt n = 2, KCl n = 2; SRF: unt n = 2, KCl n = 2; Fos: unt n = 2, KCl n = 2. **e.** Conservation score for the detected footprints at IA promoter/enhancer regions. The shaded lines indicate the s.e.m.

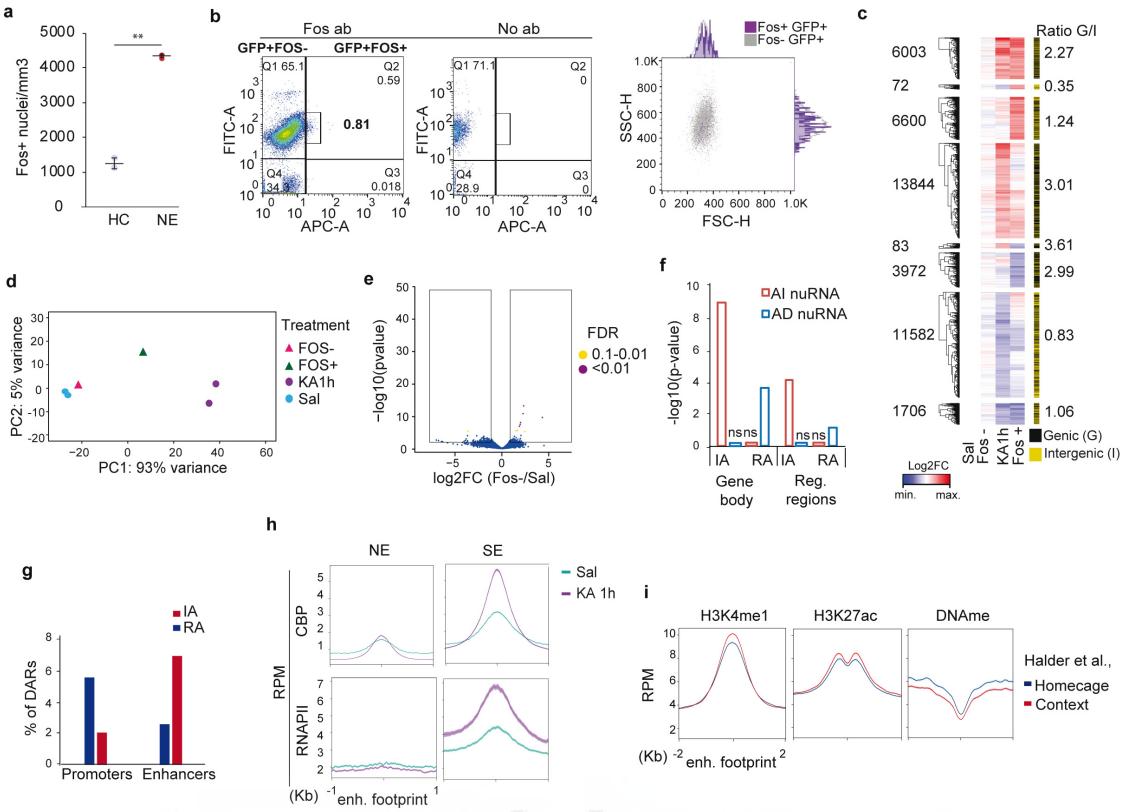

Supplementary Figure 7. Chromatin changes upon physiological neuronal activation. **a**. Number of Fos+ nuclei in the dentate gyrus of mice in their home cage (HC) and after 1 h of novelty exploration (NE). HC n = 2, NE n = 2, biologically independent samples. Bars indicate mean ± s.e.m. Two-sided t-test, **: p-value < 0.005. **b**. Flow cytometry analysis of populations by its fluorescent intensities with the presence or absence of Fos (percentage of the filtered population indicated within the channel) after channel filtering following our protocol for the specific isolation of fluorescent singlet nuclei in **Supp. Fig. 2a**. Right panel it is the co-localization of the size distribution of Fos^+ (purple) and GFP^+ cells (gray). Similar results were obtained in 3 independent experiments. **c.** Heat-map comparing DARs from SE and NE datasets, indicating common and exclusive regions between conditions**.** Last column is indicating the ratio of genic/intergenic regions on each subset. **d.** Principal component analysis for ATAC-seq datasets form physiologically (Fos^+ *vs* Fos^- neurons) and chemically activated (Sal *vs* KA-1h) neurons. Sal n = 2, KA-1h n = 2, Fos^+ n = 1, Fos^- n = 1, biologically independent samples. **e.** Volcano plot showing the significance value distribution after differential accessible regions after DESeq2 analysis in Fos^- neurons *vs* neurons from saline-treated mice. Sal n = 2, Fos^- n = 1. **f.** Predictive significance of accessibility changes at the regions annotated as promoter or enhancer and the change in expression of the gene after basic Activating/Repressive Function Prediction in BETA analysis. AI: activity-induced genes; AD: activity-depleted genes; IA: increased accessibility regions; RA: reduced accessibility regions. Single nucleus RNA-seq data from Lacar *et al.* 2016 (*Nat Comm* **7**, 11022): NE n = 96, HC n = 23; ATAC-seq: Fos^+ n = 1, Fos^- n = 1. **g.** Bar plot indicating the percentage of DARs in NE dataset at promoter and enhancer regions. **h.** Signal of activity regulated profiles 1 h after KA for RNAPII and CBP, comparing exclusive regions at detected enhancers' footprints in NE and SE. **i.** Signal for H3K4me1, H3K27ac and DNA methylation after fear conditioning (Halder *et al.* 2016, *Nat Neurosci* 19, 102-10) at detected NE-responding enhancers footprints.

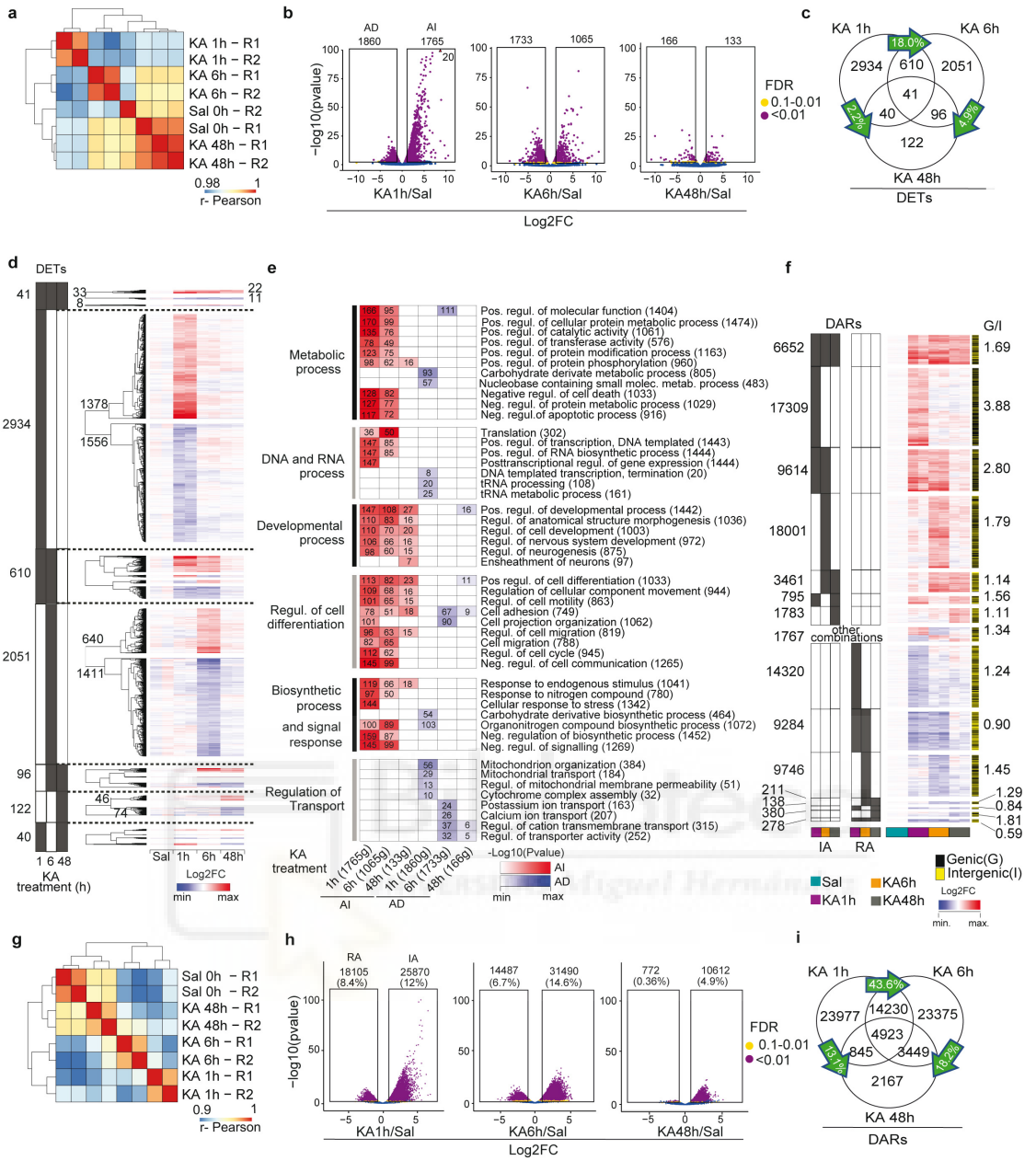
a
KA 1h − R1
KA 1h − R2
KA 6h − R1
KA 6h − R2
Sal 0h − R2
Sal 0h − R1
KA 48h − R1
KA 48h − R2
0.98
1
r- Pearson
b
AD
AI
1860
1765
1733
1065
166
133
−log10(pvalue)
KA1h/Sal
KA6h/Sal
KA48h/Sal
Log2FC
FDR
0.1-0.01
<0.01
c
KA 1h
KA 6h
KA 48h
DETs
2934
610
2051
41
40
96
122
18.0%
22.2%
4.9%
d
DETs
KA
treatment (h)
Log2FC
min
max
e
Metabolic process
DNA and RNA process
Developmental process
Regul. of cell differentiation
Biosynthetic process and signal response
Regulation of Transport
KA treatment
-Log10(Pvalue)
AI
AD
f
DARs
G/I
other combinations
IA
RA
Sal
KA1h
KA6h
KA48h
Genic(G)
Intergenic(I)
Log2FC
g
Sal 0h − R1
Sal 0h − R2
KA 48h − R1
KA 48h − R2
KA 6h − R1
KA 6h − R2
KA 1h − R1
KA 1h − R2
0.9
1
r- Pearson
h
RA
IA
18105 (8.4%)
25870 (12%)
14487 (6.7%)
31490 (14.6%)
772 (0.36%)
10612 (4.9%)
−log10(pvalue)
KA1h/Sal
KA6h/Sal
KA48h/Sal
Log2FC
FDR
0.1-0.01
<0.01
i
KA 1h
KA 6h
KA 48h
DARs
23977
14230
23375
4923
845
3449
2167
43.6%
13.7%
16.2%

Supplementary Figure 8. Chromatin accessibility dynamics shows changes that stay long after the transcriptional burst. a. Pearson correlation matrix between normalized samples clustered by Euclidian dendrogram for nuRNA-seq. Sal n = 2, KA-1h n = 2, KA-6h n = 2, KA-48h n = 2, biologically independent samples. **b.** Volcano plot showing the significance of differential gene expression by DESeq2 analysis in nuRNA-seq samples 1 h, 6 h and 48 h after KA administration. AI: activity-induced; AD: activity-depleted. Sal n = 2, KA-1h n = 2, KA-6h n = 2, KA-48h n = 2. **c.** Venn diagram presenting the overlaps between the sets of DETs at each time point in the longitudinal nuRNA-seq analysis. Almost 20% of the changes observed 1 h after KA-treatment are still detected 5 h later, whereas only 2% remain 2 days later. **d.** Heatmap for FC in nuRNA-seq analysis. **e.** Heatmap of fold enrichment for biological process GO terms detected in AI and AD genes by PANTHER analysis in the nuRNA-seq longitudinal analysis using DESeq2. The numbers indicate the number of genes associated with each term. Sal n = 2, KA-1h n = 2, KA-6h n = 2, KA-48h n = 2, biologically independent samples**. f.** Heatmap comparing DARs at the different time points**.** The last column (black/ yellow) shows the ratio of genic/intergenic regions on each subset. IA: increased accessibility; RA: reduced accessibility **g.** Pearson correlation matrix between normalized samples clustered by Euclidian dendrogram for ATAC-seq. Sal n = 2, KA-1h n = 2, KA-6h n = 2, KA-48h n = 2. **h.** Volcano plot showing the significance value of differential accessible regions after DESeq2 analysis in ATAC-seq samples 1 h, 6 h and 48 h after KA administration. IA: increased accessibility; RA: reduced accessibility. Sal n = 2, KA-1h n = 2, KA-6h n = 2, KA-48h n = 2**. i.** Venn diagram presenting the overlaps between the sets of DARs at each time point in the longitudinal ATAC-seq analysis.

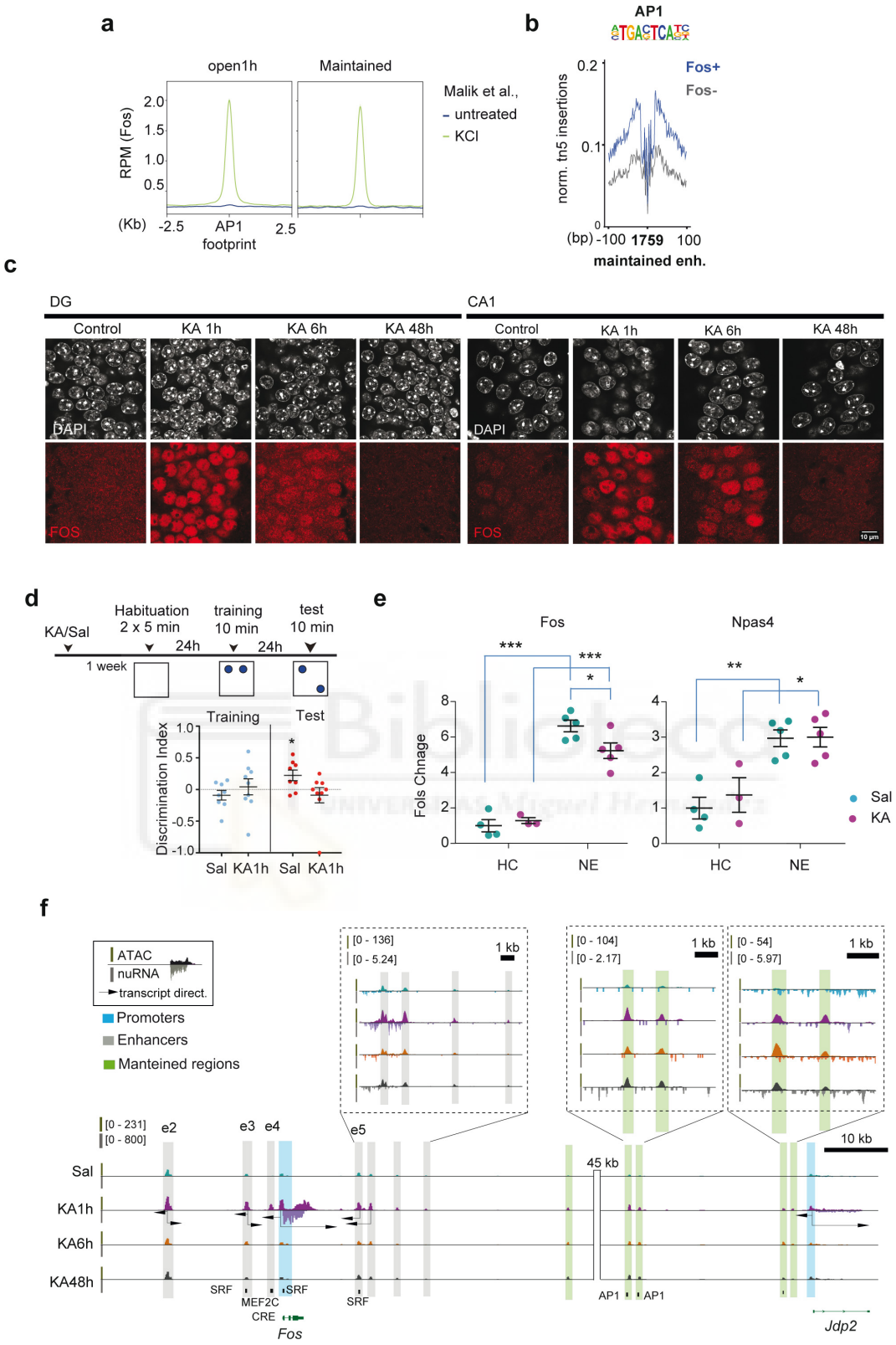
a
open1h
Maintained
RPM (Fos)
2.0
1.5
1.0
0.5
(Kb) -2.5 AP1 2.5
footprint
Malik et al.,
untreated
KCl
b
AP1
Fos+
Fos-
norm. tn5 insertions
0.2
0.1
0
(bp) -100 1759 100
maintained enh.
c
DG
CA1
Control
KA 1h
KA 6h
KA 48h
DAPI
FOS
d
KA/Sal
Habituation
2 x 5 min
training
10 min
test
10 min
24h
24h
1 week
Training
Test
Discrimination Index
Sal KA1h Sal KA1h
e
Fos
Npas4
Fols Chnage
HC
NE
Sal
KA
f
ATAC
nuRNA
transcript direct.
Promoters
Enhancers
Manteined regions
[0 - 136]
[0 - 5.24]
[0 - 104]
[0 - 2.17]
[0 - 54]
[0 - 5.97]
1 kb
[0 - 231]
[0 - 800]
e2
e3
e4
e5
10 kb
45 kb
Sal
KA1h
KA6h
KA48h
SRF
MEF2C
CRE
Fos
AP1
Jdp2

Supplementary Figure 9. Long-lasting chromatin accessibility changes are associated with AP1 binding and disease. a. Signal for Fos binding 1 h after KCl stimulation of neuronal cultures (Malik et al. 2014, *Nat Neurosci* 17, 1330-39) at the detected footprints in enhancer regions showing long-lasting changes in accessibility. **b.** Plot shows the footprinted sites at the maintained AP1 motifs detected in our longitudinal analysis (profile indicate the normalized tn5 insertions). **c.** Immunostaining for Fos in granular neurons at the DG and pyramidal neurons at the CA1 subfield at different time points after KA. Similar results were obtained in 3 independent experiments. **d.** Top: Scheme of object location memory (NOL) test. The time intervals from KA-induced SE to NOL training and testing are indicated. Bottom: Preference index for the displaced object in naïve mice and in mice that suffered SE one week earlier in the NOL test. One-sided t-test (compared to 0) *: p-value < 0.05. Furthermore, saline-treated mice show a larger discrimination index during testing than training (p = 0.03), while the mice that received KA do not show a significant difference (p = 0.56). Sal n = 8, KA-1h n = 9, biologically independent samples. Bars indicate mean ± s.e.m. **e.** RT-qPCR assay for *Fos* and *Npas4* in RNA samples extracted 1 h after NE in animals that suffered SE two weeks earlier. FC values are referred to the home cage situation. These two IEGs are strongly induced during SE but only *Fos* is in the proximity of DARs showing long-lasting changes in accessibility. HC: Sal n = 4, KA-1h n = 3; NE: Sal n = 5, KA-1h n = 5, biologically independent samples. Bars indicate mean ± s.e.m. Two-sided t-test, *: p-value < 0.05, **: p-value < 0.01, ***: p-value < 0.001. **f.** Genomic screenshots for the *Fos/Jdp2 locus* (an example of activity-regulated gene that returns to basal expression but still maintains some proximal chromatin accessibility changes after 48 h). Footprint motifs for SRF, AP1, CRE, MEF2C are labeled. DARs are colored depending on their location in a promoter or enhancer. The maintained DARs after 48 h are labeled in green. Values show counts in RPM.

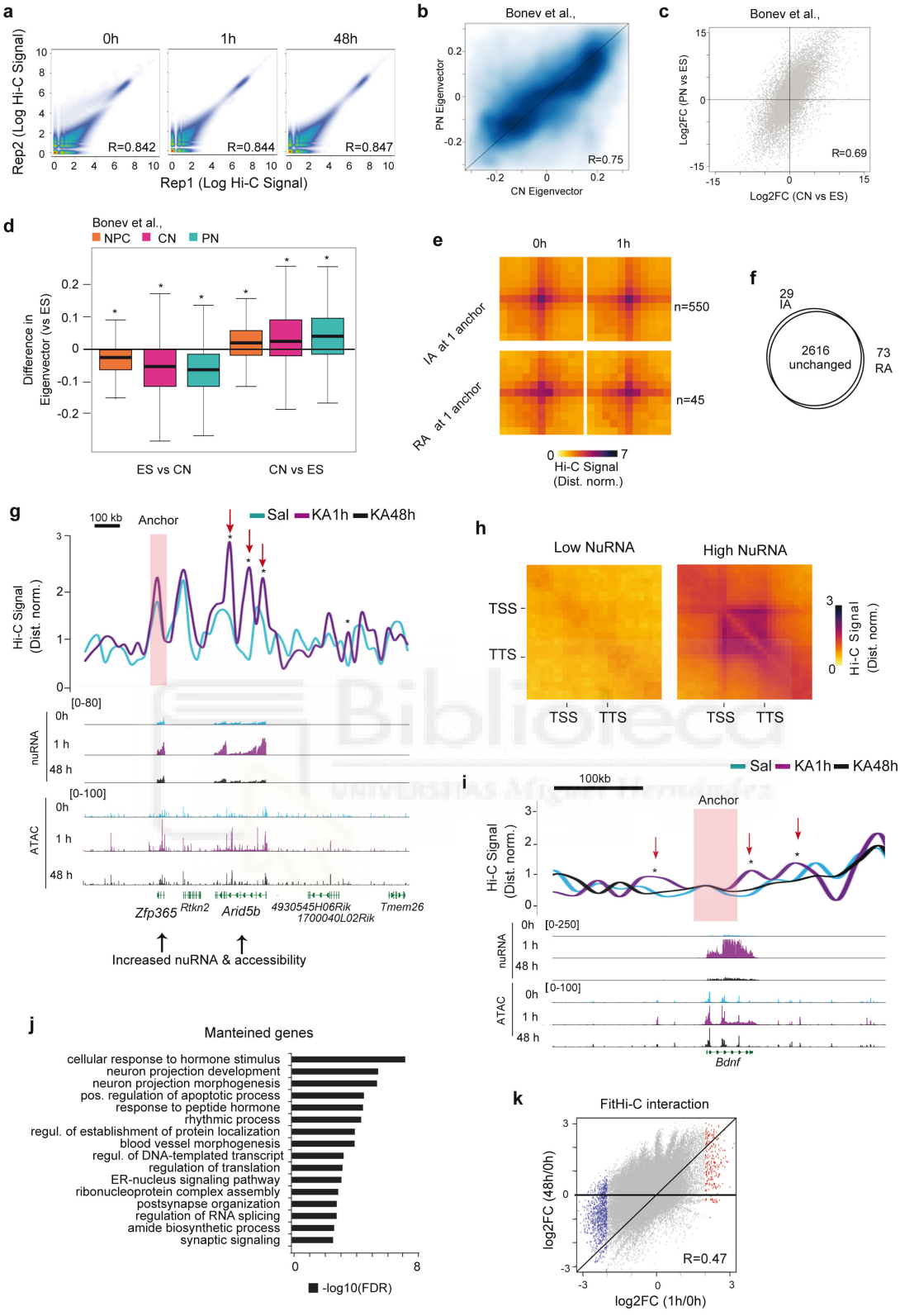
a
0h
1h
48h
Rep2 (Log Hi-C Signal)
Rep1 (Log Hi-C Signal)
R=0.842
R=0.844
R=0.847
b
Bonev et al.,
PN Eigenvector
CN Eigenvector
R=0.75
c
Bonev et al.,
Log2FC (PN vs ES)
Log2FC (CN vs ES)
R=0.69
d
Bonev et al.,
NPC
CN
PN
Difference in Eigenvector (vs ES)
ES vs CN
CN vs ES
e
0h
1h
IA at 1 anchor
RA at 1 anchor
n=550
n=45
Hi-C Signal (Dist. norm.)
f
29
IA
2616
unchanged
73
RA
g
100 kb
Anchor
Sal
KA1h
KA48h
Hi-C Signal (Dist. norm.)
nuRNA
ATAC
[0-80]
[0-100]
0h
1 h
48 h
Zfp365
Rtkn2
Arid5b
4930545H06Rik
1700040L02Rik
Tmem26
Increased nuRNA & accessibility
h
Low NuRNA
High NuRNA
TSS
TTS
Hi-C Signal (Dist. norm.)
i
100kb
Anchor
Sal
KA1h
KA48h
Hi-C Signal (Dist. norm.)
nuRNA
ATAC
[0-250]
[0-100]
Bdnf
j
Manteined genes
cellular response to hormone stimulus
neuron projection development
neuron projection morphogenesis
pos. regulation of apoptotic process
response to peptide hormone
rhythmic process
regul. of establishment of protein localization
blood vessel morphogenesis
regul. of DNA-templated transcript
regulation of translation
ER-nucleus signaling pathway
ribonucleoprotein complex assembly
postsynapse organization
regulation of RNA splicing
amide biosynthetic process
synaptic signaling
-log10(FDR)
k
FitHi-C interaction
log2FC (48h/0h)
log2FC (1h/0h)
R=0.47

Supplementary Figure 10. Hi-C analysis of activity-driven interactions. a. Pearson correlation between Hi-C replicate samples at 0 h (saline), 1 h and 48 h after KA administration. Sal n = 2, KA-1h n = 2, KA-48h n = 2, biologically independent samples. Comparison between all possible (over 600 millions) intrachromosomal bins. **b.** Comparison of compartmental eigenvectors in mature excitatory principal neurons (PN) and cortical neurons differentiated *in vitro* (iv-CN) (Bonev et al. 2017, *Cell* 171, 557-72). R = 0.75 Pearson correlation (n = 101,812 loci). **c.** Difference in gene expression between PN and iv-CN compared to embryonic stem cells (ES) (Bonev et al. 2017, *Cell* 171, 557-72). R = 0.69 Pearson correlation (n = 23,418 loci). **d.** Difference in the compartmental eigenvectors in cortical neurons (pink) and principle neurons (blue) vs embryonic stem cells for genes that are higher in ES vs iv-CN (ES vs CN) or vice versa (CN vs ES) (Bonev et al. 2017, *Cell* 171, 557-72). The boxplot indicates the median, interquartile range and min./max. Two-sided Wilcoxon rank sum test. Left side: n = 5,241. Right side: n = 14,735. All p-values are < 2.2e-16 (lower than the lowest calculated by R). **e.** Metaplot of CTCF loops where at least one anchor overlaps a differential ATAC-seq peak after DESeq2 analysis indicating that CTCF loops do not change during neuronal activation despite changes to other transcription factors. IA: increased accessibility, RA: reduced accessibility. Sample sizes are indicated at the right of the heatmaps. **f.** Venn Diagram of CTCF loops in KA-1h and saline samples. The low number of changes (< 4%, below the FDR level) indicates no real change. **g.** Snapshot of a locus presenting strong *de novo* Hi-C interactions in response to SE. Significant differences were tested for enrichment in KA-1h samples using a one-sided confidence interval using all interaction bins in the immediate vicinity (n = 81). Significance was assigned if fold change was above a 99.9% confidence interval giving rise to p < 0.001. Hi-C changes correlate with the reported changes in nuRNA production and chromatin accessibility. **h.** Heatmap of Hi-C interactions at genes with low or high nuRNA-seq signal (Hi-C signal normalized by distance). **i.** Snapshot for *Bdnf* (an example of activity-regulated gene that return to basal expression). The central area is shown with greater detail in **Fig. 7g**. Values show counts in RPM. Significant differences were tested and assigned as indicated in panel g (n = 16). **j.** GO enrichment after PANTHER analysis for the set of genes associated with long-lasting Hi-C interactions after Fit-Hi-C analysis. **k.** Total Fit-Hi-C interactions (gray) and their changes after 1 h (x-axis) or 48 h (y-axis) compared to 0 h. Dots correspond to the interactions that show

more than a 4-fold increase (red) or decrease (blue) at 1 h. Most blue points are slightly below the horizontal, while most red points are above the horizontal, indicating that some of the SE-originated interactions are still maintained after 48 h. Pearson's correlation index is shown (n = 148,732 loci).

Inventory of supplemental tables:

Supplementary Item & Number	Title or Caption
Supplementary Table 1	Differentially expressed transcripts in nuRNA-seq
Supplementary Table 2	Differentially translated genes in riboRNA-seq
Supplementary Table 3	Differentially accessed regions in ATAC-seq and comparison with DETs in nuRNA-seq (a) and DGTs in riboRNA-seq (b), and impact of TPL treatment (c) - 3 sheets
Supplementary Table 4	ATAC-seq analysis upon novelty exploration
Supplementary Table 5	Longitudinal analysis of differentially expressed transcripts in nuRNA-seq
Supplementary Table 6	Longitudinal analysis of chromatin accessibility changes
Supplementary Table 7	Fit Hi-C values at different time points after SE
Supplementary Table 8	NGS samples and datasets generated in this study (a) and generated in other studies and analyzed here (b) - 2 sheets

Data Availability: Supplementary Tables 1 to 7 provide direct access to the main results derived from the transcriptome and epigenome screens presented in this study (follow the link to access the tables: https://www.nature.com/articles/s41593-019-0476-2). In addition, raw and processed datasets generated in the study are available in the GEO repository using the accession number GSE125068.

DISCUSSION

1. *Technological innovations in functional Neurogenomics*

The way neuroscientists interrogate brain function can be divided into two main approaches: invasive and non-invasive. Non-invasive approaches are nowadays extensively used for human brain studies but provide low-resolution data. In contrast, invasive approaches provide much more detailed anatomical, cellular and molecular information. Although they represent the standard approach in animal models, they are only exceptionally applied in humans due to ethical issues. Molecular neurobiologists cannot conduct functional studies in humans except for disease-related tissue analysis from patients (e.g., electrode implants or tissue removal in severe neurological diseases) and brain donors after death. As a result most of the progress in areas such as the molecular bases of neuronal plasticity and memory formation comes from extrapolating results obtained in animal models to the human brain. This is the case of Neurogenomics studies investigating the genomic bases of plasticity.

Such studies represent an exciting and rapidly growing area of Neurosciences thanks to the introduction of the novel next-generation DNA-sequencing technologies that enable a precise and genome-wide description of a broad and diverse range of molecular events that quantitatively and qualitatively correlate with neuronal function. For applying NGS techniques in adult brain cells, it is needed the development of novel methods for cell isolation. The first attempts for the analysis of the neuronal epigenome using ChIP-seq relied on the immunostaining of the nuclear protein NeuN for the sorting of neuronal nuclei from the mouse prefontal cortex (Jakovcevski et al., 2015). Better approaches, which are not limited by the expression of cell type-specific nuclear antigens, were recently developed for chromatin analyses in the

mouse brain. These techniques use the genetic tagging of cellular compartments, like polysomes and nuclei, for the isolation of the nucleic acids of interests from specific neuronal subpopulations (Mo et al., 2015, Dougherty et al., 2017).

This thesis takes advantage of these recent developments in neurosciences and genomics to establish novel and optimized protocols for integrative functional genomics in the adult mouse brain. We used previously developed tools for cell type- and compartment-specific tagging (Mo et al., 2015, Heiman et al., 2014), and developed novel isolation methods with increased efficiency in terms of specificity and coverage that were adapted to a broad range of NGS applications. The refinements were especially important in the case of ATAC-seq, because the transposase is highly sensible to the quantity of DNA, particularly nude DNA. The introduction of our FANS protocol allows a precise control of the number of nuclei used for library preparation and removes mitochondrial DNA , which lacks nucleosomes and is very abundant in cytoplasm and whole cell preparations, therefore improving the efficiency of the library (Corces et al., 2016). The use of FANS and Sun1-GFP tagging also provided versatility to our analyses derived from their combination with secondary sorting of the cells using nuclear antigens (e.g,, the expression of the transcription factor Fos), which allowed the sorting and analysis of the chromatin in neurons activated by a discrete physiological stimulus, such as novelty exploration, for the first time. Another important asset derived from the use of FANS is the robustness of the transcriptome data obtained from sorted nuclei when compared to sorted neurons, in which the strong stress response triggered by nervous tissue dissociation may occlude the activity-induced

changes. Furthermore, the comparison of information retrieved in the nuclear and cytoplasmic compartments allowed us to describe novel molecular and network plasticity processes in neurons.

Overall, our multi-omic approach and innovative integrative analysis revealed an unexpectedly broad and dynamic scenario with multiple levels of activity-dependent regulation and novel mechanistic insights. This progress relies in original data processing methods applied to both our own generated data and externally produced data accessible at public databases. We expect that the combination of the genetic and molecular tagging of nuclei used in this thesis will become the standard approach in neurogenomics. Furthermore, the technical developments introduced here in combination with recent progress in tagging neuronal ensembles that participate in the encoding of a particular experience (DeNardo and Luo, 2017), open up the possibility of longitudinal studies of chromatin changes linked to memory engrams. Also, it is likely that in the near future similar approaches could be used in single-cell studies and adapted to novel next generation sequencing technologies, contributing to the description of other levels of genome regulation and neuronal plasticity.

2. Transcriptional plasticity program

Many important functions of the brain depends on network plasticity, which in turn relies on a large number of complex molecular mechanisms responsible for storing or modifying previously stored information. It is hypothesized that neuronal activation induces the expression of genes in sequential waves to support circuit plasticity. These genes will encode for effector proteins that are required to consolidate synaptic changes. Historically, molecular neurobiologists

made great efforts to describe all these events, but still today there are many open questions and we might be lacking molecular mechanisms activated during plasticity. As expected, the appearance of novel molecular tools and biotechnological methods has opened novel strategies to understand these mechanisms.

This is the case of the recent progresses in transcriptomics, which in the context of this study, led us to describe for first time different RNA-related mechanisms in neurons. The comparison of ongoing translation in the cytoplasm versus nuclear transcription identified transcripts in which synaptic activity specifically regulates ribosome engagement rather than its transcription. Notably, the regulation of transcripts that are retained in the cytoplasm waiting for its binding to the ribosome was previously described in other cell types (Yamazaki et al., 2005; Schott et al., 2014; Behrens et al., 2018). These seminal results suggest that additional molecular changes in the soma or dendrites may participate in the genomic memory of the cell. For instance, we cannot discard a delayed impact at the translational regulatory level, similar to the one described here at the chromatin level. Novel molecular mechanism like epi-transcriptomics could also participate in metaplasticity, as suggested by a number of recent articles (Yoon et al., 2018).

The improved temporal resolution obtained by nuRNA profiling, revealed that the robust induction of IEGs is accompanied by the downregulation of numerous metabolism-related genes, suggesting that the activity-induced transcriptional burst transiently hijacks the transcriptional machinery. In turn, the delayed downregulation of genes involved in ion transport and synaptic transmission may contribute to homeostatic plasticity mechanisms that

compensate for prolonged activation and stabilizes neuronal firing (Fernandes and Carvalho, 2016). Notably, within the downregulated geneset, we detected neuronal identity transcription factors, such as NeuroD1, that also correlates with the lower levels of accessibility of their DNA-binding sequence in epileptic and physiological activation. This result indicates that neuronal activation is such a demanding process that transiently takes over relevant resources of the cell remarkably affecting the basal state of the neuron. Probably, neuronal activation is a risky situation if there is a long-term hijack of the transcriptional machinery, and this could explain the tight coordination of the different waves of transcription during neuronal activation.

Finally, our sequencing strategy based on the deep coverage of nuRNA-seq samples allowed us to detect the expression of numerous eRNAs with better resolution and diversity than previous studies (Kim et al., 2010). The nuRNA-seq screen also revealed the production of ecRNA in activity-induced genes that may fine-tune the activity of these loci and contribute to transcriptional memory (Savell et al., 2016). The production of these ecRNAs correlates with the activity-dependent RNAPII occupancy and increased accessibility extending slightly beyond the gene limit. Unfortunately, despite the deep coverage, could not reliably interrogate alternative splicing of expressed genes and the formation of circular RNA structure previously described in neuronal cultures or dissected brain tissue in the nuclear samples because these analyses would require an even deeper coverage (You et al., 2015; Mauger et al., 2016). Other exciting questions that would be interesting to approach in the future refer to the alternative spliced micro-exons during neuronal activation *in vivo*, described to be enriched in neuronal tissue, affected

in autism spectrum disorder and linearly correlated with animal nervous system complexity (Irimia et al., 2014). Overall, our study adds to other recent transcriptomic screens describing the complex and diverse changes associated with neuronal activation.

3. Chromatin architecture dynamics in neuronal activation

A main question in neurogenomics is in what extend basal chromatin state affects activity-driven transcription and what regulatory mechanisms orchestrate the successive gene expression waves. Previous studies approached different levels of regulation in neurons such as changes in DNA methylation (Hadler et al., 2016), the production of DNA double-strand breaks (DSB) (Madabhushi et al., 2015) or the relocation of IEGs into transcription factories (Crepaldi et al., 2013). We have extended the knowledge by the combination of nuRNA-seq, ATAC-seq, RNAPII ChIP-seq and HiC experiments in the same neuronal activation paradigm. With our integrative analysis approach, we demonstrated for first time that the robust transcription of IEGs during SE correlates with the formation of gene loops that bring together the TSS and the TTS. Such organization has been described for highly transcribed genes in yeast (Hampsey et al., 2011; Laine et al., 2009) and *Drosophila* cells (Rowley and Corces, 2018), but not in neurons. This leads us to hypothesize that the characteristic strong burst of transcriptional activity in IEG relies on the formation of gene loops to favor the continuous re-loading of the RNAPII complex. It would be interesting to understand the molecular mechanism that support the formation of these chromatin loops as well as the DNA double-strand breaks (DSB) described by Madabhushi and colleagues, which might

facilitate gene loop formation (Madabhushi et al. 2015). It will be also relevant to describe the occurrence of gene loops in different cell types and paradigms of transcriptional bursting to evaluate the conservation of these mechanisms through evolution.

Our analyses also identified hundreds of *de novo* or strengthened promoter-enhancer interactions and thousands of TF binding events in the chromatin of hippocampal excitatory neurons upon activation. Interestingly some of these changes are transcription-independent and most likely rely on the post-translational modification of protein complexes such as TF, chromatin remodelers and histone modifications. The majority of the changes were transcription-dependent and the diversity of TFs families driving those chromatin changes was influenced by the strength of the neuronal activation. Although the most prominent changes were common in both physiological and pathological stimulation, such as the increased accessibility of gene bodies and *de novo* AP1 and Mef2c binding at activity-regulated enhancers, our analyses also detected remarkable differences in the scope and magnitude of the changes. Notably, our longitudinal analyses in the context of SE retrieved changes in chromatin occupancy and enhanced interactions that persisted even 2 days after stimulation. In particular, changes in the occupancy of AP1-binding sites are detected long after the shutdown of the encoding loci and constitute a prominent part of the deferred epigenomic signature of neuronal activation. This conclusion is in agreement with the recent observation of stable accessibility changes in granular neurons 24 h after electrical stimulation and the postulated role of Fos in initiating neuronal activity-induced chromatin opening (Su et al., 2017).

Interestingly, our HiC datasets did not reveal higher order architectural changes during neuronal activation, neither we observed changes in the binding of CTCF and its expression. This means that most of the activity-induced changes occur relatively close to gene bodies and the main regulation takes place at the level of local chromatin accessibility. These results add to the previous descriptions of changes in the chromatin at proximal regulatory regions of IEG induced by transcriptional activity in neurons (Yap & Greenberg, 2018). The observation is also in agreement with a very recent study that indicates that genome topology does not play a fundamental role in the control of gene expression (Ghavi-Helm et al., 2019), supporting the idea that other type of mechanisms are directly responsible for transcription regulation.

4. Potential mechanisms of long-term chromatin changes

Recent studies have shown that during cell-type enhancer selection, AP-1 binding sites are occluded by nucleosomes but became somehow primed. After the expression of the AP-1 heterodimer, this will interact with the BAF chromatin-remodeling complex at the selected enhancer sites to remodel nucleosomes and increase the accessibility in postmitotic neurons (Vierbuchen et al., 2017; Wu et al., 2007). This model is in agreement with previous descriptions of the relevance of histone turnover and exchange during neuronal activation (Zovkic et al., 2014; Maze et al., 2015; Yang et al., 2016). Moreover, the study by Yang and colleagues suggested that genes are turned off by the activity of NuRD, a nucleosome remodeler and deacetylase complex that appear to be crucial for dendritic pruning and neural coding (Yang et al., 2016).

Intriguingly, the observed long-lasting chromatin accessibility change at AP-1 biding sites does not correlate with the kinetics of Fos and Jun expression,

the main constituent protein subunits of this TF. One possibility is that other AP-1 subunits are occupying those sites after the Fos/Jun heterodimer is back to basal levels. Alternatively, other protein complexes associated with chromatin remodeling may occupy those sites, letting them prime for a second activation. There is approximately one million AP-1 binding sites in the mammalian genome, while according to ChIP experiments Fos/Jun complexes bind to approximately 10,000 sites in the mouse genome (Vierbuchen et al., 2017). Therefore, a third possibility could be that the robust induction of AP1 subunits in response to activity might produce an excess of proteins to guarantee the occupancy of these scarce sites, but we might not have yet the technology to detect the remaining low number of protein units still bound to the chromatin.

These epigenetic changes may contribute to long-lasting or permanent changes in the expression and responsiveness of genes involved in synaptic function, thereby representing a sort of genomic memory. The experimental strategy for assessing the genomic memory might start by the selective perturbation of those sites that remain open after neuronal activation. This will probably require the use of novel technologies, like CRISPR-dCas9-based perturbations of chromatin structure, to overcome the functional redundancy and compensatory effects of eliminating individual TF subunits in neurons (Kim et al., 2010).

5. *Genomic memory: implications for disease and memory*

The enduring changes in accessibility that are associated with *de novo* AP1 binding to distal regulatory regions of activity-induced genes and with enhanced promoter-enhancer interactions may influence future activity of the loci. Since

many of these loci play important roles regulating synaptic plasticity and excitability, the experience fingerprints that persist in the chromatin may act as a form of metaplasticity by influencing the future response of the neuron to the same or other stimuli.

In the case of SE, our functional genomics analyses indicate that these long-lasting changes may relate to brain disorders such as cognitive dysfunction, dementia and neurodegenetative diseases. Intriguingly, a recent large-scale study of accessible cis-regulatory elements across multiple human tissues revealed that SNPs within AP-1 motifs, including disease-associated non coding variants, are often associated with changes in chromatin accessibility (Maurano et al., 2015, Vierbuchen et al., 2017). These results could suggest that the sites detected in our study could be useful as a potential target for the genomic treatment of the consequences of epileptic episodes. Notably, this makes sense in the pathoethology of the epilepsy, characterized by the recurrent reactivation of the network which further increases the probability of activation. Therefore, returning the chromatin to the basal state could contribute to stop the negative effects.

In the context of learning, our results indicate that in addition to the well-known role of dendritic spines and synaptic contacts as physical substrate for memory, other cellular compartments such the chromatin may also participate in cellular memory. Also, the need of transcriptional induction during the different phases of memory formation, such as consolidation and retrieval, support the putative role of the epigenome during metaplasticity. Indeed, in the near future we might speak of synaptic and nuclear memory. For instance, the

formation of pathological memories like post-traumatic stress disorder could rely on changes in the neuronal epigenome (Tsai & Graff, 2014).

Finally, it will be very interesting to explore the relevance of AP1 and other induced TF in the specification of different neuronal subtypes through evolution. The close relation between neuronal depolarization and transcriptional regulation is conserved from invertebrate to vertebrates. It is also crucial at all brain stages, from circuit formation during development to environment adaptability in adults. The evidence indicates that the evolution of the regulatory genome, reflected in differences between species in the transcriptional response during neuronal activation, could be an important driver for the evolution of cognitive capabilities (Hardingham et al., 2018). Thus, understanding the role of epigenetics through the evolution of neuronal activation could be the key to decipher the functional relevance behind the genomic memory.

CONCLUSIONS

1. The technology developed here allows the interrogation of changes in nuclear transcriptional programs and translation, as well as changes in chromatin dynamics and interactions in excitatory neurons responding to stimulation in the adult mouse brain, unveiling multiple regulatory layers.

2. The comparison of riboRNA-seq and nuRNA-seq datasets identifies transcripts displaying activity-dependent ribosome engagement.

3. The investigation of nuclear transcripts unveils multiple levels of activity-dependent gene expression, including the production of several species of non-coding RNAs.

4. Synaptic activation causes a dramatic change in chromatin accessibility at activity-induced genes and enhancers.

5. RNAPII-specific inhibition blocks the displacement of the +1 nucleosome-at the promoter induced by activity as well as the increase of chromatin accessibility at the gene body of activity-regulated genes.

6. Physiological neuronal activation shows common molecular features with pathological activation, and remarkable differences in the amount of changes in the transcriptional regulatory program.

7. AP1 plays a prominent role driving chromatin changes upon both learning and status epilepticus.

8. Activity-driven transcription strengthen enhancer-promoter interactions at activity-regulated genes.

9. Activity-driven transcription induces the formation of gene loops that bring together the TSS and TTS at actively transcribed genes to sustain the fast RNAPII re-loading.

10. The longitudinal analysis of nuclear transcripts identifies specific transcriptional programs at the different time points of neuronal activation.

11. Longitudinal analysis identifies long-lasting chromatin changes at intergenic regions that correlates with past transcription, representing a form of genomic memory potentially contributing to brain metaplasticity.

12. Long-lasting chromatin occupancy and interaction changes induced by the past transcriptional activity are associated with AP1 binding and may contribute to the deleterious consequences of status epilepticus.

CONCLUSIONES

1. La tecnología desarrollada en el contexto de esta tesis permite la interrogación de los cambios en transcripción nuclear y la traducción, así como los cambios en el dinamismo de la cromatina y las interacciones en neuronas excitadoras respondiendo a la estimulación en el cerebro adulto del ratón, revelando múltiples capas reguladoras.

2. La comparación de los datos de riboRNA-seq y nuRNA-seq identifica transcritos cuya unión al ribosoma está regulada por actividad.

3. La investigación de los transcritos nucleares revela múltiples niveles de regulación de la expresión génica dependiente de actividad, incluyendo la producción de varias especies de RNAs no codificantes.

4. La activación sináptica causa un cambio dramático en la accesibilidad de la cromatina en los promotores y enhancers de genes regulados por actividad.

5. La inhibición especifica de la RNAPII bloquea el desplazamiento inducido por actividad del nucleosoma +1 en el promotor de los IEGs, así como el incremento de la accesibilidad de la cromatina en el cuerpo del gen.

6. La activación neuronal fisiológica muestra características moleculares comunes con la activación patológica, y difieren remarcablemente en la cantidad de cambios en el programa de regulación transcripcional.

7. AP-1 juega un papel prominente dirigiendo los cambios de la cromatina tanto en el contexto de aprendizaje como de epilepsia.

8. La transcripción dirigida por actividad refuerza las interacciones entre regiones enhancer y promotores de los genes regulados por actividad.

9. La transcripción dirigida por actividad induce la formación de lazos intragénicos que aproximan físicamente el TSS y el TTS de los genes que son fuertemente inducidos por actividad, permitiendo una recarga muy rápida de la RNAPII.

10. El análisis longitudinal de los transcritos nucleares identifica programas transcripcionales específicos en los diferentes puntos temporales de la activación neuronal.

11. El análisis longitudinal identifica cambios de larga duración en regiones intergénicas que correlacionan con la transcripción que tuvo lugar en el pasado, representando por tanto una forma de memoria génica que puede contribuir a la metaplasticidad neuronal.

12. Los cambios de larga duración en la ocupación y las interacciones de la cromatina inducidos por la actividad transcripcional pasada están asociados con la unión de AP1 y podrían contribuir a las consecuencias deletéreas de la epilepsia.

BIBLIOGRAPHY

- Aaron R. Quinlan & Ira M. Hall. BEDTools: a flexible suite of utilities for comparing genomic features. Bioinformatics 26, 6, 841-842 (2010).
- Alarcon, J. et al. Chromatin acetylation, memory, and LTP are impaired in CBP+/– mice: a model for the cognitive deficit in Rubinstein–Taybi syndrome and its amelioration. Neuron 42, 947–959 (2004).
- Alberini, C.M. & Kandel, E.R. The regulation of transcription in memory consolidation. CSH perspectives in biology 7, a021741 (2014).
- Anderson, E. M. et al. Overexpression of the histone dimethyltransferase G9a in nucleus accumbens shell increases cocaine self- administration, stress-induced reinstatement, and anxiety. J. Neurosci. 38, 803–813 (2018).
- Aranda, S. et al. Regulation of gene transcription by Polycomb proteins. Science advances 1, 11, e1500737 (2015).
- Ay, F. et al. Statistical confidence estimation for Hi-C data reveals regulatory chromatin contacts. Genome Res 24, 999-1011 (2014).
- Baubec, D.F. et al. Genomic profiling of DNA methyltransferases reveals a role for DNMT3B in genic methylation. Nature 520, 243–247 (2015).
- Bauer-Mehren, A. et al. DisGeNET: a Cytoscape plugin to visualize, integrate, search and analyze gene-disease networks. Bioinformatics 26, 2924-2926 (2010).
- Barrett, R. M. et al. Hippocampal focal knockout of CBP affects specific histone modifications, long-term potentiation, and long- term memory. Neuropsychopharmacology 36, 1545–1556 (2011).
- Behrens, G. et al. A translational silencing function of MCPIP1/Regnase-1 specified by the target site context. Nucleic Acids Res 46, 4256-4270 (2018).

- Belgrad, J.R.D. Fields Epigenome interactions with patterned neuronal activity. Neuroscientist 24, 471-485 (2018).

- Ben-Ari, Y. & Cossart, R. Kainate, a double agent that generates seizures: two decades of progress. Trends Neurosci 23, 580-587 (2000).

- Benito, E. & Barco, A. The neuronal activity-driven transcriptome. Mol. Neurobiol 51, 1071-1088 (2015).

- Bharadwaj, R. et al. Conserved chromosome 2q31 conformations are associated with transcriptional regulation of GAD1 GABA synthesis enzyme and altered in prefrontal cortex of subjects with schizophrenia. J. Neurosci. 33, 11839–11851 (2013).

- Bharadwaj, R. et al. Conserved higher-order chromatin regulates NMDA receptor gene expression and cognition. Neuron 84, 997–1008 (2014).

- Bito, H. et al.CREB phosphorylation and dephosphorylation: a Ca(2+)- and stimulus duration-dependent switch for hippocampal gene expression. Cell 87, 1203-1214 (1996).

- Bonev, B. et al. Multiscale 3D Genome Rewiring during Mouse Neural Development. Cell 171, 557-572 e524 (2017).

- Caroni, P. et al. Structural plasticity upon learning: regulation and functions. Nat. Rev. Neurosci. 13, 478–490 (2012).

- Cho, J., et al. Multiple repressive mechanisms in the hippocampus during memory formation. Science 350, 82-87 (2015).

- Christy, B. et al. DNA binding site of the growth factor-inducible protein Zif268. Proc. Natl. Acad. Sci. USA 86, 8737-8741 (1989).

- Chrivia, J. C. et al. Phosphorylated CREB binds specifically to the nuclear protein CBP. Nature 365, 855–859 (1993).

- Corces, M.R. et al. Lineage-specific and single-cell chromatin accessibility charts human hematopoiesis and leukemia evolution. Nat Genet. 48, 10 (2016).

- Crepaldi, L. et al. Binding of TFIIIC to sine elements controls the relocation of activity-dependent neuronal genes to transcription factories. PLoS Genet 9, e1003699 (2013).

- Crosio, C. et al. Chromatin remodeling and neuronal response: multiple signaling pathways induce specific histone H3 modifications and early gene expression in hippocampal neurons. J Cell Sci 116, 4905-4914 (2003).

- Covington, H. E. et al. A role for repressive histone methylation in cocaine- induced vulnerability to stress. Neuron 71, 656–670 (2011).

- Deisseroth, K. et al. Translocation of calmodulin to the nucleus supports CREB phosphorylation in hippocampal neurons. Nature 392, 198–202 (1998).

- Dekker, J. et al. Exploring the three-dimensional organization of genomes: interpreting chromatin interaction data. Nat. Rev. Genet. 14, 390–403 (2013).

- DeNardo, L. & Luo, L. Genetic strategies to access activated neurons. Curr Opin Neurobiol 45, 121-129 (2017).

- Dixon, J.R. et al. Topological domains in mammalian genomes identified by analysis of chromatin interactions. Nature 485, 376–380 (2012).

- Dolmetsch, R.E. et al. Calcium oscillations increase the efficiency and specificity of gene expression. Nature 392, 933-936 (1998).

- Dunn, C.J. et al. Histone hypervariants H2A.Z.1 and H2A.Z.2 play independent and context- specific roles in neuronal activity- induced

transcription of Arc/Arg3.1 and other immediate early genes. eNeuro 4, ENEURO.0040-17.2017 (2017).

- Dougherty, J.D. The Expanding Toolkit of Translating Ribosome Affinity Purification. J Neurosci 37, 12079-12087 (2017).

- Dowen, J. M. et al. Control of cell identity genes occurs in insulated neighborhoods in mammalian chromosomes. Cell 159, 374–387 (2014).

- Durand, N.C. et al. Juicer Provides a One-Click System for Analyzing Loop-Resolution Hi-C Experiments. Cell Syst 3, 95-98 (2016).

- Eagle, A.L. et al. Role of hippocampal activity-induced transcription in memory consolidation. Rev Neurosci 27, 559-573 (2016).

- Ebert, D.H. & Greenberg, M.E. Activity-dependent neuronal signaling and autism spectrum disorder. Nature 493, 327–337 (2013).

- Eferl, R. & Wagner, E.F. AP-1: a double-edged sword in tumorigenesis. Nat. Rev. Cancer 3, 859-868 (2003).

- Elliott, R.C. et al. Overlapping microarray profiles of dentate gyrus gene expression during development- and epilepsy-associated neurogenesis and axon outgrowth. J Neurosci 23, 2218-2227 (2003).

- Emmert-Buck, MR. et al. Laser capture microdissection. Science 274, 998–1001 (1996).

- Erdmann, G. et al. Inducible gene inactivation in neurons of the adult mouse forebrain. BMC neuroscience 8, 63 (2007).

- Fernandes, D. & Carvalho, A.L. Mechanisms of homeostatic plasticity in the excitatory synapse. J Neurochem 139, 973-996 (2016).

- Finnsson, J. et al. LMNB1-related autosomal-dominant leukodystrophy: clinical and radiological course. Ann. Neurol. 78, 412–425 (2015).

- Fiorenza, A. et al. Blocking miRNA Biogenesis in Adult Forebrain Neurons Enhances Seizure Susceptibility, Fear Memory, and Food Intake by Increasing Neuronal Responsiveness. Cereb Cortex 26, 1619-1633 (2016).
- Flavell, S.W. & Greenberg, M.E. Signaling mechanisms linking neuronal activity to gene expression and plasticity of the nervous system. Annu. Rev. Neurosci. 31, 563–590 (2008)
- Gabel, H.W. et al. Disruption of DNA-methylation-dependent long gene repression in Rett syndrome. Nature 522, 89–93 (2015).
- Gavin, D. P. et al. Active DNA demethylation in post-mitotic neurons: a reason for optimism. Neuropharmacology 75, 233–245 (2013).
- Ghavi-Helm, Y. et al. Highly rearranged chromosomes reveal uncoupling between genome topology and gene expression. Nat. Gen. 51, 1272–1282 (2019).
- Goldberg, A. D. et al. Epigenetics: a landscape takes shape. Cell 128, 635–638 (2007).
- Gräff, J. et al. Epigenetic priming of memory updating during reconsolidation to attenuate remote fear memories. Cell 156, 261–276 (2014).
- Greenberg, M.E. & Ziff, E.B. Stimulation of 3T3 cells induces transcription of the c-fos proto-oncogene. Nature 311, 433-438 (1984).
- Guo, X. et al. Structural insight into autoinhibition and histone H3-induced activation of DNMT3A. Nature 517, 640–644 (2015). (a)
- Guo, Y. et al. CRISPR inversion of CTCF sites alters genome topology and enhancer/promoter function. Cell 162, 900–910 (2015). (b)
- Gupta, S. et al. Histone methylation regulates memory formation. J. Neurosci. 30, 3589–3599 (2010).

- Guy, H. et al. The role of MeCP2 in the brain. Annu. Rev. Cell Dev. Biol. 27, 631–652 (2011).

- Halder, R. et al. DNA methylation changes in plasticity genes accompany the formation and maintenance of memory. Nat Neurosci 19, 102-110 (2016).

- Hampsey, M. et al. Control of eukaryotic gene expression: gene loops and transcriptional memory. Adv Enzyme Regul 51, 118-125 (2011).

- Hardingham, G.E. et al. Distinct functions of nuclear and cytoplasmic calcium in the control of gene expression. Nature 385, 260-265 (1997).

- Hardingham, G. E. et al. Lineage divergence of activity-driven transcription and evolution of cognitive ability. Nat Rev Neurosci. 19,1, 9 (2017)

- Hargreaves, D.C. & Crabtree, G.R. ATP- dependent chromatin remodeling: genetics, genomics and mechanisms. Cell Res. 21, 396–420 (2011).

- Heiman, M. et al. Cell type-specific mRNA purification by translating ribosome affinity purification (TRAP). Nat Protoc 9, 1282-1291 (2014).

- Heintzman, N.D. et al. Histone modifications at human enhancers reflect global cell-type-specific gene expression Nature 459, 108-112 (2009).

- Henikoff, S. & Smith, M.M. Histone variants and epigenetics. Cold Spring Harb. Perspect. Biol. 7, a019364 (2015).

- Herring, B. E. & Nicoll, R. A. Long-term potentiation: from CaMKII to AMPA receptor trafficking. Annu. Rev. Physiol. 78, 351–365 (2016).

- Hevroni, D. et al. Hippocampal plasticity involves extensive gene induction and multiple cellular mechanisms. J Mol Neurosci 10, 75-98 (1998).

- Hofer, S. B. et al. Experience leaves a lasting structural trace in cortical circuits. Nature 457, 313–317 (2009).

- Holt, C.E. & Schuman, E.M. The central dogma decentralized: new perspectives on RNA function and local translation in neurons. Neuron 80, 648-657 (2013).

- Hong, E.J. et al. Transcriptional control of cognitive development. Curr. Opin. Neurobiol. 15, 21–28 (2005).

- Hrvatin, S. et al. Single-cell analysis of experience-dependent transcriptomic states in the mouse visual cortex. Nat. Neurosci. 21, 120–129 (2018).

- Hu, P. et al. Dissecting cell-type composition and activity-dependent transcriptional state in mammalian brains by massively parallel single-nucleus RNA-seq. Mol. Cell 68, 1006–1015.e7 (2017).

- Huang, Y. et al. Altered histone acetylation at glutamate receptor 2 and brain-derived neurotrophic factor genes is an early event triggered by status epilepticus. J Neurosci 22, 8422-8428 (2002).

- Irimia, M. et al. A highly conserved program of neuronal microexons is misregulated in autistic brains. Cell. 159(7):1511–1523 (2014).

- Jakovcevski M. et al. Neuronal Kmt2a/Mll1 histone methyltransferase is essential for prefrontal synaptic plasticity and working memory. *J Neurosci*. 35,13,5097–5108 (2015).

- Jenuwein, T. & Allis, C. D. Translating the histone code. Science 293, 1074–1080 (2001).

- Jones, P.A. Functions of DNA methylation: Islands, start sites, gene bodies and beyond. Nat. Rev. Genet. 13, 484–492 (2012).

- Joo, J.Y. et al. Stimulus-specific combinatorial functionality of neuronal c-fos enhancers. Nat. Neurosci. 19, 75–83 (2016).

- Kagey, M.H. et al. Mediator and cohesin connect gene expression and chromatin architecture. Nature 467, 430–435 (2010).

- Keung, A.J. et al. Chromatin regulation at the frontier of synthetic biology Nat Rev Genet, 16 (2015), pp. 159-171

- Ki-Jun, Y. et al. Epitranscriptomes in the Adult Mammalian Brain: Dynamic Changes Regulate Behavior. Neuron. Volume 99, Issue 2, 25 July 2018, Pages 243-245 (2018).

- Kim, D. et al. HISAT: a fast spliced aligner with low memory requirements. Nature methods 12, 357-360 (2015).

- Kim, T.K., et al. Widespread transcription at neuronal activity-regulated enhancers. Nature 465, 182-187 (2010).

- Kobow, K. & Blumcke, I. Epigenetic mechanisms in epilepsy. Prog Brain Res 213, 279-316 (2014).

- Kouzarides, T. Chromatin modifications and their function. Cell 128, 693–705 (2007).

- Korb, E. et al. BET protein Brd4 activates transcription in neurons and BET inhibitor Jq1 blocks memory in mice. Nat. Neurosci. 18, 1464-1473 (2015).

- Korzus, E. et al. CBP histone acetyltransferase activity is a critical component of memory consolidation. Neuron 42, 961–972 (2004).

- Korzus, E. Rubinstein-Taybi syndrome and epigenetic alterations. Adv. Exp. Med. Biol. 978, 39–62 (2017).

- Lacar, B. et al. Nuclear RNA-seq of single neurons reveals molecular signatures of activation. Nat. Commun. 7, 11022 (2016).

- Lahm, A. et al. Unraveling the hidden catalytic activity of vertebrate class IIa histone deacetylases. Proc. Natl Acad. Sci. USA 104, 17335–17340 (2007).

- Laine, J.P. et al. A physiological role for gene loops in yeast. Genes Dev 23, 2604-2609 (2009).

- Langmead, B. & Salzberg, S.L. Fast gapped-read alignment with Bowtie 2. Nature methods 9, 357-359 (2012).

- Leach, P. T. et al. Gadd45b knockout mice exhibit selective deficits in hippocampus- dependent long- term memory. Learn. Mem. 19, 319–324 (2012).

- Levenson, J. M. et al. Evidence that DNA (cytosine-5) methyltransferase regulates synaptic plasticity in the hippocampus. J. Biol. Chem. 281, 15763–15773 (2006).

- Li, H. et al. The Sequence Alignment/Map format and SAMtools. Bioinformatics 25, 2078-2079 (2009).

- Liao, Y. et al. featureCounts: an efficient general purpose program for assigning sequence reads to genomic features. Bioinformatics 30, 923-930 (2014).

- Lieberman-Aiden, E. et al. Comprehensive mapping of long-range interactions reveals folding principles of the human genome. Science 326, 289–293 (2009).

- Lin, Y. et al. Activity-dependent regulation of inhibitory synapse development by Npas4. Nature 455, 1198-1204 (2008).

- Lister, R. et al. Global epigenomic reconfiguration during mammalian brain development. Science 341, 1237905 (2013).

- Liu, X. S. et al. Optogenetic stimulation of a hippocampal engram activates fear memory recall. Nature 484, 381-385 (2012).

- Long, H.K. et al. Ever-changing landscapes: transcriptional enhancers in development and evolution Cell 167, 1170-1187 (2016).

- López, A.J. & Wood, M.A. Role of nucleosome remodeling in neurodevelopmental and intellectual disability disorders. Front. Behav. Neurosci. 9, 100 (2015).

- Lopez-Atalaya, J.P. et al. Genomic targets, and histone acetylation and gene expression profiling of neural HDAC inhibition. Nucleic Acids Res 41, 8072-8084 (2013).

- Lopez-Atalaya, J.P. & Barco, A. Can changes in histone acetylation contribute to memory formation? Trends Genet 30, 529-539 (2014a).

- Lopez-Atalaya, J.P et al. Epigenetic factors in intellectual disability: the Rubinstein-Taybi syndrome as a paradigm of neurodevelopmental disorder with epigenetic origin. Prog Mol Biol Transl Sci. 128, 139–176 (2014b)

- Love, M.I. et al. Moderated estimation of fold change and dispersion for RNA-seq data with DESeq2. Genome Biol 15, 550 (2014).

- Ma, D. K. et al. Neuronal activity- induced Gadd45b promotes epigenetic DNA demethylation and adult neurogenesis. Science 323, 1074–1077 (2009).

- Madabhushi, R., et al. Activity-Induced DNA Breaks Govern the Expression of Neuronal Early-Response Genes. Cell 161, 1592-1605 (2015).

- Maddox, S.A. et al. p300/CBP histone acetyltransferase activity is required for newly acquired and reactivated fear memories in the lateral amygdala. Learn. Mem. 20, 109–119 (2013).

- Malik, A.N. et al. Genome-wide identification and characterization of functional neuronal activity–dependent enhancers. Nature Neuroscience 17, 1330-1339 (2014).

- Malvaez, M. et al. CBP in the nucleus accumbens regulates cocaine-induced histone acetylation and is critical for cocaine- associated behaviors. J. Neurosci. 31, 16941–16948 (2011).

- Mardinly, A.R. et al. Greenberg. Sensory experience regulates cortical inhibition by inducing IGF1 in VIP neurons. Nature 531, 371-375 (2016). (a)

- Mardinly, A.R. et al. Sensory experience regulates cortical inhibition by inducing IGF1 in VIP neurons. Nature 531, 371–375 (2016) (b)

- Martin, M. Cutadapt removes adapter sequences from high-throughput sequencing reads. EMBnet Journal 17, 10-12 (2011).

- Martin, K.C. & Zukin, R.S. RNA trafficking and local protein synthesis in dendrites: an overview. J. Neurosci. 26, 7131-7134 (2006).

- Mauger, O. et al. Targeted Intron Retention and Excision for Rapid Gene Regulation in Response to Neuronal Activity. Neuron 92, 1266-1278 (2016).

- Maurano, M.T. et al. Systematic localization of common disease-associated variation in regulatory DNA. Science 337, 1190–1195 (2012).

- Maurano, M.T. et al. Role of DNA methylation in modulating transcription factor occupancy. Cell Reports 12, 1184–1195 (2015). (a)

- Maurano, M.T. et al. Large-scale identification of sequence variants influencing human transcription factor occupancy in vivo. Nat. Genet. 47, 1393–1401 (2015). (b)

- Maze, I. et al. Essential role of the histone methyltransferase G9a in cocaine- induced plasticity. Science 327, 213–216 (2010).

- Maze, I. et al. Critical role of histone turnover in neuronal transcription and plasticity. Neuron 87, 77–94 (2015).

- McLean, C.Y. et al. GREAT improves functional interpretation of cis-regulatory regions. Nature biotechnology 28, 495-501 (2010).

- Mellén, M. et al. 5-hydroxymethylcytosine accumulation in postmitotic neurons results in functional demethylation of expressed genes. Proc. Natl. Acad. Sci. USA 114, E7812–E7821 (2017).

- Milbrandt, J. Nerve growth factor induces a gene homologous to the glucocorticoid receptor gene. Neuron 1, 183-188 (1988).

- Miller, C. A. & Sweatt, J. D. Covalent modification of DNA regulates memory formation. Neuron 53, 857–869 (2007).

- Miller, C. A. et al. Cortical DNA methylation maintains remote memory. Nat. Neurosci. 13, 664–666 (2010).

- Mo, A. et al. Epigenomic Signatures of Neuronal Diversity in the Mammalian Brain. Neuron 86, 1369-1384 (2015).

- Mullins, C. et al. Unifying views of autism spectrum disorders: a consideration of autoregulatory feedback loops. Neuron 89, 1131–1156 (2016).

- Nasmyth, K. & Haering, C. H. Cohesin: its roles and mechanisms. Annu. Rev. Genet. 43, 525–558 (2009).

- Neri, F. et al. Intragenic DNA methylation prevents spurious transcription initiation. Nature 543, 72–77 (2017).

- Nora, E.P. et al. Spatial partitioning of the regulatory landscape of the X-inactivation centre. Nature 485, 381–385 (2012).

- Padeken, J. & Heun, P. Nucleolus and nuclear periphery: velcro for heterochromatin. Curr. Opin. Cell Biol. 28, 54–60 (2014).

- Phillips-Cremins, J.E. et al. Architectural protein subclasses shape 3D organization of genomes during lineage commitment. Cell 153, 1281–1295 (2013).

- Piper, J. et al. Wellington: a novel method for the accurate identification of digital genomic footprints from DNase-seq data. Nucleic Acids Res 41, e201 (2013).

- Pollard, K.S. et al. Detection of nonneutral substitution rates on mammalian phylogenies. Genome Res 20, 110-121 (2010).

- Poo, M.M. et al. What is memory? The present state of the engram. BMC Biol. 14, 40 (2016).

- Queralt-Rosinach, N. et al. DisGeNET-RDF: harnessing the innovative power of the Semantic Web to explore the genetic basis of diseases. Bioinformatics 32, 2236-2238 (2016).

- Ramirez, F. et al. deepTools2: a next generation web server for deep-sequencing data analysis. Nucleic Acids Res 44, W160-165 (2016).

- Rao, S.S. et al. A 3D map of the human genome at kilobase resolution reveals principles of chromatin looping. Cell 159, 1665–1680 (2014).

- Reik, W. Stability and flexibility of epigenetic gene regulation in mammalian development. Nature 447, 425–432 (2007).

- Risca V.I. & Greenleaf WJ. Unraveling the 3D genome: genomics tools for multiscale exploration. Trends Genet. 31, 7, 357–372 (2015).

- Ronan, J.L. et al. From neural development to cognition: unexpected roles for chromatin. Nat. Rev. Genet. 14, 347–359 (2013).

- Rowley, M.J. & Corces, V.G. Organizational principles of 3D genome architecture. Nat Rev Genet 19, 789-800 (2018).

- Rudenko, A. et al. Tet1 is critical for neuronal activity regulated gene expression and memory extinction. Neuron 79, 1109–1122 (2013).

- Sanz, E. et al. Cell-type-specific isolation of ribosome-associated mRNA from complex tissues. Proc. Natl. Acad. Sci. USA 106, 13939–13944 (2009).

- Savell, K.E., et al. Extra-coding RNAs regulate neuronal DNA methylation dynamics. Nature communications 7, 12091 (2016).

- Saxena, A. et al. Trehalose-enhanced isolation of neuronal sub-types from adult mouse brain. Biotechniques 52, 381–385 (2012).

- Sawicka, A. & Seiser, C. Histone H3 phosphorylation - a versatile chromatin modification for different occasions. Biochimie 94, 2193-2201 (2012).

- Scandaglia, M. et al. Loss of Kdm5c Causes Spurious Transcription and Prevents the Fine-Tuning of Activity-Regulated Enhancers in Neurons. Cell reports 21, 47-59 (2017).

- Schaukowitch, K. et al. Enhancer RNA facilitates NELF release from immediate early genes. Mol. Cell 56, 29–42 (2014).

- Schep, A.N. et al. Structured nucleosome fingerprints enable high-resolution mapping of chromatin architecture within regulatory regions. Genome Res 25, 1757-1770 (2015).

- Schott, J. et al. Translational regulation of specific mRNAs controls feedback inhibition and survival during macrophage activation. PLoS Genet 10, e1004368 (2014).

- Sudhof, T.C. Molecular neuroscience in the 21st century: a personal perspective. Neuron 96, 536–541 (2017).

- Sheng, M. & Greenberg, M.E. The regulation and function of c-fos and other immediate early genes in the nervous system. Neuron 4, 477-485 (1990).

- Sheng, M. et al. CREB: a Ca(2+)-regulated transcription factor phosphorylated by calmodulin-dependent kinases. Science 252, 1427-1430 (1991).

- Siepel, A. et al. Evolutionarily conserved elements in vertebrate, insect, worm, and yeast genomes. Genome Res 15, 1034-1050 (2005).

- Silva, A.J. et al. CREB and memory. Annu. Rev. Neurosci. 21, 127–148 (1998).

- Spruston, N. Pyramidal neurons: dendritic structure and synaptic integration. Nat. Rev. Neurosci. 9, 206–221 (2008).

- Stadler, M.B. et al., DNA-binding factors shape the mouse methylome at distal regulatory regions. Nature 480, 490–495 (2011).

- Stanley, S. et al. Profiling of Glucose-Sensing Neurons Reveals that GHRH Neurons Are Activated by Hypoglycemia. Cell metabolism 18, 596-607 (2013).

- Stefanelli, G. et al. Learning and age- related changes in genome- wide H2A.Z binding in the mouse hippocampus. Cell Rep. 22, 1124–1131 (2018).

- Su, Y. et al. Neuronal activity modifies the chromatin accessibility landscape in the adult brain. Nat. Neurosci. 20, 476-483 (2017).

- Sugino, K. et al. Molecular taxonomy of major neuronal classes in the adult mouse forebrain. Nat. Neurosci 9, 99–107 (2006).

- Sultan, F.A. et al. Genetic deletion of Gadd45b,a regulator of active DNA demethylation, enhances long- term memory and synaptic plasticity. J. Neurosci. 32, 17059–17066 (2012).

- Sweatt, J.D. The emerging field of neuroepigenetics. Neuron 80, 624-632 (2013).

- Taniura, H. et al. Histone modifications in status epilepticus induced by kainate. Histol Histopathol 21, 785-791 (2006).

- Teissandier, A. & Bourchis, D. Gene body DNA methylation conspires with H3K36me3 to preclude aberrant transcription. EMBO J. 36, 1471–1473 (2017).

- Telese, F. et al. “Seq-ing" insights into the epigenetics of neuronal gene regulation”. *Neuron* 77, 4, 606-23 (2013).

- Thomas, G.M. & Huganir, R.L. MAPK cascade signalling and synaptic plasticity. Nat. Rev. Neurosci. 5, 173-183 (2004).

- Thorvaldsdottir, H. et al. Integrative Genomics Viewer (IGV): high-performance genomics data visualization and exploration. Brief Bioinform 14, 178-192 (2013).

- Tonnesen, J. & Nagerl, U. V. Dendritic spines as tunable regulators of synaptic signals. Front. Psychiatry 7, 101 (2016).

- Tsai, L.H. & Graff, J. On the resilience of remote traumatic memories against exposure therapy-mediated attenuation. EMBO Rep 15, 853-861 (2014).

- Tsankova, N.M. et al. Histone modifications at gene promoter regions in rat hippocampus after acute and chronic electroconvulsive seizures. J Neurosci 24, 5603-5610 (2004).

- Tullai, J.W. et al. Cooper Immediate-early and delayed primary response genes are distinct in function and genomic architecture J. Biol. Chem. 282, 23981-23995 (2007).

- Turrigiano, G. Homeostatic synaptic plasticity: local and global mechanisms for stabilizing neuronal function. Cold Spring Harb. Perspect. Biol. 4, a005736 (2012).

- Tyssowski, K.M. et al. Different neuronal activity patterns induce different gene expression programs. Neuron 98, 530-546.e11 (2018).

- Urdinguio, R.G. et al. Epigenetic mechanisms in neurological diseases: genes, syndromes, and therapies. Lancet neurology 8, 1056-1072 (2009).

- Vierbuchen, T. et al. AP-1 Transcription Factors and the BAF Complex Mediate Signal-Dependent Enhancer Selection. Mol Cell 68, 1067-1082 e1012 (2017).

- Vernimmen, D. & Bickmore, W. A. The hierarchy of transcriptional activation: from enhancer to promoter. Trends Genet. 31, 696–708 (2015).

- Vietri Rudan, M. et al. Comparative Hi-C reveals that CTCF underlies evolution of chromosomal domain architecture. Cell Rep. 10, 1297–1309 (2015).

- Vogel-Ciernia, A. et al. The neuron-specific chromatin regulatory subunit BAF53b is necessary for synaptic plasticity and memory. Nat Neurosci 16, 552-561 (2013).

- Vogel-Ciernia, A. et al. Mutation of neuron- specific chromatin remodeling subunit BAF53b: rescue of plasticity and memory by manipulating actin remodeling. Learn. Mem. 24, 199–209 (2017).

- Watson, L.A. et al. Dual effect of CTCF loss on neuroprogenitor differentiation and survival. J. Neurosci. 34, 2860–2870 (2014).

- Wayman, G.A. et al. Soderling. Calmodulin-kinases: modulators of neuronal development and plasticity. Neuron 59, 914-931 (2008).

- Webb, W.M. et al. Dynamic association of epigenetic H3K4me3 and DNA 5hmC marks in the dorsal hippocampus and anterior cingulate cortex following reactivation of a fear memory. Neurobiol. Learn. Mem. 142, 66–78 (2017).

- Weber, C.M. et al. Nucleosomes are context- specific, H2A.Z- modulated barriers to RNA polymerase. Mol. Cell 53, 819–830 (2014).

- Wefelmeyer, W. et al. Homeostatic plasticity of subcellular neuronal structures: from inputs to outputs. Trends Neurosci. 39, 656–667 (2016).

- West, A.E. et al. Greenberg Calcium regulation of neuronal gene expression. Proc. Natl. Acad. Sci. USA 98, 11024-11031 (2001).

- West, A.E. & Greenberg, M.E. Neuronal activity-regulated gene transcription in synapse development and cognitive function. Cold Spring Harb. Perspect. Biol. 3, 3 (2011).

- Wood, M. A. et al. Transgenic mice expressing a truncated form of CREB- binding protein (CBP) exhibit deficits in hippocampal synaptic plasticity and memory storage. Learn. Mem. 12, 111–119 (2005).

- Wood, M.A. et al. A transcription factor- binding domain of the coactivator CBP is essential for long term memory and the expression of specific target genes. Learn. Mem. 13, 609–617 (2006).

- Worley, P.F. et al. Thresholds for synaptic activation of transcription factors in hippocampus: correlation with long-term enhancement. J. Neurosci. 13, 4776-4786 (1993).

- Wu, G.Y. et al. Spaced stimuli stabilize MAPK pathway activation and its effects on dendritic morphology. Nat. Neurosci. 4, 151-158 (2001).

- Wu, H. et al. Dnmt3a-dependent nonpromoter DNA methylation facilitates transcription of neurogenic genes. Science 329, 444–448 (2010).

- Wu, J.I. et al. Regulation of dendritic development by neuron- specific chromatin remodeling complexes. Neuron 56, 94–108 (2007).

- Wu, Y.E. et al. Detecting activated cell populations using single-cell RNA-seq. Neuron 96, 313–329.e6 (2017).

- Xing, J. et al. Coupling of the RAS-MAPK pathway to gene activation by RSK2, a growth factor-regulated CREB kinase. Science 273, 959-963 (1996).

- Yamazaki, S. et al. Stimulus-specific induction of a novel nuclear factor-kappaB regulator, IkappaB-zeta, via Toll/Interleukin-1 receptor is mediated by mRNA stabilization. J Biol Chem 280, 1678-1687 (2005).

- Yang, G. et al. Stably maintained dendritic spines are associated with lifelong memories. Nature 462, 920–924 (2009).

- Yang, Y. et al. Chromatin remodeling inactivates activity genes and regulates neural coding. Science 353, 300–305 (2016).

- Yap, E.L. & Greenberg, M.E. Activity-Regulated Transcription: Bridging the Gap between Neural Activity and Behavior. Neuron 100, 330-348 (2018).

- Ye, T. et al. seqMINER: an integrated ChIP-seq data interpretation platform. Nucleic Acids Res 39, e35 (2011).

- Yin, J. C. & Tully, T. CREB and the formation of long-term memory. Curr. Opin. Neurobiol. 6, 264–268 (1996).

- Yiu, A.P. et al. Neurons are recruited to a memory trace based on relative neuronal excitability immediately before training. Neuron 83, 722-735 (2014).

- Yoo, M. et al. BAF53b, a neuron- specific nucleosome remodeling factor, is induced after learning and facilitates long- term memory consolidation. J. Neurosci. 37, 3686–3697 (2017).

- You, X., et al. Neural circular RNAs are derived from synaptic genes and regulated by development and plasticity. Nat Neurosci 18, 603-610 (2015).
- Zeisel, A. et al. Cell types in the mouse cortex and hippocampus revealed by single-cell RNA-seq. Science 347, 1138–1142 (2015).
- Zhang, Y. & Reinberg, D. Transcription regulation by histone methylation: interplay between different covalent modifications of the core histone tails. Genes Dev. 15, 2343–2360 (2001).
- Zhang, Y. et al. Model-based analysis of ChIP-Seq (MACS). Genome Biol 9, R137 (2008).
- Zhou, V.W. et al. Charting histone modifications and the functional organization of mammalian genomes. Nat. Rev. Genet. 12, 7–18 (2011).
- Zhu, H. et al. Transcription factors as readers and effectors of DNA methylation. Nat. Rev. Genet. 17, 551–565 (2016).
- Zovkic, I.B. et al.Histone H2A.Z subunit exchange controls consolidation of recent and remote memory. Nature 515, 582–586 (2014).